Experimental Coherent Laser Control of Physicochemical Processes

ARTICLE *in* CHEMICAL REVIEWS · MAY 2004

Impact Factor: 46.57 · DOI: 10.1021/cr020668r · Source: PubMed

2 AUTHORS:

Marcos Dantus
Michigan State University
281 PUBLICATIONS **5,376** CITATIONS
SEE PROFILE

Vadim V Lozovoy
Michigan State University
155 PUBLICATIONS **2,532** CITATIONS
SEE PROFILE

Experimental Coherent Laser Control of Physicochemical Processes

Marcos Dantus* and Vadim V. Lozovoy

Department of Chemistry and Department of Physics and Astronomy, Michigan State University, East Lansing, Michigan 48824

Received October 3, 2003

Contents

* To whom correspondence should be addressed. Phone (517) 355-9715 (ext-315). Fax (517) 353-1793. E-mail dantus@msu.edu.

1. Introduction

The observation of coherent dynamics ensuing from the excitation of molecular systems by femtosecond laser pulses is at the heart of femtochemistry. The time-dependent evolution of coherent superpositions of quantum states, the physical basis for the observation of coherent dynamics and their manipulation are of central importance to coherent control of physicochemical processes. In the early days of femtochemistry, there was significant skepticism regarding the type of information that could be learned from spectroscopic experiments using very short pulses. There were arguments that one could infer the dynamics from frequency-resolved experiments and that the femtosecond experiments did not offer new information. It was also assumed that experiments with very short pulses would smear the available spectroscopic information because of their broad bandwidths. Approximately two decades after the initial experiments, it has become clear that femtosecond experiments have opened an extremely valuable window into the dynamic behavior of atomic and molecular systems that is influencing how we think about physics, chemistry, and biology. In particular, we highlight the fact that some of the highest resolution spectroscopic measurements being carried out employ femtosecond laser pulses. These experiments, specifically those taking advantage of rotational coherence, provide resolution that rivals microwave spectroscopy. The reason spectroscopic information is not lost in femtochemistry experiments is coherence, a property that can be manipulated to control physicochemical processes by a number of different approaches, which will be reviewed here.

This review presents a summary of some of the most salient contributions to the field of coherent laser control from an experimentalist's perspective. While a number of theoretical papers have made key contributions to the field, it is from the experimental successes, as well as failures, that we can best learn how to implement new strategies and develop future applications. Coherent laser control, in the context of this review, encompasses experiments in which the coherent properties of the laser and/or the molecule are required for controlling a particular physicochemical process. We distinguish for each of the experiments between coherence in the laser field(s),

10.1021/cr020668r CCC: $48.50
Published on Web 03/27/2004

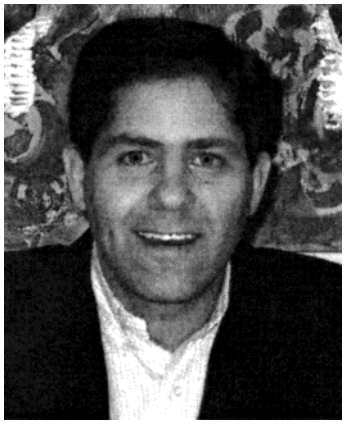

Professor Marcos Dantus was born in Mexico. He received B.A. and M.A. degrees from Brandeis University and a Ph.D degree in chemistry from Caltech under the direction of Professor Ahmed H. Zewail. His Ph.D. work focused on the development of femtosecond transition state spectroscopy, and his postdoctoral work on the development of ultrafast electron diffraction. He is presently Profesor of Chemistry and Adjunct Professor in Physics at Michigan State University. Professor Dantus has received many honors and awards. He received the Herbert Newby McCoy Award (for best Ph.D. Thesis in Chemistry); and the Milton and Francis Clauser Doctoral Prize (for the most significant Ph.D thesis) both from Caltech. In 1992, he was honored with the Nobel Laureate Signature Award for Graduate Education in Chemistry. He received the Camille and Henry Dreyfus New Faculty Award; the General Electric Foundation Faculty Award in 1994; the Beckman Young Investigator Award; the Packard Fellowship for Science and Engineering; the Eli Lilly Teaching Fellowship; the Alfred P. Sloan Research Fellowship; and the Camille Dreyfus Teacher-Scholar Award. Professor Dantus was featured in the ACS 125th Anniversary Issue of *Chemical and Engineering News*, 2001. He is founder and member of the Board of Directors of KTM Industries. Professor Dantus' teaching interests include enhancing critical thinking in the classroon through activities involving discovery, student presentations, and competition-based games. One of his favorite challenges is teaching freshman students about what is NOT known in chemistry. Professor Dantus' research interests include ultrafast dynamics, coherent laser control of laser–matter interactions, and quantum computation. Professor Dantus has 78 publications, and four patents.

Vadim V. Lozovoy was born in Novosibirsk, USSR, in 1960. He received his M.S. degree in physics from Novosibirsk State University in 1983 where he studied ion radicals and their reactions in solutions with optically detected electron spin resonance of ion pairs and positron annihilation. He received his Ph.D. degrees in physics and mathematics from the Institute of Chemical Kinetics and Combustion Siberian Branch Academy of Science USSR, Novosibirsk, in 1989. His dissertation research involved the discovery of fast energy transfer by excitons in liquid cyclic hydrocarbons using a picosecond pulse radiolysis system and picosecond streak camera registration built with his active participation. From 1991 to 1998 he worked in the N. N. Semenov Institute of Chemical Physics, Russian Academy of Science, Moscow. He was involved in the design and construction of a femtosecond laser system with supersonic jet, intracavity laser spectroscopy, adsorption, fluorescence and depolarization registrations. He conducted a group of students in the experiments on ultrafast chemical dynamics in gas and condensed phases and made theoretical analysis of the coherent intramolecular dynamics. In 1999, he joined the Marcos Dantus research laboratory at Michigan State University, where laser control of intramolecular dynamics with four-wave mixing spectroscopy is studied experimentally and theoretically. Currently he works at MSU on the theory and intrepretation of experiments on coherent laser control of multiphoton microscopy and quantum computing with molecules. Dr. Lozovoy is a member of the American Chemical Society and Optical Society of America.

and microscopic (intramolecular) and macroscopic (intermolecular) coherence in the sample. We consider coherence in the various degrees of freedom available to the sample—among them, electronic vibrations, rotations, and collective dynamics. We have included a wide range of experiments, not only those aimed at controlling chemical reactions, because there are several important lessons to be learned from them.

The accelerated progress and the very exciting successes in this field have increased the demand for reviews. During the past few years, a number of reviews have been written on coherent control, the majority of them emphasizing theoretical concepts rather than experimental implementation.[1−32] This review takes a different approach. Instead of focusing on the theory, we focus on the experiments, their requirements, the signals, and their interpretation. We analyze the present degree of success, the present limitations, and the future applications. This review is aimed at the experimentalist who is interested in pursuing or understanding coherent control methods and at the theoretician who wants to know what currently limits experimental implementation.

Coherent control methods exploit a number of constructive and destructive interferences that are manipulated to obtain a desired outcome. In 1801, Young's double-slit experiment demonstrated the interference of light, a fact that became important in the development of quantum mechanics. Young's experiment, depicted in Figure 1, entailed the propagation of light through two closely spaced slits. The light was projected onto a screen, and a very interesting phenomenon was observed. When either of the slits was closed, a smooth, bell-shaped intensity pattern was recorded; however, when both slits were opened, the amplitude of light varied sinusoidally with position, because of interference between the beams emerging from the two slits. The phase of the light traversing through each of the slits determines the intensity of light that is observed at a specific location on the detection screen. The path length from each slit to the location of the detector on the screen (r_1 and r_2) determines if constructive or destructive interference takes place (see Figure 1A). This experiment could also be considered one of the first successful experiments in coherent control. One could control the intensity of light reaching a detector fixed in space by advancing or delaying the phase of light going through one of the two slits. In Figure 1B, we illustrate such a setup, in which an optic retards the phase of light going through one of the slits. When phase retardation equivalent to half an optical period (π) is introduced, the interference pattern on the

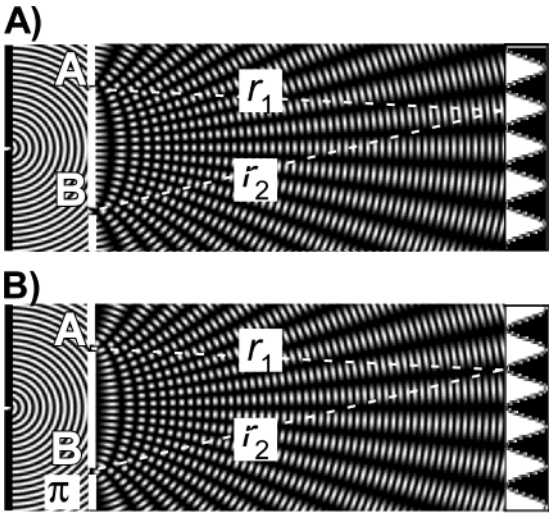

Figure 1. Schematic simulation of Young's double-slit experiment in which the distance between the slits A and B is equal to 10 λ. (A) A plane wave is diffracted by a small pinhole, and the resulting wave encounters two small slits. The emerging light interferes and is detected at the screen. (B) Same as above, but in slit B a phase delay of π is introduced. Notice that this delay shifts the intensity pattern on the screen from a maximum to a minimum, and vice versa.

screen changes, and the amount of light reaching the fixed detector changes from being a maximum to being a minimum. This principle could be extended to a molecular system, where the phase delay can be used to control the excitation of a particular quantum-mechanical state, provided two optical pathways connect the initial state to the final state. In this review, we present a number of experiments that fit this general description, namely, the interference between two or more pathways allows one to control the outcome of laser−matter interactions.

A number of nonlinear optical processes could also be considered important in a review on coherent control—given the broad definition of the field as being any experiment that takes advantage of the coherent properties of light to control processes by constructive and destructive interference. Nonlinear optical experiments have been performed since the laser was invented.[33−36] In all these cases, electromagnetic fields are combined coherently to generate new polarizations in the sample through interference. Here, we review some of the principles and then concentrate on recent experiments carried out expressly to demonstrate coherent control.

The combination of two or more electromagnetic fields can be used to introduce constructive and destructive interference in the sample, thereby achieving coherent control of population transfer. Coherent control, therefore, can be defined as the ability to control optically driven processes, using the coherent properties of lasers and/or the sample. In most cases, optically driven processes imply nonlinear optical processes. Coherent-control strategies, in some cases, can achieve 100% contrast between two outcomes by small adjustments in the phase of the field. An incoherent strategy, on the other hand, depends on the specific wavelength of excitation or on the secondary processes occurring after the laser−sample interaction.

We begin by defining coherence and its different manifestations. Coherence, a property of waves, defines the degree with which waves are in step with each other. Spatial coherence is defined as the degree with which waves remain in step in space, across a beam, or in the region where two or more beams cross. Coherence time is the time it takes waves to lose their coherence. The coherence of a quantum-mechanical system refers to the extent with which two or more of its constituent states remain in step. In the absence of intermolecular interactions, coherence can persist in a molecule for a long time, and a coherent light source can be used to manipulate this coherence with great efficiency. This review includes a number of experiments that have successfully exploited this simple concept.

In addition to defining the coherence of the light source, it is important to define the type of coherence that can be induced on a sample. The polarization that electromagnetic waves induce on a sample, i.e., the induced electronic polarization, is short-lived, except when the field is resonant with a spectroscopic transition. Laser pulses with duration shorter than the inherent molecular dynamics of the system impulsively excite coherent superpositions of quantum-mechanical states such as rotations and vibrations, which are observable as coherent wave packet dynamics. For example, the short pulse resonant excitation of gas-phase iodine molecules leads to the creation of coherent superpositions of vibrational states in the ground and excited states. The ensuing oscillatory motion in both states can be recorded by the interactions of one or more additional laser pulses. Molecular coherence is usually considered an intramolecular property; however, it is possible to induce macroscopic (intermolecular) coherences in a sample. This type of coherence plays an important role in four-wave mixing (FWM) experiments. The fundamental goal of laser control is to find the electromagnetic field, which through its interaction with the sample causes specific excitation of quantum states, or manipulates molecules so that they form or break specific chemical bonds. In particular, for coherent control, the goal is to achieve the desired outcome by taking maximum advantage of the phase in the electromagnetic field and the quantum-mechanical phase of the sample.

In this review, we present a number of approaches that have been proven experimentally successful so that we may glean from them the most important parameters required for control. We illustrate each of the main strategies with the description of one or more relevant experiments. We include a table listing additional experiments using the same general tactic being applied to a number of different systems. The review is structured as follows: Section 2 presents an overview of experimental tools available for coherent control experiments, from laser sources to phase-control systems and methods of registration. Section 3 presents a summary of control experiments with narrow bandwidth lasers. Section 4 presents a summary of experiments with femtosecond pulses, in which we include one- and two-pulse methods, involving timing and phase changes for coherent con-

trol. Section 5 presents a summary of experiments, based on FWM, that take advantage of optical as well as molecular coherence to control the signal that is observed. Section 6 is reserved for a review on particular challenges in the field of coherent control, foremost among these concerns is control of chemical reactions. We discuss separately some of the aspects that have prevented laser control of chemical reactions, such as coherence dephasing and energy redistribution. In conclusion, Section 7 covers some of the future applications that are likely to derive from the field of coherent control.

2. Experimental Methods

Here, we give a brief presentation of some of the most modern experimental instruments for coherent control. We emphasize the experimental requirements for coherent control studies. Particular attention is placed on phase locking of different beams. Femtosecond sources are discussed more fully, although a number of systems are already commercially available. We outline the most important characteristics that should be considered when planning coherent control experiments with these sources. The attention to detail and didactic style of this section is intended to highlight the importance of studies in coherent control where all the relevant parameters, such as laser pulse characteristics, need to be accurately and thoroughly determined. We have also included a section on very advanced laser systems that are not commercially available but, we believe, could play an important role in coherent control in the future.

2.1. Laser Sources

2.1.1. Nanosecond and CW Laser Sources

Various narrow bandwidth laser sources are commercially available. These laser systems range from very small laser diodes to very large excimer-pumped dye lasers. Coherent control schemes based on narrow bandwidth sources depend on tunability, frequency stability, and intensity stability. Solid-state diode lasers provide the highest stability and resolution. They also provide limited tunability over specific regions in the spectrum. For coherent control schemes that entail multiphoton excitation, high-peak intensities are required; continuous wave diode lasers are not suitable for those applications. Pulsed YAG or excimer nanosecond laser sources are employed directly or as pumps of tunable laser sources that are then used in those coherent control experiments.

Long-range wavelength tunability in nanosecond systems is presently achieved with dye lasers or with the more modern solid-state optical parametric oscillator. The more advanced systems include active stabilization of the frequency and can provide millijoule pulses at the desired frequency.

A number of coherent control experiments require the phase-stabilized combination of two different laser pulses. In general, these experiments include the fundamental frequency ω_0, and its second or third harmonic with frequency $2\omega_0$ or $3\omega_0$, respectively. This combination can be easily achieved by having both the fundamental and its harmonic propagating collinearly into the experimental setup. For improved phase stability, the fundamental and its harmonic are not separated into different optical paths. Additionally, the time delay introduced by the harmonic generation crystal ($\sim$10 ps) is negligible compared to the duration of the pulses ($\sim$1$-$10 ns). In the beam path, a gas cell is used to introduce a frequency-dependent time delay. This delay can be accomplished by regulating the pressure in the cell. The wavelength-dependent refractive index of the gas provides a delay between the two incident beams that varies linearly with pressure. For example, a 2π phase delay between ω_0 (336 nm) and $3\omega_0$ (112 nm) required a pressure difference of 0.51 ± 0.02 Torr or 0.43 ± 0.01 Torr in a 46-cm cell filled with H_2 or Ar, respectively.[37] The experimental implementation of this type of phase delay has been shown to provide excellent phase stability.[37]

2.1.2. Femtosecond Laser Sources

Femtosecond laser sources with a wide range of parameters are commercially available from a number of companies. The majority of the models utilize the titanium sapphire laser medium. Their pulses, centered at 800 nm, have durations that range from 20 to 200 fs and their pulse energies range from 1 nJ to 1 J. Other femtosecond lasers available are erbium-doped fiber lasers, used primarily for communications because of their wavelengths at 1.5 μm, the chromium fosterite lasers with a wavelength centered at 1.26 μm, and the ytterbium doped lasers with a wavelength centered at 1.04 μm. The availability and long-term stability of these systems, particularly that of Ti:Sapphire lasers, has permitted the construction of very sophisticated equipment for tuning, shaping, and characterizing their pulses. Here, we focus on the most critical parameters required for coherent control experiments.

For a review on the principles of ultrafast laser pulse generation, the reader is referred to a number of excellent and timely reviews in print.[38$-$43] Here, we concentrate only on the main characteristics that are essential for coherent control experiments, namely, pulse-to-pulse stability, pulse duration, coherence, wavelength, and phase homogeneity. Pulse-to-pulse stability limits the precision with which one can estimate the effect of a particular control experiment. Intensity variations have a detrimental effect on the statistical evaluation of an experiment. For an nth-order nonlinear optical experiment, the average value obtained after N measurements on a signal, where fluctuations are of magnitude $\pm\sigma$, is determined by $\pm n\sigma N^{-0.5}$. Given that most coherent control experiments involve nonlinear excitation, it is important to keep σ as small as possible. Pulse duration is of importance for two major reasons. For many experiments, it is important to excite on a time scale that is short with respect to the dynamics of the system. Among the relevant dynamics, we mention rotational (1$-$100 ps) and vibrational motion (10 fs$-$1 ps), intramolecular energy randomization (0.5 ps $-$ 1 ns), electronic dephasing (10 fs $-$ 10 ns), and bond

cleavage or formation (50−500 fs). Pulse duration also determines the bandwidth of the pulse, because of the inverse relation between the two. Bandwidth is important, because it determines what quantum-mechanical states can become resonantly accessible to the laser pulse at the one-photon level as well as at the multiphoton excitation levels. This is of particular importance at relatively low powers of excitation. For high-power excitation, the electric field interaction is very strong, and resonant excitation becomes of secondary importance.

The coherence of the laser pulses is of great importance. For continuous-wave lasers, one is concerned with the coherence length, which is inversely proportional to the bandwidth. When femtosecond pulses are used for coherent control, the concern is to what extent the phases of the different frequencies in the bandwidth can be defined by a deterministic function. For example, if the spectral phase can be described by a quadratic function of the frequency, an optical arrangement consisting of a pair of prisms or gratings can be used to eliminate the phase distortion and render a pulse in which all the frequencies are in step. This parameter can be determined by finding the time-bandwidth product of the pulse, i.e., the product between the full-width at half-maximum (FWHM) of the pulse spectrum and pulse duration, provided the pulses are not phase modulated. This measurement, when made on pulses with spectral and temporal profiles that resemble Gaussian functions, and in the absence of phase distortions, should approximate the transform limit $\Delta\nu\ \Delta\tau_{TL} = (2/\pi)\ln 2$. The transform limit implies that all of the frequencies in the bandwidth are in step, and the pulse is as short as possible. Transform-limited (TL) pulses are the ideal starting point for coherent control experiments. With pulse shaping technology, it is possible to prepare pulses with small phase distortions when $\Delta\tau/\Delta\tau_{TL} \approx 1.001$. Non-TL pulses have phase deformations that, in some cases, cannot be compensated and could be detrimental in a coherent control experiment. The center wavelength, or carrier frequency, of the pulse is of importance for experiments in which resonant excitation of a specific transition is desired. Stability of the carrier frequency and phase will be discussed in the next section.

Last, we need to address spatial homogeneity in the laser pulse. It is quite common that a laser pulse will emerge from a system with phase or frequency inhomogeneities across the mode. This type of distortion is very common in laser systems using prisms for pulse compression. Frequency inhomogeneity across the laser front can be detected by carefully acquiring spectra at various positions across the beam. If a frequency shift is detected, it implies that the laser pulse is composed of a number of different subpulses with different characteristics. This type of distortion, known as spatial chirp, can be misleading in coherent control experiments. The overall bandwidth of these laser pulses is always greater than the transform limit. This problem can be overlooked if pulse characterization uses only a small portion of the beam profile, for example, when an iris is used as an aperture. Spatial chirp can usually be corrected by careful positioning of the prisms at their minimum deflection angle in the oscillator and the pulse compressor. Phase inhomogeneity, or front-phase distortions, refers to spatial deformations of the phase front. These distortions usually result from defective optics, from having the laser reflect from an edge of a dielectric mirror, or from faulty positioning of compression prisms. Front-phase deformations are easiest to detect by interferometry. More on pulse characterization is given in Section 2.5.

2.1.3. Advanced Laser Sources

So far, we have considered laser systems that are commercially available or that require minor user modifications. There are more advanced laser sources available that require customized construction at very large facilities. In the realm of facility laser sources, we mention the Deutsches Elektronen Synchrotron (DESY) laboratory in Hamburg and the Stanford Linear Accelerator Center (SLAC) in California. Both of these laboratories are partners in the construction of free-electron laser sources producing femtosecond X-ray laser beams. These facilities will generate intense X-ray laser light ranging from wavelengths of 10 nm down to 0.1 nm, with pulses lasting just 50−500 fs. These sources provide wavelengths that are very difficult to obtain from tabletop systems. It is hoped that the achieved brightness, stability, and coherence will make them ideal for coherent control experiments.

A second type of advanced laser source is the carrier phase locked laser system. In this type of laser, all the pulses have a fixed carrier frequency and are phase locked with great stability.[44−52] This type of phase stability is most important for very short pulses. In Figure 2, we show the calculated electric field for 5.4-fs pulses from a titanium sapphire laser with a different common phase. For these very short pulses, the phase is very important in determining the maximum amplitude of the field. Until recently, control of the common phase as shown in Figure 2A,B was not possible. Synchronization and phase-locking of separate femtosecond laser systems have been demonstrated experimentally.[49] The data shown in Figure 2C present a pulse obtained from the coherent addition of two pulses from different femtosecond oscillators operating at slightly different carrier frequencies.[49] When the two lasers are not phase locked or synchronized, the autocorrelation shows the same interference pattern but a much broader temporal envelope. Absolute phase stability is also of great importance, if one wants to use subsequent pulses from an oscillator for coherent control. In a typical experiment, beam splitters are used to produce synchronized laser pulses that can be phase locked using actively controlled optical paths.[50] The pulses are typically separated by 10 ns, yet they all have the same phase.

Another approach is to broaden the output pulses to produce a broad spectrum that contains an octave, for example, an 800 nm pulse that has some amplitude at 532 nm and at 1064 nm. The 1064 nm light is frequency doubled and interfered with 532 nm light. Stabilizing the interference between these two beams stabilizes the phase.[46]

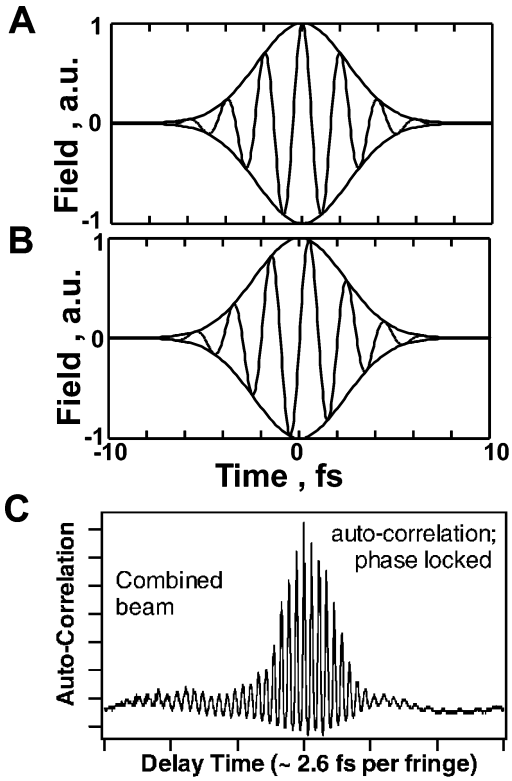

Figure 2. Interferometric autocorrelation (calculated) for 5.4-fs pulses. The electric field is shown with a carrier phase of 0 and $\pi/2$ in panels A and B, respectively. (C) Second-order autocorrelation measurement of the combined pulse. When two lasers are both synchronized and phase-locked, the second-order autocorrelation data show the pulse width is narrowed and pulse amplitude increased by >20% (Reprinted with permission from ref 49. Copyright 2002 Springer-Verlag).

These sources can be used to achieve perfect constructive interference. This aspect of perfect constructive interference has been shown to be useful in the construction of an amplifier in which there is no gain medium. The principle of operation depends on the coherent addition of phase-locked pulses. This principle can be used to synchronize pulses with different carrier frequencies and may eventually be used to produce sub-femtosecond pulses.[1−3,5,6,49] Phase stabilization requires a means to detect the carrier frequency and phase of the pulses.[51,52] This information is used inside a feedback loop to control positioning devices inside the laser cavity. On the basis of this idea, one can synchronize and phase lock femtosecond pulses from one or more laser systems. In Section 4.2, we discuss a number of experiments that have implemented active phase locking for coherent control.

2.2. Wavelength Tuning of Short Pulses

A number of nonlinear optical processes, such as second harmonic generation (SHG), continuum generation, and noncollinear optical parametric amplification, are used to prepare ultrashort pulses at different wavelengths. These nonlinear processes can be strongly affected by the phase distortions on the pulse. Here, we give some practical rules on frequency conversion for coherent control experiments.

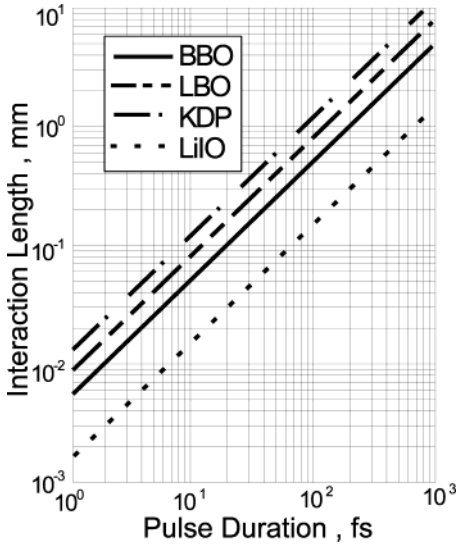

Figure 3. Dependence of the interaction length (maximum crystal thickness) on pulse duration for four different commonly used SHG crystals. Data for the plot were obtained from www.eksma.lt.

Frequency doubling is one of the most common methods used for obtaining femtosecond pulses at a different wavelength; it also plays an important role in phase characterization. Therefore, it deserves special attention. The first and most important aspect in frequency doubling is that the conversion efficiency increases with the square of the thickness of the doubling crystal.[33,53] However, the bandwidth over which phase matching can be achieved decreases with its thickness. This is because of phase−velocity mismatch. For a monochromatic pulse, the mismatch caused by the difference in the refractive indices of the fundamental and the second harmonic is eliminated by crystal orientation (phase-matching condition) to achieve $(n_e(2\omega_0) - n_o(\omega_0) = 0)$. For short pulses it is impossible to eliminate the mismatch for all spectral components within their broad bandwidth.[54] The interaction length over which SHG conversion takes place is defined by $L = \tau/\delta v$, where τ is the pulse duration and δv is the group−velocity mismatch between the fundamental (v_f) and the second harmonic (v_{SHG}), given by $|1/v_f - 1/v_{SHG}|$. The interaction length should be considered the maximum crystal thickness that can be used to avoid temporal broadening and spectral narrowing of the pulses. This parameter is plotted as a function of pulse duration for some of the most common SHG crystals in Figure 3. The interaction length depends on the crystal and the incident wavelength; here, we assume frequency doubling of 800-nm pulses. Fortunately, the efficiency of SHG increases as the pulse duration decreases, allowing for efficient SHG from very short pulses, ~10 fs, with crystals that are only 20−50 μm thick. For pulses that are shorter than 10 fs, there are additional parameters of concern, which reduce the conversion efficiency of bluer wavelengths. Baltuska et al. have studied SHG with single optical cycle femtosecond pulses.[55] They concluded that a 10 μm thick BBO crystal, cut for Type I phase matching at 700 nm, is a good compromise for frequency doubling a 5-fs pulse centered at 800 nm.

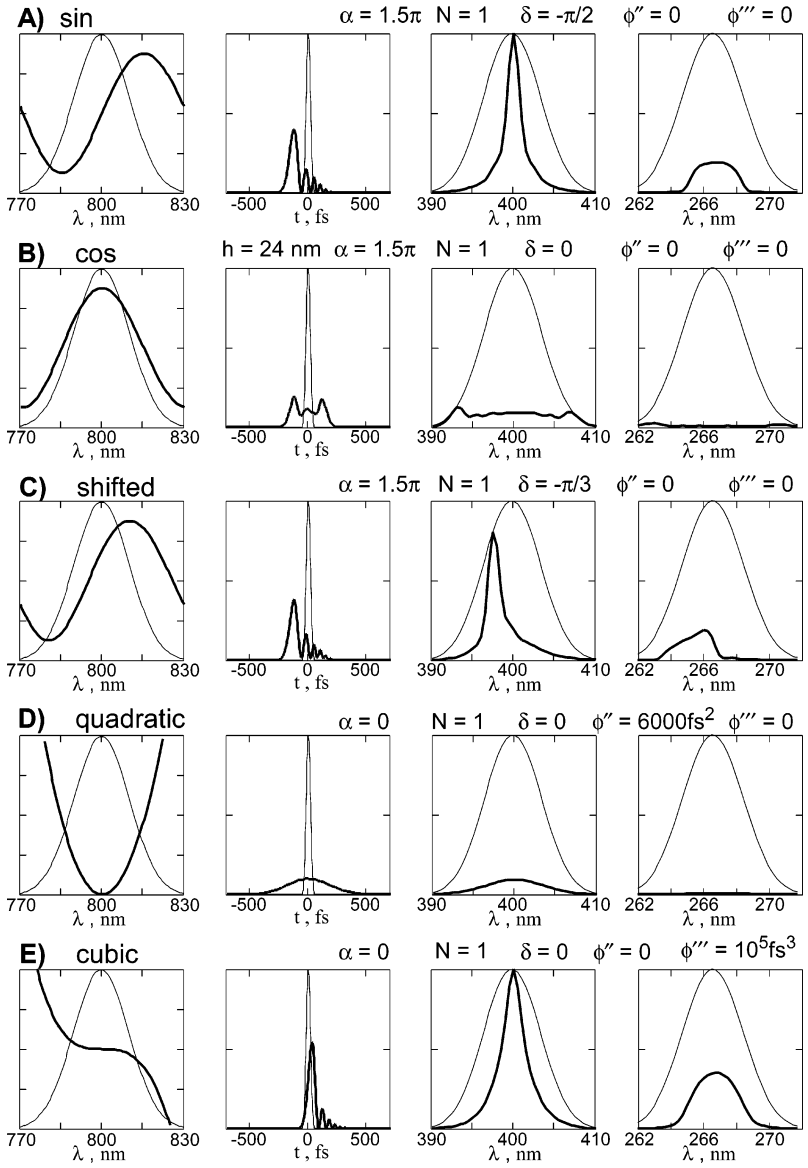

Figure 4. (A−E) Effect of phase modulation on the temporal intensity and second and third harmonic generation spectra (calculated). The first column shows the spectrum of the pulse and the spectral phase (thick line) as a function of wavelength. The second column shows the intensity of the field as a function of time for TL and shaped pulses (thick line). The third and fourth columns show the second- and third-order nonlinear power spectrum of the laser for TL and shaped pulses (thick line), respectively. (Reprinted with permission from ref 61. Copyright 2003 American Institute of Physics.)

Frequency doubling depends also on the spectral phase of the pulses. It is important to note that, if one desires phase modulated pulses at a frequency that is to be obtained by frequency doubling, it is not a good practice to modulate the phase prior to SHG. The main reason for this is that the SHG spectrum is intimately dependent on the spectral phase of the fundamental. This dependence has been studied by a number of groups.[56−62] In general, phase modulation can be expanded in a Taylor series given by

$$\phi(\omega) = \sum_{n=0}^{\infty} \frac{1}{n!} \left| \frac{d^n \phi(\omega)}{d\omega^n} \right|_{\omega=\omega_0} (\omega - \omega_0)^n \qquad (1)$$

The first- and second-order terms affect the common phase (important only in pulses with less than three optical cycles) and the overall time delay. The second-order term affects the intensity of the SHG that is detected, but it does not affect the spectrum of the pulse. Higher-order terms do affect the spectrum of the shaped pulse after SHG. The effect of specific phase functions on the second- and third-order nonlinear power spectrum of the pulse are illustrated in the third and fourth columns of Figure 4, respectively. The pronounced changes in the SHG and THG spectra shown in Figure 4 highlight the importance of accurate phase characterization for all experiments involving multiphoton transitions. When phase modulation is required at a wavelength that corresponds to the second harmonic of the laser and it cannot be easily accomplished with the available optics, then phase modulation can be done on the fundamental, and the fundamental can be upconverted by a second TL pulse. One must take into account that the shaped pulse can be several times longer than it was prior to phase shaping, and the amplifying pulse intensity should not vary considerably during this time. There-

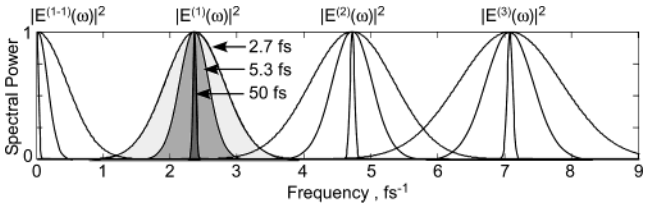

Figure 5. Calculated power spectra for 800-nm Gaussian pulses with pulse duration equal to 2.7 fs (one optical cycle), 5.3 fs (two optical cycles), and 50 fs (19 optical cycles). In addition to the fundamental spectrum (shaded), we show the power spectra responsible for two-photon excitation $|E^{(2)}(\omega)|^2$ and three-photon excitation $|E^{(3)}(\omega)|^2$. In the spectral region between 0 and 1 fs^{-1}, we show the rectification spectrum responsible for Raman transitions. Notice that single-cycle pulses can be used to excite transitions anywhere in the spectrum.

fore, it is important that the second pulse be at least 10 times longer (and consequently narrower in frequency) than the shaped pulse.

Noncollinear optical parametric amplification (NOPA) is a method that has close similarities to frequency doubling.[63−65] In NOPA, the seed pulse is generated by continuum generation, and this provides a very wide spectrum that can be used to produce extremely short pulses. The seed pulse is amplified by a more intense pulse that overlaps the seed pulse in the nonlinear optical crystal. The NOPA has been used to produce pulses as short as 4 fs[66−68] and has also been used to generate and amplify shaped pulses.[69−71]

The need for wavelength tuning decreases with pulse duration. A short laser pulse may induce linear excitation and nonlinear processes such as two- and three-photon excitation and Raman transitions. As the bandwidth of the pulse increases, a wider range of the spectrum can be accessed by the pulse by either linear or nonlinear transitions. A typical amplified titanium sapphire laser system produces 50-fs pulses and is centered at 800 nm; this pulse has 19 optical cycles within the FWHM and has a 20 nm spectral width (312 cm^{-1}) and covers only a small portion of the electromagnetic spectrum between 0 and 12 500 cm^{-1}. To understand how, through nonlinear transitions, an ultrashort pulse can cover a wide range of the electromagnetic spectrum, the reader is referred to Figure 5, where multiple harmonics of the fundamental pulse are plotted. The laser pulses that can be generated from an ultrashort pulse titanium sapphire oscillator are 10 fs in duration and give five times greater coverage with a concomitant advantage for coherent control. For a titanium sapphire laser pulse to have 100% overlap over the entire spectrum, one would need single cycle, 2.67-fs pulses FWHM, as shown in Figure 5. The shorter the pulses are the greater the probability for nonlinear excitation and the greater the overlap to a number of electronic transitions. In principle, with a single optical cycle pulse, one can reach any spectroscopic transition in the spectrum. It is important for one to have the means to enhance the desired transition while suppressing the others. This goal is addressed in Section 2.4, and from this discussion the importance of pulse duration for coherent control should be clear. Until recently, most of the experiments in coherent control have used pulses that are more than 40 optical cycles long FWHM, and only a few groups have used laser pulses with significantly shorter pulses. In conclusion, the flexibility afforded by ultrashort laser pulses has yet to be harnessed by coherent control experiments.

2.3. Methods of Registration

For every experiment in laser control, it is important to determine the most appropriate method to monitor progress. Some methods of registration offer single-ion detection capabilities, others offer spectroscopic information that can be used to learn more about the control pathway, and still others offer a number of discrimination tactics that ensure only the desired signal is analyzed without contamination. Here, we will explore successful experiments in control, using multiphoton-induced fluorescence, FWM, and charged-particle detection.

2.3.1. Absorption and Fluorescence

Absorption and fluorescence are well-known spectroscopic methods that can play an important role in probing the progress of control strategies. Absorption is difficult to measure due to the significant background inherent in the measurement. In condensed phase samples, lock-in amplification can be used to measure, with confidence, absorption on the order of 10^{-4} of the incident beam. Laser-induced fluorescence is a much more sensitive method that can detect signal from 10^3 molecules in the sample region, and, with photon-counting equipment, even from a single molecule. Dispersed fluorescence spectra carry information about the final state (electronic, vibrational, and rotational) of the molecules and has played an important role in femtosecond pump−probe experiments.

2.3.2. Four-Wave Mixing (CARS, CSRS, PE, and TG)

FWM methods implicate the coherent interaction of three different waves to produce a fourth wave that corresponds to the output. Because the interactions must be phase coherent, these types of experiments are advantageous for carrying out coherent control experiments that involve sequences of pulses. In the most general implementation, three separate laser pulses impinge on the sample at different angles, as shown in Figure 6. The signal emerges at the phase-matching direction given by a linear superposition of the wave vectors of the incident beams. FWM experiments have the advantage that one can discriminate the output signal in frequency, time, and space. This leads to very clean signals that depend on the input pulses and their phase.

There are a number of experimental setups for carrying out FWM measurements. In Figure 6, we show a number of such setups involving two or three different laser pulses in a collinear, planar, or three-dimensional arrangement. As mentioned above, the signal beam, in FWM experiments, results from the linear combination of the three incident waves. Energy conservation requires that $\omega_{out} = \pm \omega_1 \pm \omega_2 \pm \omega_3$. Similarly, momentum conservation requires

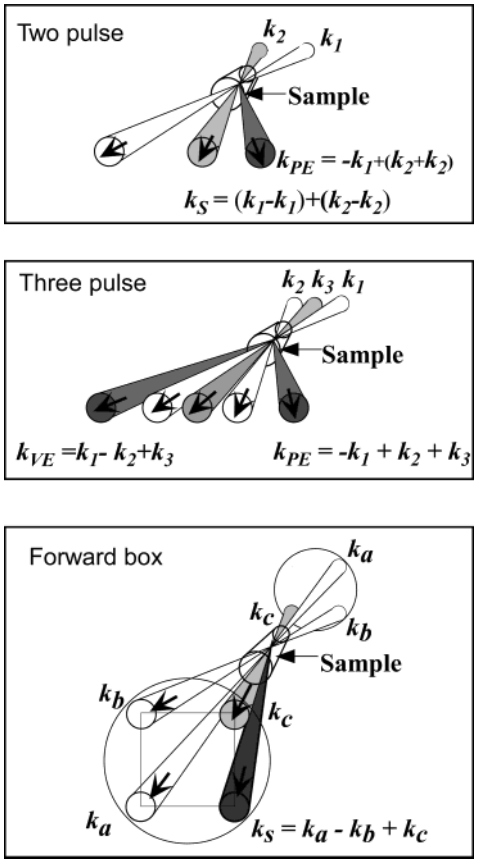

Figure 6. Different geometries and phase-matching angles for FWM experiments. (Reprinted with permission from ref 19. Copyright 2000 Wiley-VCH.)

that $k_{out} = \pm k_1 \pm k_2 \pm k_3$. The coherent addition of the three waves results in third-harmonic generation, a special case of FWM. In most cases, however, the output corresponds to sums and differences. Each of the cases receives a special name, even though they arise from the same principle.

In general, the FWM methods are recognized by their phase-matching condition as follows: when $k_{out} = k_1 - k_2 + k_3$, the measurements are recognized as transient grating (TG) for off-resonance excitation or virtual echo (VE) for resonance excitation, and $k_{out} = -k_1 + k_2 + k_3$ is known as photon echo (PE). When pulses of different frequencies are used to match Raman transitions, the measurements are known as coherent Stokes Raman scattering (CSRS) and coherent anti-Stokes Raman scattering (CARS). Both of these methods follow the same phase-matching conditions outlined above.

In FWM experiments, the input beams, as well as the output signal, are coherent. For CARS and CSRS experiments, it is possible to select the input wavelengths such that the output beam has a distinct wavelength that can be isolated by dispersion. In these cases, a spectrometer or a simple prism can be used to isolate the signal beam. When the input pulses are degenerate (same wavelength), it is important to use a setup that isolates the output beam in space. This can be easily accomplished because of the phase-matching condition. In Figure 6, we showed some of the typical arrangements used in FWM. The two most common arrangements are two-pulse FWM, where the directions for TG and PE are different, and the forward-box geometry,[72,73] where both TG and PE coincide. The simplicity of the two-pulse setup is that one of the pulses acts twice on the sample; however, this reduces the number of controllable parameters. In the forward-box geometry, one is able to control the frequency and time for each of the pulses and, with this control, the type of signal that is detected at the phase-matching geometry.[74,75]

The advantage of FWM experiments over collinear pump−probe experiments is that the signal is coherent (similar to a laser beam) and corresponds to the coherent interaction of three waves with the sample. No active or passive locking of the phase among the different input laser beams is required to maximize coherence, nor is a lock-in amplifier required to filter out the incoherent contributions to the signal. To illustrate why the signal arises from the coherent interaction of the incoming beams, we analyze a TG experiment in detail. All the observations we make for this case can be easily extended to the other pulse sequences, because they are all based on the same principle. In a TG experiment, the first two beams cross at the sample and create an interference grating. The spacing of the interference is given by the crossing angle and the wavelength of the incoming beams. This spacing d can be calculated using formula $d \approx \lambda/\alpha$, where λ is wavelength and α is a small angle (radian) between the two beams. The third beam, as it interacts with the transient grating in the sample, undergoes Bragg diffraction and is scattered toward the phase-matching angle where the detector is placed. As indicated earlier, this coherent interaction is achieved without the need for active or passive phase locking of the three beams.

The position of the grating fringes in space depends on the relative phase between the first two beams. Changes in their relative phase affect the absolute position in space of the grating, but the grating characteristics are not changed. The third beam is diffracted toward the phase-matching direction, which is determined by the fringe spacing, not by the position of the fringes in space. Note that the phase of the signal beam is affected by the relative phase of the other beams. Phase-sensitive detection of the output beam requires phase locking of two pairs of beams: the first two beams, and the third and fourth beams. The fourth beam (also known as the local oscillator) is used to analyze the phase and amplitude of the coherent signal emission. Phase locking among all four beams is not required. The Jonas group has done very accurate phase sensitive detection of FWM.[76−79] In general, FWM experiments are ideal for testing some coherent control strategies, because the signal results exclusively from the coherent interaction of the three beams with the sample.

2.3.3. Ionization and Mass-Spectrometry

Ion detection coupled to a time-of-flight mass spectrometer (TOF-MS) can be used to provide mass discrimination, an important advantage for experiments in which breakage of different chemical bonds produces different fragment ions. This detection method is capable of single-particle sensitivity. Some

of the most successful coherent control experiments have taken advantage of the fact that TOF ion detectors collect a number of ion masses concurrently, providing the yield of different product ions resulting from multiple dissociation pathways, every laser pulse.

The TOF-MS has a few drawbacks that need to be considered when designing a control experiment. First, this method is best used under low-pressure conditions (10^{-6} Torr) typically achieved in molecular beams. The method is not practical for liquid-phase experiments. Second, the method requires ionization, and unless the goal of the control target is to produce a particular ion, and not a neutral molecule, the ionization process itself can be misleading. Consider an experiment in which selective bond cleavage (for example ABC → AB + C) is desired. The ideal setup would be able to detect the percent of desired products over the total yield. By detecting only ions (C^+, for example), we lose information about the neutral species. We also have no information on how the fragment ions were formed. One would like to think that the desired fragment ions were generated by selective bond cleavage followed by prompt ionization; however, fragment ions could be generated as a result of fast ionization (ABC^{*+}) followed by fragmentation, a pathway that does not involve the neutral species at all. However, there is a possibility that fragment C was formed as a neutral species and its ionization is phase dependent as well, further complicating the observed solution.

To follow bond-selective cleavage, resulting in neutral fragments, a very general ionization step is needed after the interaction of the sample with the laser field. For example, after the control laser field, a VUV laser pulse could be used to monitor the total yields of all species and to determine percent yield of the desired product. It is important to note that the TOF-MS provides only mass-over-charge information about the products. For example, the signal from O_3^{3+} would coincide with that of O_2^{2+} and that of O^+. No information is revealed about the structure of the ions that are collected, preventing one from determining the bond-breakage pattern that leads to a specific mass-over-charge signal, or the atom−atom connectivity, which could be useful in establishing the structure of the product.

There are other more subtle shortcomings of the TOF-MS when used for coherent control experiments. One of the most important is the intensity gradient near the focus of the beam and the dependence of multiphoton ionization on the intensity of the laser. In Figure 7, we show regions of equal intensity near the focus of a perfect Gaussian beam. The lines are drawn for every 10% change in the intensity of light. Under strong field excitation, the sample molecules, dispersed in different regions, will yield different signal ions because of the changes in the local intensity. Avoiding such intensity differences requires no focusing or mild focusing of the beam and the use of a top-hat spatial mode with a flat intensity distribution instead of a Gaussian transverse mode. Intensity changes in the ion detection chamber can be reduced with a slit that limits the passage of ions to those that come from a narrow region where the laser is focused on the sample. Ideally, the sample is introduced as a skimmed molecular beam and the laser interrogates the sample at right-angle geometry.

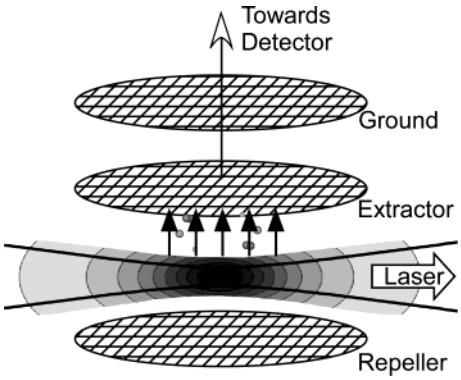

Figure 7. Spatial intensity variations near the focal region during multiphoton ionization experiments. Under high intensities, different regions produce different product ions.

A number of different charge-particle detection methods are more powerful than mass spectrometry. Photoelectron spectroscopy, where the electron being ejected during ionization is detected and its energy is resolved, is one such powerful method. Photoelectron spectroscopy has already been used in some coherent control experiments.[80−92] In all cases, the spectroscopic information provided by the method has been essential for the proper interpretation of the result. Coincidence ion-imaging methods, as introduced by Continetti and Hayden,[93−97] can provide valuable information about photodissociation dynamics. Their incorporation into coherent control experiments would be a very powerful addition, and enable better mechanistic interpretation of the results.

2.4. Pulse Shapers

One of the most important technical developments in the field of coherent control is the pulse-shaping apparatus.[98−103] Originally introduced by Weiner, Heritage and Nelson,[98,104] the initial purpose of the pulse shaper was to eliminate phase deformations in the pulse to achieve TL pulses. Pulse shapers have been reviewed elsewhere;[100] here, we concentrate on the most important experimental parameters for laser control experiments.

In simple terms, the role of the pulse shaper is to advance or retard individual frequencies within a laser pulse. For example, in a TL pulse, all the frequencies are locked and have a net zero retardation. In this case, the spectral phase is flat. The pulse shaper can be used on a TL pulse to make some frequencies arrive before others. In these general terms, a pulse shaper can be defined by a number of parameters: input bandwidth, frequency resolution, and maximum retardance. The spectral resolution of a pulse-shaper setup is determined at the Fourier plane, where the pulse is resolved in the frequency domain. The phase retardation must be calibrated and checked for accuracy and reproducibility.

In Figure 8 we present the typical design of a pulse shaper showing the 4*f* configuration.[100] This arrange-

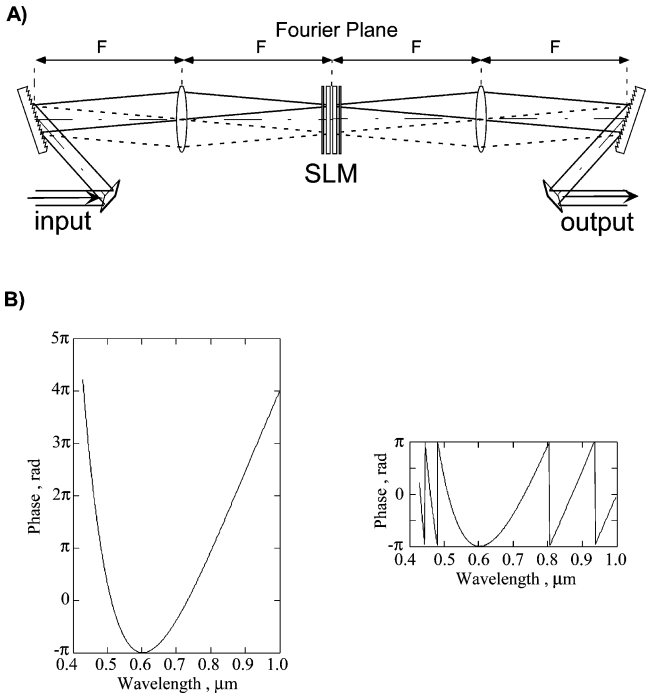

Figure 8. (A) Schematic design of a 4f pulse shaper, using diffraction gratings and spatial light modulator. (B) Wrapping of optical phase: left, unwrapped phase; right, wrapped phase. A spectral phase that enters from $-\pi$ to 4π (left) can be reproduced by a "folded" phase from $-\pi$ to π (right).

ment is also known as the zero-dispersion compressor. The main elements are dispersion gratings, collimating lenses, and the phase-retardation unit, which, in this case, is a liquid crystal spatial light modulator (SLM). The SLM unit is located at the Fourier plane of the shaper. As mentioned above, at the Fourier plane, the pulses are spread into their frequency components where each can be delayed separately. Experimentally, spatial light modulators have a finite resolution that is determined by the number of individual liquid crystal elements (pixels) and the optics that disperse the spectrum over the SLM. The liquid crystal is birefringent; therefore, depending on the polarization of the incoming light, a voltage can introduce pure phase retardation or a combination of phase retardation and polarization rotation. Both types of SLM systems are used for pulse shaping, as described below. For a laser pulse centered at 800 nm and pulse duration of 20 fs, the full spectrum spreads from 750 to 850 nm. If that spectrum is spread over the central 100 pixels of a 128-pixel SLM, then the resolution is limited by the SLM to ~1 nm per pixel. However, the optical setup can further reduce the spectral resolution. The key parameter for determining the optical resolution is the focal spot size that is projected by the lens across the SLM. A typical setup, with an input beam 5 mm in diameter, grating having 600 lines per millimeter, and 300 mm focal length lens, projects a spot size of 60 μm on the SLM. A typical SLM pulse shaper has 100 μm-pixel width; seemingly, the lens choice is correct. One should be careful of the thickness of the SLM. The dual-mask SLM, for example, is very thick; the spot size 10 mm away from the focus, in the example above, is 170 μm. The resulting value is excessive, thus reducing the effective optical resolution by almost a factor of 2. To preserve the spectral resolution, one must use a different optical arrangement with greater confocal parameter. Using a 500-mm focal length lens, the diameter at the focus is 100 μm, and 10 mm away is 108 μm. This optical setup would preserve the ~1 nm spectral resolution.

The input bandwidth of the shaper should be sufficient to accommodate the bandwidth of the laser pulses. Lenses are appropriate for shaping pulses 50 fs or longer; chromatic aberration prevents their use for shaping shorter pulses. Grating pairs have been used successfully to shape pulses as short as 20 fs,[105] but for shorter pulses gratings are too dispersive, and it is advantageous to use a setup that is less dispersive. Prisms are about an order of magnitude less dispersive than gratings and provide an excellent alternative to gratings for shaping ultrashort pulses. Prism pair compressors have been used down to sub-10-fs pulses. [106]

The frequency resolution of the pulse shaper is determined by the number of pixels in the SLM, as described above. Frequency resolution plays two different roles. First, one can think of frequency resolution in the time domain. Because of the Fourier transform relation between spectral and time resolution, the higher the spectral resolution, the longer the pulses that can be produced by the pulse shaper and the higher the finesse with which one can control narrow frequency resonances in the sample. This is of particular importance for samples that have narrow resonances, like gas-phase systems. The frequency resolution also plays a role in shaping experiments that require broad and smooth phase functions. If the pulse shaper has a limited number of pixels, then the resolution is restricted and the function is jagged. This limitation places unwanted distortions in the spectral phase.

Pulse shapers are also defined by the maximum retardance that can be introduced by the shaping element. Typically, liquid crystal SLM systems provide retardance equal to 4π. The systems that provide the greatest retardance are those based on acousto-optic modulators, capable of an order of magnitude greater retardance. In theory, only 2π retardance is required, because the phase can be folded (distributed into separate $0-2\ \pi$ segments) to produce any type of total retardance (see Figure 8B). Experimentally, folding the phase has two principal limitations. The abrupt phase changes required for folding can introduce additional unwanted modulation into the pulse, and the finite resolution of the shaper prevents clean phase jumps from one pixel to the next.

When the optical axis of the liquid crystal mask is oriented at a 45° angle with respect to the polarization of the incident electric field, polarization rotation is introduced in addition to retardance. When two such SLM units are lapped back-to-back and in opposite angles of rotation, and they are flanked by input and output polarizers, one can control phase and amplitude of the transmitted light.[107−109] In Figure 9, we show how the double-mask SLM unit works. A light incident from the left goes through a polarizer and then transmits through the first liquid

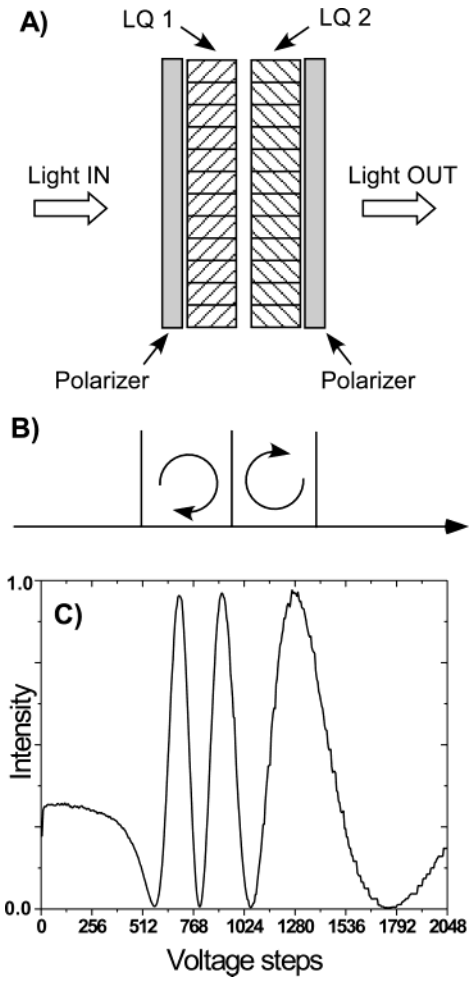

Figure 9. (A) Schematic of an SLM-256 (CRI, Inc.) amplitude/phase mask. (B) The electric field's polarization rotates in each of the liquid crystal masks in opposite directions. (C) Experimentally measured transmission as a function of voltage used for calibration of the SLM.

crystal plate, where it undergoes retardation and polarization rotation (see Figure 9B). When the light reaches the second liquid crystal plate, it undergoes retardation, but this time polarization rotation takes place in the opposite direction (see Figure 9B). Finally, a second polarizer is used for amplitude control. When the polarization is rotated away from the incident, horizontal direction, it is attenuated by the second polarizer. A rotation of 90 degrees results in zero transmission. This polarization dependence is very useful for calibration of the pulse shaper. Ramping the voltage of one of the liquid crystal plates while maintaining the other at a constant voltage results in the transmission function, shown in Figure 9C, which can be used to accurately calibrate the dependence of retardance on voltage. The total retardation ϕ is determined experimentally taking advantage of changes in the transmission given by

$$T = \cos^2[\pi(R_1(V_1) - R_2(V_2))/\lambda] \qquad (2)$$

where $R(V)$ is the retardance as a function of voltage introduced by each SLM unit. By fixing V_2 and scanning V_1, one can measure $T(V_1)$ and calculate $R_1(V_1)$ (except for a constant). By measuring $T(V_2)$ while keeping V_1 constant, one can obtain $R_2(V_2)$. Knowing $R_1(V_1)$ and $R_2(V_2)$, one can calculate the phase delay ϕ according to

$$\phi = \pi(R_1(V_1) + R_2(V_2))/\lambda) \qquad (3)$$

It is possible to program the pulse shaper to provide amplitude-only or phase-only pulse shaping, using the formulas given above. Phase-control work with sub-20-fs pulses requires that this type of calibration be carried out as a function of the pixel (because the index of refraction is wavelength dependent). This can be accomplished by dispersing the output spectrum and obtaining a frequency-dependent calibration curve.

The Gerber,[110−112] Wiener,[113] and Silberberg[114] research groups have begun to explore removal of the second polarizer to synthesize shaped pulses with frequency-dependent polarization. These types of laser pulses are expected to induce torques on molecules that would, in turn, lead to more sophisticated control of chemical processes such as enantiomeric synthesis. No experimental results on this subject have been reported so far.

A number of different pulse-shaping systems have been successfully demonstrated. As we have indicated above, the liquid crystal SLM[100,107,115] is one of the most popular. It is possible to implement a purely reflective phase shaper using independently addressable mirrors, instead of the SLM at the Fourier plane. The deformable mirror setup consists of a small number (typically 18) of electrostatically controlled membrane mirrors.[67,116,117] The deformable mirror is placed at the Fourier plane. These units have the advantage of a very small insertion loss, but they cannot be used for amplitude control. Their reduced number of optical elements further restricts the types of phase functions that can be synthesized.

There are two different types of pulse shapers based on acousto-optic modulators. One of the designs uses an acousto-optic crystal that is placed at the Fourier plane of a zero-dispersion compressor.[118,119] A radio frequency wave is programmed and introduced on the crystal. This wave induces changes in the index of refraction. The input laser pulse refracts and is phase shaped according to the stationary wave. This type of pulse shaper has the advantage of not being limited by the number of pixels; however, the refraction efficiency can be lower than 50%. The second type of acousto-optic pulse-shaper design operates on a completely different principle. In this setup, the pulse shaper is not at the Fourier plane. Instead, a linearly chirped laser pulse propagates through an acousto-optic programmable dispersive filter (AOPDF), which uses a time-dependent acoustic signal to control the group delay of the diffracted optical pulse. Simultaneously, the spectral amplitude of the diffracted optical pulse is driven by the acoustic signal's intensity. Therefore, the optical output, diffracted by the transient acoustic wave, is a function (convolution) of the optical input pulse and the electrical signal corresponding to the programmed RF pulse.[120] Typical parameters of an AOPDF device (2.5-cm long TeO_2 crystal) are a maximum diffraction efficiency of 30%, a temporal resolution of 6.7 fs, and a 3-ps group-delay range.[120] Compared to an SLM

unit placed at the Fourier plane, the AOPDF has lower efficiency and temporal resolution, but it has orders-of-magnitude-greater group-delay range. Being able to introduce a large group delay can be useful to delay a pulse in time. Alternatively, one can use the large group delay to compensate or to introduce very large phase deformations without the need for other compensation optics such as prisms and chirped mirrors. Recently, an AOPDF was programmed to perform pulse characterization on the input pulse according to the spectral phase interferometry direct electric-field reconstruction method (see Section 2.5).[121]

Pulse-shaping technology is advancing at a very fast pace. One of the most advanced systems to date employs a reflective, two-dimensional SLM originally designed for phase front compensation in atmospheric imaging. These units are available commercially with 640 × 480 and 1024 × 768 pixels. Each pixel is electrically addressed using an image-transmitting element to couple an optically addressed parallel-aligned nematic liquid crystal spatial light modulator (PAL-SLM). Itoh et al. demonstrated the power of this type of pulse shaper first, with 70-fs pulses.[122] Nelson's group has constructed a pulse shaper based on this type of system.[101] The units are designed to blur the sharp edges of the pixels so that pixelation is no longer noticeable. These SLM systems can be placed at the end of a 2*f* zero-dispersion reflective compressor to build a pulse shaper. The pixels can be binned vertically to achieve the same results obtained with conventional one-dimensional SLMs. More interestingly, these units can be used for two-dimensional pulse shaping of surface polaritons.[101−103]

Last, we consider the accuracy with which phase can be controlled by the pulse shaper. Control over the retardance introduced by a certain pixel in the SLM is determined by the voltage that causes alignment in the liquid crystal constituent. The voltage control is extremely accurate; the key here is overall differences between pixels (a device problem) and the changes in retardance introduced by the difference in optical frequencies that transmit through the SLM. Both of these problems can be assessed by a full calibration. For very short pulses, when differences in the frequency-dependent index of refraction become significant, the location of the central wavelength has to be maintained throughout the calibration and the experiments. The calibration should include interferometric data for each pixel/wavelength of the system. A computer program can be written to carry out the calibration of the systems, taking into account the transmission from each pixel and frequency region.[123,124] Only with a well-calibrated pulse shaper can one carry out experiments that require specific, user-defined, shaped pulses.

2.5. Phase Characterization

The most important step in laser control experiments with shaped pulses is accurate phase characterization of the pulse that interacts with the sample. Strictly speaking, the phase of every frequency component within the spectral bandwidth of the pulse must be determined accurately. This information cannot be obtained from an autocorrelation of the pulse or by determination of a time-bandwidth product, as discussed earlier. Pulse characterization is extremely important for experiments using a genetic algorithm (GA) to find the spectral phase of the pulse that interacts with the sample and optimizes a specific target. Experiments that require specific phase functions to achieve coherent control also require very accurate phase characterization.

Presently, there are two types of units available commercially that provide spectral phase characterization of laser pulses. These are second-harmonic frequency-resolved optical gating (FROG) and spectral-phase interferometry for direct electric-field reconstruction (SPIDER). The FROG instruments have been in use for years and have been described thoroughly in a number of publications.[43,125−142] Their main advantage is their sensitivity, stability, and ease of setup. However, SHG-FROG methods have some ambiguities regarding the sign of phase distortions and have certain accuracy limitations.

The SPIDER setup is much more complicated and requires interferometric stability. The concept behind this method is to take individual frequency components of a replica pulse and to interfere them with the original pulse.[143−145] This process was made much more practical when the reference frequencies were replaced by a heavily chirped pulse.[146−154] This method is more accurate than FROG, but it obtains the phase in $0-2\pi$ segments that need to be pieced together. Both FROG and SPIDER cannot determine $\phi^{(0)}(\omega)$ or $\phi^{(1)}(\omega)$, the absolute and first-order components of the spectral phase as defined in eq 1. The SPIDER method measures the change of phase, as a function of frequency, and integrates to obtain the overall phase across the pulse.[150,151] The FROG method measures a frequency and time-resolved autocorrelation and then attempts to simulate the resulting two-dimensional data using a learning algorithm that evaluates different phase and amplitude values on a grid. The field amplitude and phase values that most closely simulate the FROG trace are given as the result. The two methods have been compared in the literature.[155,156] Both SPIDER and FROG data are limited by the spatial and temporal overlap of beams in the optical interferometers. For an in-depth discussion on established methods for femtosecond laser pulse characterization, the readers are referred to ref 43.

Attempts to merge pulse shaping and characterization have either used a GA-controlled shaper to optimize a nonlinear optical signal,[67,69,115,116,157−174] or implemented time-domain interferometry with an acousto-optic programmable filter.[120,121,175] A newer method, multiphoton intrapulse interference phase scan (MIIPS),[123,124] takes advantage of the influence that phase modulation has on the probability of nonlinear optical processes at specific frequencies.[56,58,60,61] The experimental setup for MIIPS is straightforward, requiring only a thin SHG crystal and a spectrometer, provided a pulse shaper is already available. The method is not based on autocorrelation, so no overlapping of beams in time or space is required, nor is the tweaking of beam

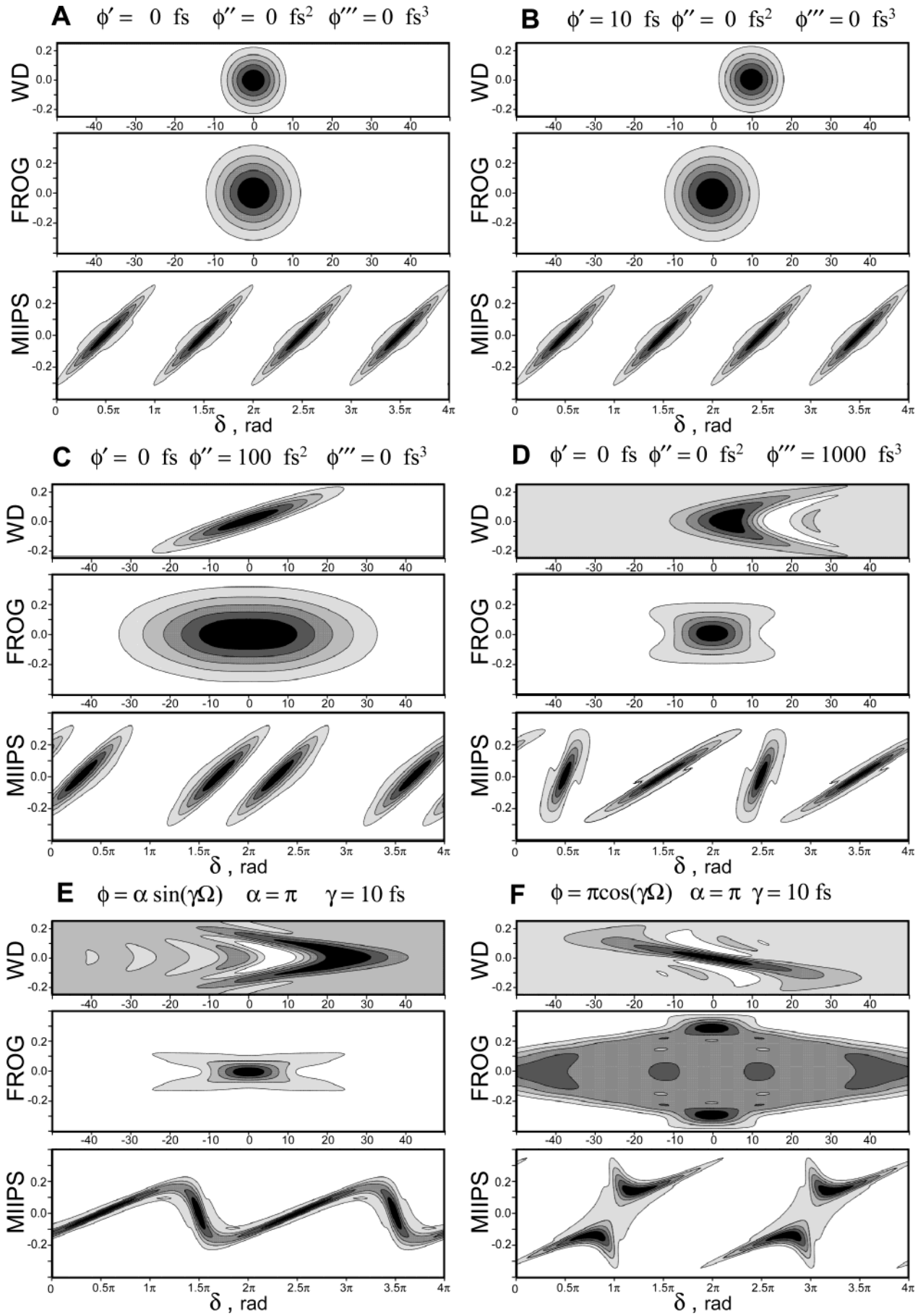

Figure 10. (A−F) Calculated Wigner distribution function, SHG-FROG, and MIIPS for pulses with different spectral phase modulations.

intensity and pointing to achieve symmetric scans. A series of calibrated reference phase functions are introduced, and the SHG spectrum resulting from each one is collected. The two-dimensional data (spectra vs phase parameter) contain enough information for the complete and accurate phase retrieval.

Phase retrieval using MIIPS involves introduction of reference phases given by $f(\Delta) = \alpha \cos(\gamma\Delta - \delta)$, where Δ is the detuning frequency from the fundamental ω_0, which, when scanned across the spectrum, reduces or cancels phase distortions in one or more regions of the spectrum. The MIIPS trace shows features of maximum SHG signal that are observed when phase distortions in $\varphi(\Delta) = \phi(\Delta) + f(\Delta)$ are minimized, where $\phi(\Delta)$ is the spectral phase of the input pulse before the shaper and $\varphi(\Delta)$ is the spectral phase of the output pulse. By setting the second derivative of the phase equal to zero, we obtain

$$\varphi''(\Delta) = \phi''(\Delta) + f''(\Delta) = 0 \quad (4)$$

Equation 4 gives the condition when the SHG generated at frequency Δ has a maximum. Scanning the parameter δ in the reference function and collecting the SHG spectrum for each value generates the two-dimensional MIIPS trace from which one can find the condition $\delta_{max}(\Delta)$ where the maximum SHG signal is obtained. From these values, $\phi(\Delta)$ is determined by integration. For TL pulses $\phi''(\Delta) = 0$, and δ_{TLmax} is given by

$$\delta_{TLmax}(\Delta) = \gamma\Delta \pm \pi/2 \quad (5)$$

This implies that, in a MIIPS scan, TL pulses are described by parallel diagonal lines separated by π. When $\phi(\Delta)$ is determined, the function $-\phi(\Delta)$ is programmed into the pulse shaper as a compensation function to obtain TL pulses, $\phi(\Delta) \equiv 0$. If deviations are still observed in a subsequent MIIPS, a second or third iteration of measurement and compensation are carried out. The goal is to introduce increasingly fine compensation functions $\phi(\Delta)$ until TL pulses are obtained according to

$$\phi(\Delta) - \{\phi^{I}(\Delta) + \phi^{II}(\Delta) + \phi^{III}(\Delta) + ...\} \approx 0 \quad (6)$$

After two or three iterations, the accumulated phase, according to eq 6, corresponds to the accurate phase $\phi(\Delta)$ across the spectrum in the original, uncorrected, pulse.

In Figure 10, we illustrate the effect of spectral phase on a 10-fs pulse centered at 800 nm. In all cases, we give three different images. The top corresponds to the Wigner representation,[176,177] below that we give the SHG-FROG, and below that we give the MIIPS trace. The illustrations are given for TL pulses (panel A). Notice that the Wigner representation and the FROG trace show a circular pattern. The MIIPS trace shows parallel lines separated by π. In panel B, we show pulses with a first-order phase delay of 10 fs. This delay can only be seen in the Wigner representation and is not observed in SHG-FROG or MIIPS. Figure 10C shows pulses with quadratic phase distortion corresponding to linear chirp in the time domain. In this case, the SHG-FROG shows an elongation in the time domain. The MIIPS trace shows that the spacing between the parallel lines has changed. Depending on the pair of lines that are closer, one can determine the sign of the quadratic phase, a parameter that is not determined by SHG-FROG. Figure 10D shows pulses with cubic spectral distortion. In this case, the angle of the features in the MIIPS trace changes; depending on the sign of the change in the angle one determines the sign of the third-order phase deformation. The magnitude of the change determines the magnitude of the third-order phase deformation. SHG-FROG does not provide the sign of the cubic phase distortion directly. In Figure 10E,F, we show the result from sinusoidal and cosinusoidal phase modulation.

While the methods discussed here are quite accurate in determining the spectral phase of femtosecond pulses, these methods are not capable of retrieving an arbitrarily complex spectral phase (especially one with discontinuities) that might result from a coherent control experiment. This concern arises from experiments in which the phase at each pixel is allowed to change freely. Until a method capable of accurate phase characterization of arbitrarily complex pulses is developed, one can use a method such as MIIPS to first determine the condition for the pulse shaper when TL pulses are produced at the sample $\varphi(\Delta) = 0$. During an optimization experiment, the phase of each pixel is allowed to vary, resulting in the arbitrarily complex phase function $\varphi_{control}(\Delta)$ at the sample.

3. Coherent Control with Narrow Bandwidth Lasers

3.1. Two-Wavelength Experiments

In the early days of laser control, it was thought that monochromatic laser light would be sufficient to cause selective bond cleavage by mode selective overtone excitation by single or multiphoton excitation processes.[178] Mode selective excitation, a strategy that does not depend on coherence, has proven to be successful only in systems with extremely slow intramolecular vibration redistribution (IVR).[179,180] Eventually, multiphoton excitation with narrow bandwidth lasers was shown to yield the thermodynamically favored pathway. These two strategies will not be discussed further in this review.

The general goal behind coherent laser control with two narrow bandwidth pulses is to provide two or more excitation pathways from the initial to the final state of an atom or molecule and to use interference between them as the control parameter. In 1986, Brumer and Shapiro proposed a scheme that closely resembled Young's double-slit experiment.[181] In their scheme, the probability of excitation of a laser transition is modulated by the relative phase between two different laser pathways reaching that transition. This control method is similar to the modified double-slit experiment illustrated in Figure 1B, where the phase of one pathway can be adjusted to control the amount of light that reaches a static detector.

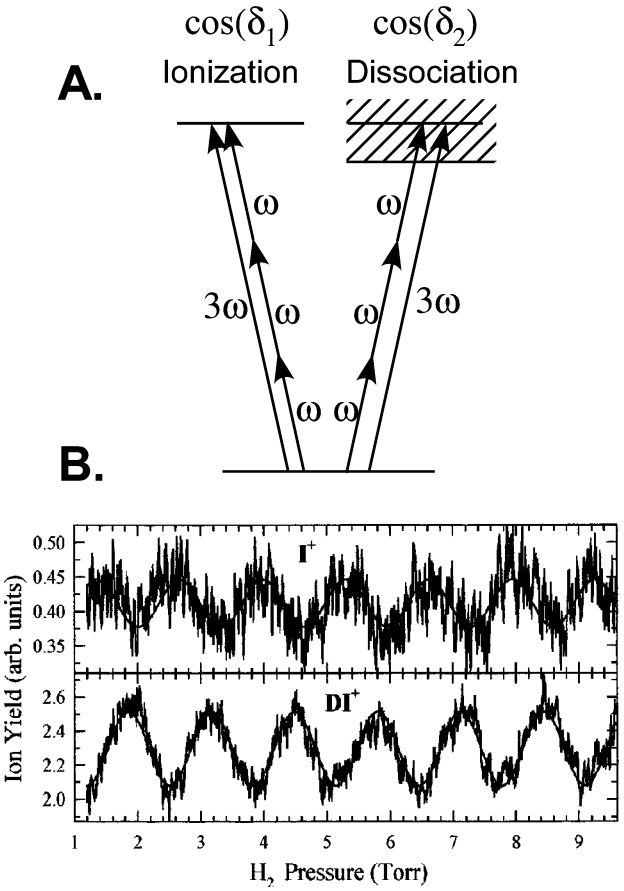

Figure 11. (A) Schematic representation of the Brumer-Shapiro coherent control approach. (B) Experimentally measured modulation curves following excitation of deuterium iodide (DI), showing variations in the yield of fragment ions DI^+ and I^+. (Reprinted with permission from ref 209. Copyright 1997 The American Physical Society.)

The combination of a laser at frequency ω, and its second harmonic, at frequency 2ω, has been used to control the direction of photoinduced current[182] and the direction in which fragments are ejected.[183]

In 1991, Gordon's group demonstrated coherent control over the dissociation or ionization of deuterium iodide (DI). The experiment entailed excitation above the ionization potential with two different laser sources, the fundamental laser light, at frequency ω, and its third harmonic, at frequency 3ω. Both excitation sources deposited the same amount of energy in the sample, one via one-photon and the other via three-photon excitation. As the relative phase between the two laser fields was changed, it was found that the probability of ionization or dissociation changed. Gordon's experimental findings can be interpreted in terms of two independent double-slit experiments, one controlling the probability for ionization and the other the probability for dissociation. This interpretation can be deduced as follows: there are two optically induced pathways to reach the ionization state (see Figure 11a). The probability of population transfer to the ionization state depends on the square of the sum between the two pathways, from which an interference term arises containing the relative phase $\delta_{\text{ionization}}$. Similarly, there are two optical pathways connecting the ground state with the dissociative state, and similarly a second interference term δ_{dissoc} arises. When $\delta_{\text{ionization}} \neq \delta_{\text{dissoc}}$, it is possible to enhance one pathway while the other is minimized (as shown in Figure 11). The difference between $\delta_{\text{ionization}}$ and δ_{dissoc} is known as the phase lag.[184] When δ is equal to π, maximum contrast between the two pathways can be achieved. The value of δ depends on the detuning of the incident beams with respect to a particular resonance. In fact, Gordon, Seideman, and co-workers have demonstrated that the value of δ can be used to obtain valuable spectroscopic information regarding resonance states imbedded in the ionization continuum of molecules.[185,186]

Experimental implementation of the Brumer-Shapiro control method has been found to yield modest results. In the case of the DI experiment, the depth of modulation found was ~20% (see Figure 11B). The nearly 100% depth of modulation predicted by most calculations is not realized experimentally. The Brumer-Shapiro method requires narrow wavelength excitation (long pulses or CW beams), because the interference condition is fulfilled only at a specific frequency. In Table 1, we list a number of experimental studies based on the concept of narrow bandwidth laser interference. The experiments are divided into control over amplitude of excitation and ionization (Table 1A),[37,187−204] and control over chemical reaction branching ratio (Table 1B).[190,205−210] From these experiments, we learn that interference is one of the most powerful processes available for achieving coherent control. We also see that theoretical predictions must take into account all relevant quantum states of the system and the various degrees of freedom, such as thermally averaged rotational populations, to more closely determine what is experimentally possible.

3.2. The STIRAP Scheme

One of the principal goals in laser control is to achieve 100% population transfer to a specific quantum state. In a two-level system, the fast Rabi oscillations induced by the electromagnetic field cycle the population between the initial and final state. With radio frequency, it is quite easy to design π pulses that cause complete population transfer. In the visible and ultraviolet range, the fast oscillations of the field ($10^{14}-10^{15}$ s^{-1}) prevent one from achieving 100% excitation and restrict the excitation to the average 50% over Rabi period. For multiple pulse experiments, if each laser pulse can only achieve 50% population transfer, then, after two pulses, the best one can expect is a 25% yield. This limitation was lifted with the demonstration of a method involving the coherent interaction between two pulses and a three-level system. The method, a stimulated transition induced by Raman adiabatic passage (STIRAP), depends on a Raman-type transition that is induced by the pair of pulses.[10,211−233] The concept for this method is shown in Figure 12. The goal is to transfer as much population as possible from level $|1\rangle$ to level $|3\rangle$. Because level $|2\rangle$ is optically coupled to level $|1\rangle$ and $|3\rangle$ and decays by spontaneous emission, population in level $|2\rangle$ would lead to a loss in the efficiency of population transfer. The tactic, therefore,

Table 1. CW - Control over (A) Amplitude of Excitation and Ionization and (B) Chemical Reaction Branching

(A) CW − Control over Amplitude of Excitation and Ionization

method	system	refs
$(\omega+\omega+\omega)(3\omega)$	Hg; 6s → 6p	187
$(\omega+\omega)(2\omega)$	Kr; tunnel e^-	188
$(\omega+\omega+\omega)(3\omega)$	Hg; 6s → 6p	189
$(\omega+\omega+\omega)(3\omega)$	HCl; $v''=0 \rightarrow v' \rightarrow HCl^+$	37
$(\omega+\omega+\omega)(3\omega)$	HCl; $v''=0 \rightarrow v' \rightarrow HCl^+$	190
$(\omega+\omega+\omega)(3\omega)$	CO; → CO^+	190
$(\omega+\omega)(2\omega)$	Ru; → e^-	191
$(\omega+\omega+\omega)(3\omega)$	HCl; X → HCl^*	192
$(\omega+\omega+\omega)(3\omega)$	CO; X → B	192
$(\omega+\omega)(2\omega)$	Kr n → e^-	193
$(\omega+\omega)(2\omega)$	NO; A → F → e^-	194
$(\omega+\omega+\omega)(3\omega)$	$H_2S \rightarrow H_2S^+/HS^+/S^+$	208
$(\omega+\omega+\omega)(3\omega)$	CH_3I	195
$(\omega+\omega+\omega)(3\omega)$	NH_3	196
$(\omega+\omega+\omega)(3\omega)$	c-C_8H_8	196
$(\omega+\omega+\omega)(3\omega)$	$(CH_3)_2N_2H_2$	196
$(\omega+\omega+\omega)(3\omega)$	$N(CH_3)_3$	196
$(\omega+\omega+\omega)(3\omega)$	$N(C_2H_5)_3$	196
$(\omega+\omega+\omega)(3\omega)$	CH_3I	196
$(\omega+\omega+\omega)(3\omega)$	Hg; 6s → 6p → e^-	197
$(\omega+\omega+\omega+\omega)(3\omega+\omega)$	Kr, Xe; 3s → 5p → e^-	198
$(\omega+\omega)(2\omega)$	Kr, Xe; n → e^-	199
$(\omega_1+\omega_2)(\omega_2+\omega_1)$	NO; A → E, H → NO^+	200
$(\omega_1+\omega_2)(\omega_2+\omega_1)$	Ba; $6s^2$ → 6s6p, 6s7p → e^-	201
$(\omega_1+\omega_2)(\omega_2+\omega_1)$	Ba; $6s^2$ → 6s6p, 6s7p → e^-	202
$(\omega+\omega+\omega)(3\omega)$	Ca; 4s4s → e^-	203
$(\omega+\omega)(2\omega)$	Ru; → e^-	204
$(\omega+\omega)(2\omega)$	IBr; → $I(^2P_{1/2})+Br(^2P_{3/2})^-$	558
$(\omega_1+\omega_2)(\omega_2+\omega_1)$	BBO, crystal	559
$(\omega+\omega)(2\omega)$	IBr; → $I(^2P_{1/2})+Br(^2P_{3/2})^-$	558

(B) CW − Control over Chemical Reaction Branching

method	system	refs
$(\omega+\omega+\omega)(3\omega)$	HCl; → HCl^+/H^+	190
$(\omega+\omega+\omega)(3\omega)$	HI → HI^+/I^+	205
$(\omega+\omega)(2\omega)$	$HD^+ \rightarrow H + D^+/H^+ + D$	206
$(\omega+\omega+\omega)(3\omega)$	$CH_3I \rightarrow CH_3 + I^* \rightarrow I^+/CH_3^+$	207
$(\omega+\omega+\omega)(3\omega)$	HI → HI^+/I^+	209
$(\omega+\omega+\omega)(3\omega)$	DI → DI^+/I^+	209
$(\omega+\omega+\omega)(3\omega)$	HI → HI^+/I^+	210
$(\omega+\omega+\omega)(3\omega)$	DI → DI^+/I^+	210

is to minimize the population at level |2> during the experiment. The STIRAP method was found to require a counterintuitive timing of the pulses, whereby the pulse ω_{23} arrives at the sample first, and is followed by the pulse ω_{12}. While the two fields are on, the population is transferred to level |3>. Because field ω_{23} turns off before ω_{21} the population in |3> cannot return to level |1>. The presence of both fields directly couples the ground state and the final state adiabatically.

This scheme has been used to achieve 100% population transfer in atoms and diatomic molecules. An extension of this method has been introduced recently where the two laser pulses are replaced by a single, chirped pulse. In this case, also known as CHIRAP, the higher frequencies arrive before the lower ones, achieving the STIRAP effect by using only a single laser pulse.[216,217,227,228,233] This scheme has been expanded theoretically for selective control of population transfer involving four or more states. These more-complicated schemes have not yet been

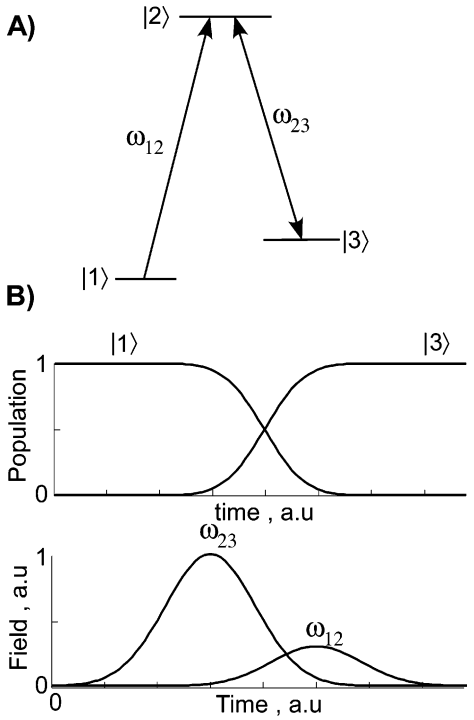

Figure 12. (A) Optical scheme for the STIRAP experiments. (B) Dependence of state population on the intensity of the two laser pulses as a function of time. Note that the population of state |2⟩ remains equal to zero at all times.

Table 2. STIRAP

method	system	refs
cw, RAP	NH_3; one photon; pop inversion	211
cw, RAP	NH_3; two photon; pop inversion	212
cw STIRAP	Na_2; Xv0 → Av7 → Xv5	213
cw STIRAP	Na_2; X → A → X	214
cw STIRAP	C_2H_4; $\nu_{gs}(413) \rightarrow \nu_7(505) \rightarrow \nu_{7+9}(514)$	215
ps CHIRAP	I_2; X → B → X	216
ps CHIRAP	Na: 3s → 3p → 5s	217
cw STIRAP	Na_2; X → A → X	218
fs STIRAP	Ru; 5s → 5p → 5d	219
ns STIRAP	NO; v0 → v6	220
ps STIRAP	Na 3s → 5s → 3p	221
ps STIRAP	I_2; X → B → X	221
ps STIRAP	pentacene/*p*-terphenyl crystal	221
ns STIRAP	C_6H_6; $S_0 \rightarrow S_1 \rightarrow S_0$	222
ns STIRAP	C_6H_6; $S_0 0_0 \rightarrow S_1 6_1 \rightarrow S_0 6_2$	223
cw STIRAP	Na_2; vibrational excitation	224
ns STIRAP	SO_2; (000) → (910)	225
cw STIRAP	Ne; $^3P_0 \rightarrow {}^3P_1 \rightarrow {}^3P_2$	226
ps CHIRAP	Cs; 20p → 26p → 50p	227
ps CHIRAP	NO; v0 → v3	228
ns STIRAP	NO; v0 → v6	229
cw STIRAP	Ne; $^3P_0 \rightarrow {}^3P_1 \rightarrow {}^3P_2$	10
ns STIRAP	NO; v0 → v6	10
cw STIRAP	Ne; $^3P_0 \rightarrow {}^3P_1 \rightarrow {}^3P_2$	230
cw STIRAP	Na_2; v0 → v25	231
ns STIRAP	K_2; X → B → X	232
fs CHIRAP	Rb; 5s → 5p → 5d	233

realized experimentally. In Table 2, we list a number of experimental studies based on the STIRAP concept.[10,211−233] These experiments range from single atoms to polyatomic molecules and from continuous wave lasers to chirped femtosecond laser pulses. The STIRAP concept is very powerful. Its only limitation appears to be the requirement of sharp resonances in the spectrum of the sample to be controlled.

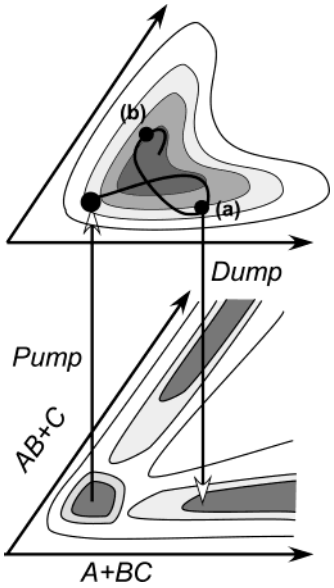

Figure 13. Schematic representation of the pump−dump experiments. The dump pulse can be timed to catch the wave packet at point (a) to produce A + BC, or at point (b) to produce AB + C.

4. Coherent Control with Femtosecond Pulses

4.1. The Pump–Probe and The Pump–Dump Methods

In 1980, once it was realized that energy in the molecules becomes delocalized by IVR, Zewail proposed that selective bond excitation for controlling chemical reactions would require the use of short laser pulses to compete with IVR.[234] Short pulse excitation leads to the formation of wave packets whose motion can remain relatively localized for picoseconds or nanoseconds in liquid or gas-phase environments, respectively.[235−250] Wave packet localization was exploited for probing chemical reaction dynamics in the Zewail group, as well as in other groups.[251−259] At approximately the same time, the concept of pump−dump was introduced by Tannor and Rice for controlling the outcome of chemical reactions.[260−262] The localized wave packet formed by the femtosecond pump pulse explores different regions of the potential energy surface and permits a second short pulse to "dump" the excitation and leave the wave packet in a specific region on the ground-state potential from which the desired product is obtained (as shown in Figure 13). This time-dependent sensitivity, which depends only on the vibrational coherence but not on the phase coherence between the two laser pulses, has been used in many pump−probe experiments to follow the evolution of wave packets.[263]

We illustrate how wave packet motion can be used to access two different electronic states with a 1990 experiment from Zewail's group on diatomic molecular iodine.[264] The relevant potential energy curves are shown in Figure 14A. The pump pulse (50 fs in duration and centered at 620 nm) prepares a localized wave packet in the B state, and the wave packet oscillates in the anharmonic well. The probe pulse (50 fs in duration and centered at 620 nm) promotes

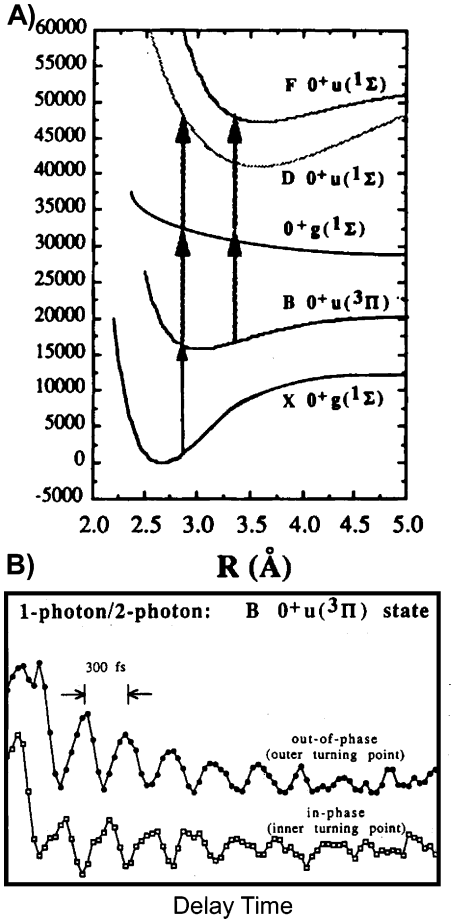

Figure 14. (A) Potential energy curves and optical pathways for multiphoton excitation of gas-phase I_2. (B) Experimentally recorded transients obtained by collecting fluorescence from the F or the D ion pair states. The dynamics correspond to the vibrational period in the B state. (Reprinted with permission from ref 264. Copyright 1990 Elsevier B. V.)

the wave packet to the D or F excited ion-pair states by two-photon excitation. Notice that the transition probability to either of the ion-pair states depends on the location of the wave packet (see Figure 14A). Transitions to the D state are favored when the wave packet is at the inner turning point, while transitions to the F state are favored when the wave packet is at the outer turning point. This dependence is shown in Figure 14B, where out-of-phase vibrations are observed when detecting the D−X or F−X fluorescence as a function of time delay between the pump and probe pulses.

We have not included a table to summarize all experiments based on pump−dump or pump−probe, where the time delay between pump and probe beams is the variable that "controls" the outcome. The reason for this omission is that many pump−probe experiments depend on the time-dependent wave packet motion for probing the molecular dynamics of the system; however, only in a few cases particular emphasis has been placed on using the time delay to control the preparation of different products and to cast the experiment in the language of control. Baumert et al. demonstrated in 1991 how the time delay between pump and probe lasers could be used to control the production of Na_2^+ and Na^+.[265] When

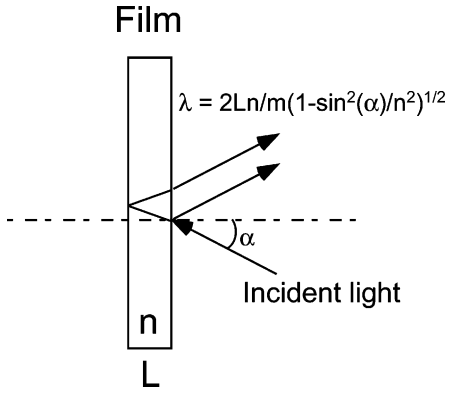

Figure 15. Interference of light from a thin film with refractive index *n*.

the wave packet visited the inner turning point, the probe laser produced Na_2^+; when the wave packet visited the outer turning point, Na^+ was produced.

When pump and probe beams have different wavelengths (no spectral overlap), the relative optical phase between the pump and probe beams plays no role. There is no need or advantage gained by locking the phase between pump and probe pulses. Each of the electric fields induces a population with partial molecular coherence but no coherence with the optical field. Methods that achieve coherent control by phase locking the two incoming fields are discussed in Section 4.2.

Here, we remark that impulsive excitation leads to the formation of coherent wave packet dynamics in all samples from single atoms to large biomolecules and crystals. A second, short pulse can interact with the system at different times during the coherent motion thereby controlling the final state that is reached. This is an extremely powerful method with few limitations. This method has played an important role since microsecond light flashes were available, and will probably play an important role in subfemtosecond (attosecond) experiments.

4.2. Linear Intensity Dependence Control

4.2.1. Interferometry of Laser Pulses and Wave Packets

Although Young's double-slit experiment has been credited with the demonstration that light has wave properties, the linear interference of light had been known by Newton. This type of interference can be observed in everyday objects such as the colors observed on the surface of an oily puddle in the street, the colors in the surface of a soap bubble, or the bright colors in the wings of a butterfly. All of these are the manifestation of linear interference. The textbook explanation for the colors observed in these everyday examples is simple. One or more layers have a distinct refractive index. As light propagates through a film with an index of refraction *n* (see Figure 15), a small portion is reflected from the front and back surfaces. The reflected light from the back surface is delayed by a time that is proportional to the phase velocity of the particular wavelength and twice the thickness *L* of the layer. The delay can give rise to constructive or destructive interference for each particular wavelength, resulting in vivid color patterns.

Table 3. Phase-Locked Pumps

method	system	refs
ns 2 locked pumps, LIF	Na, $3^2S \rightarrow 4^2D$, gas	266
ns N locked pumps, LIF	Na, 3S → 5S, gas	267
ns, 4 locked pumps, LIF	I_2, X → B	268
fs, 2 locked pumps, LIF	I_2; X → B, gas	269
fs, 2 locked pumps, LIF	I_2; X → B, gas	50
fs, 2 locked pumps, LIF	I_2; X → B, gas	270
fs, 2 locked pumps, ion probe	K, 3d → 12−18f, gas	271
fs, 2 locked pumps, LIF	I_2; X → B, solution	272
fs, 2 locked pumps, ion probe	Cs_2, X → B, beam	273
ps, 2 locked pumps, ion probe	K, n(Ry) = 66, beam	274
ps, 2 locked pumps, ion probe	K, n(Ry) = 66, beam	275
fs, 2 locked pumps, ion^- probe	Cs, 6s → 7d, beam	276
fs, 2 locked pumps, LIF	Cs, 6S → 8S, gas	277
ps, 2,3 locked pumps, ion probe	K, n(Ry) = 66, beam	278
fs, 2 locked pumps, ion probe	Cs_2, X → B, beam	279
fs, 2 locked pumps, ion probe	K, 4s → 4p, beam	280
fs, 2 locked pumps, ion probe	Cs, 6s → 7d, beam	280
fs, 2 locked pumps, transmission probe	AlGaAs, crystal	281
fs, 2 locked pumps, ion probe	K, 4s → 4p, beam	282
fs, 2 locked pumps, ion probe	K, 4s → 4p, beam	283
fs, 2 locked pumps, e^- probe	Ca, 4s → ns, beam	85
fs, 2 locked pumps, ion probe	K, 4s → 5p	284
fs, 2 locked pumps, ion probe	Ca, 4s → ns, beam	84
fs, 2 locked THz pumps, e^- probe	Rb, → n40, gas	285
fs, 2 locked pumps, ion probe	Ca, 4s → ns, beam	83
fs, 2 locked pumps, e^- probe	K, 4s → 4p → e^-, beam	286
fs, 2 locked pumps, e^- probe	Na_2, gas	81
ps, 2 locked pumps, field ionization	Xe, 6p → n = 30−50, beam	332
fs, 2 locked pumps, LIF probe	Rb, 5s → 5p(3/2,1/2), gas	287
ps, 2 locked pumps, field ionization	Xe, 6p → n = 30−50, beam	333
ps, 2 locked pumps, field ionization	NO, *n* = 30−40, p(0) or f(2), beam	334
fs, 2 locked pumps, e^- probe	K, 4s → 4p → e^-, beam	80
Fs, 2 locked pumps, LIF probe	Hg−Ar, X → A(*v* = 3,4,5) → E, jet	560

There are a number of coherent control experiments based on the use of two phase-locked pulses. These experiments are referenced in Table 3.[50,80,81,83−85,266−287] Although most of these experiments use short laser pulses, some use broad bandwidth nanosecond pulses.[266,267] The interpretation of these experiments is as follows: the incident field generates a coherent superposition of vibronic states (a wave packet). The second pulse generates a second superposition of vibronic states. Because the phase between the two pulses is locked, certain states within the two wave packets interfere, leading to what is known as wave packet interference. The resulting fluorescence from this type of experiment reflects the interference experienced by the wave packets. The first demonstration of this type of experiment for coherent control was carried out by Scherer et al.[269] They used lock-in amplification to isolate the signal resulting from the constructive or destructive interference. Their data clearly show constructive (positive signal) and destructive (negative signal) interference, as shown in Figure 16. When the phase-locking mechanism was turned off, the very fast fluctuations in phase result in an average signal that is subtracted by the lock-in detection system.

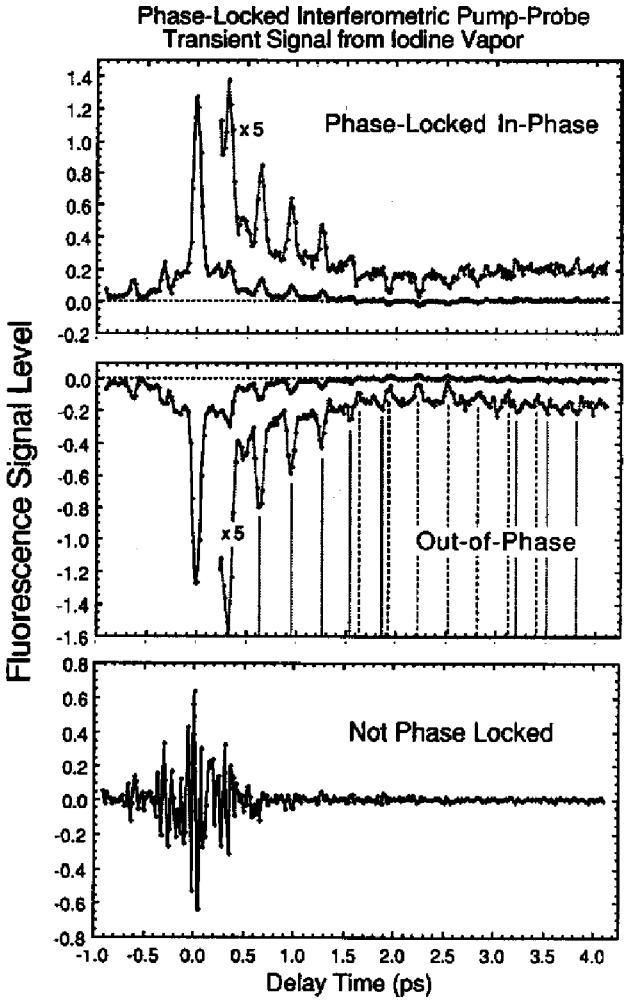

Figure 16. Phase-locked pump−probe signals detected from iodine vapor at 300 K. Both pump and probe pulses are centered at 611 nm with 65−70 fs duration. Fluorescence is detected at right angles as a function of time delay between the pulses. Notice that the best signals come from pump and probe pulses, which are phase locked and in-phase. (Reprinted with permission from ref 269. Copyright 1990 American Institute of Physics.)

The setup was similar to a pump−probe experiment, with a Mach-Zhender interferometer arrangement used to provide the time delay between the two pulses. The beams are recombined collinearly before impinging on the gas-phase sample. Phase locking required Scherer and co-workers to add a piezoelectric actuator in one of the optical-delay mirrors to adjust the time delay between the two pulses with sub-femtosecond accuracy. The piezoelectric actuator was under the control of a feedback servo loop that monitored the phase difference between the two arms of the interferometer. The researchers added a spectrometer to have better phase resolution at the carrier frequency of the pulse. Using a spectrometer to narrow the frequency bandwidth, they were able to observe clear interference, even for delays that were many times longer than the pulse duration.

Prior and Shapiro realized that there was no need for complicated phase-locking equipment to carry out interferometry experiments. They independently demonstrated that similar results could be obtained when they purposely introduced random phase fluctuations in the optical delay between the two laser pulses.[288−291] These fluctuations caused sharp changes in the signal because of constructive and destructive interference. By tracking the amplitude of the changes in the signal, they were able to reproduce the type of results observed by Scherer with a simpler setup. This type of experiment became known as "coherence observation by interference noise" or COIN spectroscopy. It was realized that there was no need to use femtosecond lasers for these types of experiments. All that was needed was a source with broad bandwidth, such as can be generated from a nanosecond pumped dye laser without wavelength tuning optics. These observations were preceded by similar studies in nonlinear optics.[292−294] Linear interferometry is also used in Fourier transform infrared spectrometers.

Girard utilized an interferometer to follow the time-resolved signal in a setup that had some similarities to Scherer's. Instead of phase locking the pulses, Girard acquired the data with extremely high temporal resolution. The resulting scans revealed the constructive and destructive interference at the frequency of the incoming laser pulses (2.67 fs).[276,279,280,282,295] The most interesting part of this work has been the comparison between one- and two-photon excitation. For two-photon excitation, the interference is observed at twice the frequency.[284]

There is a simpler interpretation for experiments involving linear interference. As mentioned in Sections 2.1.2 and 2.1.3, femtosecond pulses are coherent superpositions of electromagnetic waves of different frequency. When a femtosecond pulse is analyzed with a spectrometer, as the frequency resolution of the spectrometer is increased, the portion of the pulse that is detected increases in time duration. In fact, the output of a femtosecond pulse oscillator can be dispersed in a high-resolution spectrometer until the individual longitudinal modes that make up the femtosecond pulse can be individually resolved. It is only when all the individual modes are phase-locked that the femtosecond pulse is formed. On the basis of this understanding, there is a simpler interpretation for linear interferometry experiments.

Wave packet interferometry experiments are carried out with pairs of identical phase-locked femtosecond pulses. The time delay between the pulses is several times longer than the pulse duration; hence, they are considered by many to be noninteracting. However, on the basis of the discussion above, and because the pulses are identical, they share all their frequency components. This implies that, for a given time delay between the two pulses, one or more of their frequency components undergoes destructive interference. This condition is depicted in Figure 17, where we show how the spectrum of a pair of pulses changes as the delay between them is changed. Notice that the distance between the nodes is determined by the ratio between the time delay and the time duration of the pulses. The position of the nodes can be fine-tuned by controlling the phase delay within an optical cycle (2−3 fs). This interpretation has also been given by Girard.[280]

Linear interference experiments are much easier to carry out in gas-phase samples, containing very sharp transitions, usually of atoms and diatomics.

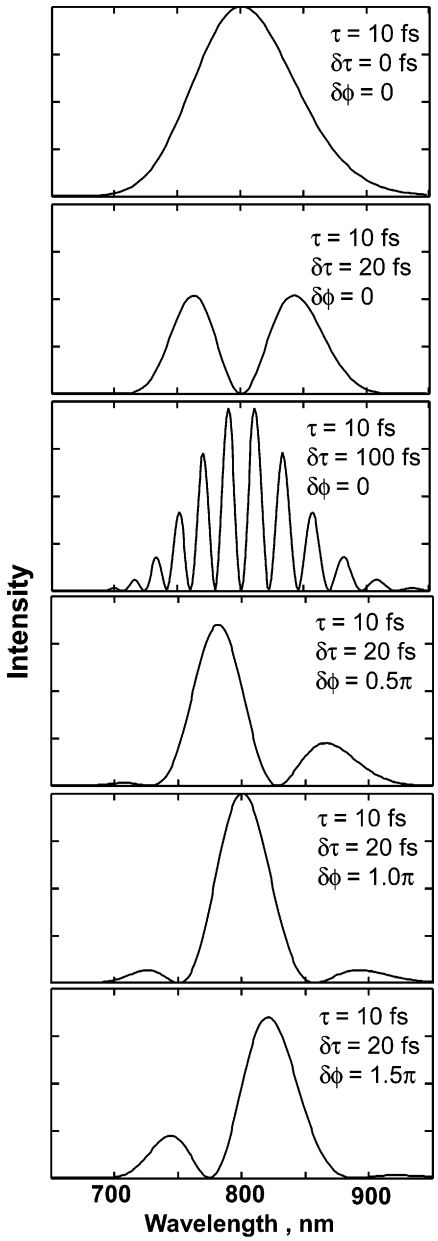

Figure 17. Calculated spectral interference obtained when two pulses of duration τ are separated by a time delay $\delta\tau$ and have a phase difference of $\delta\phi$. Notice that in the first panel, both pulses interfere constructively. In subsequent panels, destructive interference produces nodes. The number of nodes is controlled by $\delta\tau$, and their position is controlled by $\delta\phi$.

Similar results can be achieved for larger molecules, even in condensed phase, if the time delay between the two pulses and their pulse duration is reduced considerably. For example, in Figure 17, we show the spectrum of a pair of 10-fs pulses as a function of time. It is clear that large changes in the spectrum can be achieved by controlling the linear interference, and these changes can be used for controlled excitation. Strictly speaking, linear interferometry depends on the amplitude modulation of the spectrum of the incoming laser caused by interference. The frequency-resolved picture explains why these experiments can be carried out with an incoherent light source.

In conclusion, the spectrum of a pair of phase-locked femtosecond pulses is different from the spectrum of a single pulse; it is modulated by linear interference. On the basis of this observation, experiments based on wave packet interferometry and COIN spectroscopy measure the absorption spectrum of the sample.

Interference between two incoherent broad-bandwidth sources has been used to develop a very powerful method for Raman spectroscopy.[296−300] The method, known as noisy CRS spectroscopy, or $I^{(2)}$CRS, is carried out with three beams (two are incoherent and broad bandwidth and the third is narrow bandwidth) in a forward-box arrangement similar to that used for FWM experiments (see Figure 6). Raman transitions are induced by a narrow bandwidth laser pulse and one of the broad bandwidth lasers. Scattering in the phase-matching direction carries the Stokes signal. The main advantage of this setup is that the interference occurs at the center wavelengths where the Raman transition takes place; therefore, in the time domain, slow oscillations (picosecond) near the Raman transition correspond to the signal of interest. This is in contrast to Fourier transform infrared spectroscopy or selective excitation Raman active transitions, where oscillations in the time domain occur in the picosecond time scale.[301] This effect has been interpreted as a down conversion of the vibrational frequencies.[302] In these experiments, the interference between the two incoherent broad-bandwidth fields requires the interaction with the molecular system.

4.2.2. Wave Packet Manipulation

The spectral phase of a femtosecond pulse can be used to manipulate the shape and evolution of a wave packet. Upon excitation by a femtosecond pulse, the wave packet that is formed can be described by the following expression:

$$\psi(t) \sim \sum_n a_n \exp(-iE_n t/\hbar + \theta_n)|n> \qquad (7)$$

where a_n are the quantum amplitudes determined by the transition from the ground to the nth excited state, E_n is the energy of the nth state, $|n>$ is the nth wave function in the excited state, and θ_n is the phase introduced by the pulse shaper. From eq 7, one can ascertain that changes in θ_n introduced by the pulse shaper can manipulate the shape and time evolution of the wave packet. The Wilson group demonstrated this type of control experimentally with wave packet focusing and other wave packet manipulations on diatomic iodine molecules.[303−305] Gerber's group demonstrated that the single-pulse, multiphoton-ionization of Na_2 was strongly dependent on the chirp of the laser pulse. Furthermore, they found that the ionization of Na atoms using 618 nm laser pulses was enhanced with negatively chirped pulses. They explained that, for negatively chirped pulses, the high-energy photons (closer to resonance at 589 nm to the p state) precede the lower-energy photons responsible for the ionization. For positively chirped pulses, the ionization of atomic sodium was not observed.[306]

The early experiments concentrated on the use of linear chirp, characterized by a frequency sweep

Table 4. Chirped Pump

method	system	refs
ps, chirped pump, e^-	Rb, → n 25−30, beam	56
ps, chirped pump, e^-	Rb, → n 25−30, beam	309
fs, chirped pump, absorption	GaAs, crystal	310
ps, chirped pump, e^-	Rb, → n 25−30, beam	311
ps, chirped pump, ion probe	Rb, 5s → 5p → 5d, gas	312
fs, chirped pump, LIF probe	LD690, $S_0 \rightarrow S_1$, solution	347
fs, chirped pump, LIF probe	I_2, X → B, gas	303
fs, chirped pump, LIF probe	I_2, X → B, gas	304
fs, chirped pump, LIF probe	I_2, X → B, gas	313
fs, chirped pump, LIF probe	LDS570, $S_0 \rightarrow S_1$, solution	348
fs, chirped pump, LIF probe	I_2, X → B, gas	305
fs, chirped pump, LIF probe	I_2, X → B, Kr matrix	305
fs, chirped pump, LIF probe	NaI, NaI → NaI* → Na* + I, gas	314
fs, chirped pump, ion probe	NO, $v0 \rightarrow v5$, beam	315
ps, 1 chirped pump, e^-	Cs, np → n′s → n″s, beam	227
fs, chirped pump, LIF probe	bacteriorhodopsin, $S_0 \rightarrow S_1$, solution	349
fs, chirped pump, LIF probe	GFP, IR125 solution	316
ps, chirped pump, absorption	$W(CO)_6$, $v0 \rightarrow v1,2$, solution	317
fs, chirped pump, LIF probe	I_2, X → B, gas	318
fs, chirped pump, LIF probe	I_2, X → B, gas	319
fs, chirped excitation, ion probe	NO, $v0 \rightarrow v3$, beam	228
fs, chirped pump, LIF probe	CH_2I_2, gas	320
fs, chirped pump, LIF probe	I_2, X → B, gas	321
fs, chirped pump, LIF probe	I_2, X → B, gas	322
fs, chirped pump, LIF probe	I_2, X → B, solid Kr	323
fs, chirped pump, ion probe	NO, $v0 \rightarrow v4$, beam	324
fs, chirped pump, birefringence probe	D_2, N_2, NO_2, gas	325
fs, chirped pump, birefringence probe	D_2, N_2, NO_2, gas	326
fs, chirped pump, LIF	NH_3, gas	327
fs, chirped pumps, LIF probe	Rb, 5s → 5p → nd,n′s, gas	328
fs, chirped pump, LIF probe	Rb, 5s→5p (3/2,1/2), gas	329

across the laser pulse. In a positively chirped pulse, for example, the frequency sweeps from red to blue. Femtosecond pulses acquire a positive chirp when they propagate through water or glass. The measured introduction of positive or negative chirp can be accomplished by the use of prism or grating pairs.[307,308] More sophisticated phase modulation required the introduction of pulse shapers. Experimental demonstrations of wave packet manipulation, using phase-modulated pulses, are listed in Table 4.[56,227,228,303−305,309−329] For example, Bucksbaum's group has demonstrated Rydberg-state wave packet sculpting based on phase shaping.[330−334] Leone has taken this method one step further with relative control over the phase of rotational and vibrational levels in a diatomic molecule.[335−339] In Leone's experiment, they used a narrow bandwidth laser to excite a single rovibrational state from which they could launch the wave packets. This initial step served to circumvent the initial thermal distribution. Lozovoy studied the effect of chirp for pump-and-probe pulses on the preparation and subsequent evolution of wave packet dynamics of I_2 molecules.[319,340] In principle, wave packet manipulation can be used in combination with the pump−dump scheme to improve the yield of a particular chemical reaction. This approach was used by Wilson to control the predissociation of NaI.[314]

There is a number of studies that follow the interference between resonant and nonresonant two-photon transitions to a final state. Among these studies, we mention the work of Silberberg, where he demonstrated that TL pulses are not optimal to cause two-photon excitation when an intermediate state is resonant at the one-photon level. Leone has taken advantage of the interference that takes place between the resonant and the off-resonant pathways, to observe a transient change in the phase between two states in a coherent superposition.[338,339,341−346]

Coherent vibrational motion has been observed in a number of pump−probe experiments on polyatomic molecules in the gas and condensed phases. These wave packet dynamics usually involve a small number of states, and the dynamics are quite regular (quantum beats). In these cases, one can use the time delay between pump and probe pulses for control purposes, as discussed above. However, there are no experiments where the superposition of states was designed a priori, so that the subsequent motion of the wave packet in the multidimensional state of the poliatomic molecule can be predicted, and focused on different dimensions or local modes. Here, we refer to cases in which the dynamics involve several different modes, and the time evolution is complex. There is no fundamental impediment for this realization. The experiments that come closest to controlling wave packet motion in polyatomic molecules are those that use chirp to determine the state (ground or excited) where the wave packet is formed. Shank and Wilson, independently, have shown that, for one-photon transitions in large molecules, positively chirped pulses lead to formation of a wave packet in the excited state while negatively chirped pulses lead to formation of a wave packet in the ground state.[316,322,347−355] Experiments that attempt to control the wave packet evolution in polyatomic molecules would be valuable in teaching us about the flow of energy in these complex systems.

4.2.3. Wave Packet Manipulation in Real Space

We have concentrated, so far, on coherent control of intramolecular degrees of freedom, and we have not paid attention to the spatial component of these dynamics. Here, we discuss manipulation of molecules in real space. We start with rotational wave packet manipulation; we then discuss control of the position of wave packets in space.

In the previous section, we considered the impulsive interaction of an ultrashort pulse and the emergence of a vibrational wave packet. Similarly, we can consider the interaction of an ultrashort linearly polarized laser pulse with a gas-phase molecular sample. Here, we concentrate on the emergence of a rotational wave packet, aligned at time zero with the polarization of the laser pulse and evolving in time. The evolution of such a rotational wave packet was demonstrated by Heritage et al. by passing a pair of picosecond laser pulses through CS_2 vapor.[356] The most important observation was the recurrence of the initial alignment with a period equal to $(1/4B)$, where B is the rotational constant of

the molecule. For molecules with inversion symmetry, half recurrences or revivals are observed for times equal to $(1/8B)$.[74,357−361] The recurrent observation of rotational alignment has been used to develop a spectroscopic method for the determination of accurate rotational constants—this method is known as rotational coherence spectroscopy.[246,248]

A number of experiments have explored properties in the laser field that may be used to manipulate rotational wave packets. These experiments must be divided into resonance and off-resonance excitation. When the incident field is resonant, it is possible to manipulate the phase of the light that excites a particular rovibronic transition. This degree of finesse has been demonstrated by Leone's research group.[335,336,338,339,344,362−365] The effect of different phase modulation, for example, chirp, on the rotation of diatomics has been explored by Sarkisov and Lozovoy.[325]

The interaction between a linearly polarized off-resonance laser pulse with anisotropically polarizable molecules leads to the observation of rotational wave packet dynamics, as was first demonstrated for CS_2.[356] One of the explanations for the initial alignment observed arising from the laser−molecule interaction is that the electric field creates a potential that acts on the polarized molecules.[366,367] This interaction requires some time for the molecules to align with the incident electric field. Demonstrations of the laser-induced alignment technique using nanosecond pulses have been conducted by Kim and Felker on large nonpolar molecules[368,369] and by Stapelfeldt and co-workers on smaller molecules.[370−372] When a femtosecond pulse interacts with the sample, the long time of interaction required for the molecules to align with the electric field is not available. Alignment with femtosecond pulses can be understood as resulting from an impulsive kick imparted by the polarized laser.[373] Posthumus et al. examined the multiphoton dissociative ionization of H_2, N_2, and I_2 with 50-fs pulses and found that only H_2 and N_2 showed alignment characteristics.[374] This observation was confirmed when alignment experiments were carried out on a series of halogen molecules. Heavier molecules such as I_2 showed enhanced ionization but not alignment. For lighter molecules, such as Cl_2, the 80-fs pulses were able to induce the desired alignment.[375] The Dantus group has demonstrated off-resonance alignment of CS_2 molecules.[20] In the Dantus setup, two intense femtosecond beams generate a transient grating, and then a laser pulse is diffracted from the grating to probe the degree of alignment. The probe pulse arrives 76 ps after the two alignment pulses, the time of the first rotational recurrence. The molecules rotate field free during this time. These experiments have demonstrated alignment; and, under the highest intensities, the linear molecules have deformed, the S−C−S changing from 180 to 160 deg.[20,376]

There are a number of additional experiments in the literature regarding alignment of molecules with short laser pulses.[377] Rather than giving an exhaustive list, here we concentrate on a single experiment

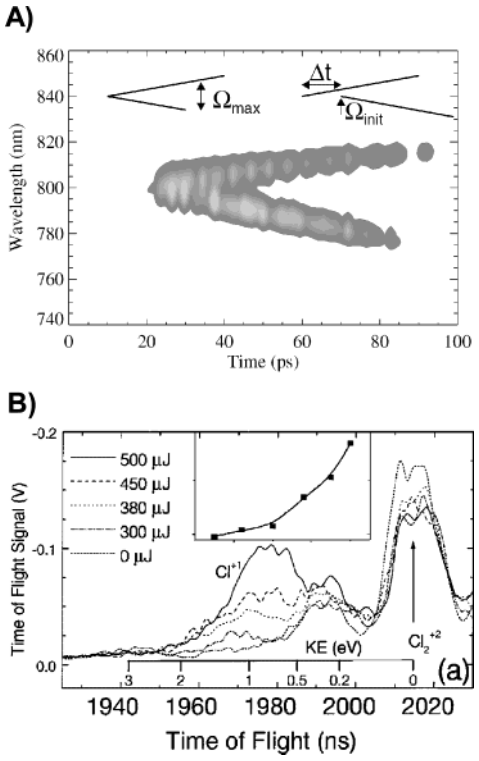

Figure 18. (A) Time dependence of the carrier frequency in the centrifuge pulse. (B) Distribution of ions observed under strong chirped field excitation. (Reprinted with permission from ref 378. Copyright 2000 American Physical Society.)

where manipulation of a rotational wave packet led to a chemical reaction. For this experiment, Corkum and co-workers created an intense rotating electric field for the molecules to follow, using an off-resonance chirped circularly polarized pulse. As the circularly polarized field rotated, the molecules rotated faster and faster until the centrifugal force overcame the chemical bond. The induced rotational acceleration resulted in a molecular centrifuge.[378] In Figure 18, we show a plot of the chirped electric field used for the experiment. The bottom plot shows how, as the intensity of the laser was increased, the amount of Cl^+ detected increased, resulting from the centrifuge-induced dissociation. Control of the external degrees of freedom of molecules beyond rotation includes the manipulation of molecules in space. This manipulation has been demonstrated in small, isolated molecules,[377] as well as in large molecules in solution using the laser intensity at its focus as "tweezers".[379−382]

Spatial manipulation has also been used to manipulate wave packets on the surface of materials. The Nelson group has demonstrated the generation of two-dimensional wave packets that are sculpted by a two-dimensional pulse shaper.[102] The excitation fields were directed toward distinct regions of a crystalline sample. As the waves emanated from their multiple origins, interferences among them resulted in focusing or amplified wave fronts.[103] These experiments are the culmination of early efforts into the manipulation and amplification of molecular motions in solids for inducing a phase transformation.[98,383]

Table 5. Shaped Pump Using GA

method	system	refs
fs, shaped pump, LIF	IR125 → IR125*, solution	384
fs, shaped CARS	CCl_4, CH_3OH, vibrations, liquids	391
fs, shaped pump, probe transmit	AlGaAs crystal	412
fs, shaped pump, LIF probe	Na, 3s → 3p, gas	387
fs, shaped pump, LIF probe	Na, 3s → 5s,gas	387
fs, shaped pump, LIF	DCM/$Ru(dpb)_3^{2+}$, solution	388
fs, Raman shaped, Raman,	CF_6, CO_2, gas	392
fs, shaped pump, Raman	CCl_4, CH_3OH, C_6H_6, C_6D_6, CO_2, vibr. liquids	393
fs, shaped pump, DFWM	K_2, molecular beam, vibrations	413
fs, shaped pump, probe LIF	Na, 3s → 5s, gas	389
fs, shaped pump, probe LIF	Rb, 5S → 5P → 4D, gas	390
fs, shaped pump, ion probe	Li_2, X → A → E → X^+, gas	365
fs, shaped pump, probe absorp	LH_2, S0 → Car/(B800,B850), solution	414
fs, Raman shaped, Raman	CCl_4, CH_3OH, C_6H_6, C_6D_6, CO_2, vibr., liquids	26
fs, shaped CARS	PDA, vibrations, crystal	394
fs, multiphoton shaped, LIF	$Ru(dpb)_3(PF_6)_2$, solution	415

4.3. Optimized Coherent Control and the Use of Learning Algorithms

In 1997, the Wilson group implemented an experimental setup in which a computer optimized the phase and amplitude of femtosecond pulses, with the goal of optimizing the measured experimental signal in a closed loop.[384] This experimental setup, where the apparatus learns to excite specific transitions based on the success of each laser pulse, was the first implementation of the scheme proposed in 1992 by Judson and Rabitz.[385] The Wilson group used an amplified femtosecond laser system that was coupled to a pulse shaper under the control of an evolutionary learning algorithm, also known as GA.[384] The experiment had the simple goal of optimizing the amount of two-photon induced fluorescence observed by the detector. For the first time, a computer program using a GA was used to change individual phase and amplitude parameters to optimize the excitation of a molecule, without being guided by theory. The computer program was guided only by the signal amplitude, which it used to determine its progress.

During the same year, the groups of Silberberg[158] and Gerber[163] demonstrated the use of adaptive pulse shaping for pulse compression. The principle behind these experiments was that TL pulses would generate the maximum SHG because they would have the highest peak intensity. Soon after implementing the pulse shaping methodology, Gerber's group applied it to control the branching of a chemical reaction in a complex polyatomic molecule.[386] Experiments using pulse shapers controlled by GAs have been applied for optimization of laser-induced fluorescence,[384,387−390] stimulated Raman emission,[26,391−394] high-harmonic generation,[392,395−398] ultrafast semiconductor switching,[399] pulse propagation through optical fibers,[400,401] and control of molecular dissociation and selective bond breaking.[386,402−411] Experiments aimed at control of molecular excitation (not reaction), based on a shaped laser pulse controlled by a GA, are referenced in Table 5.[26,365,384,387−394,412−415]

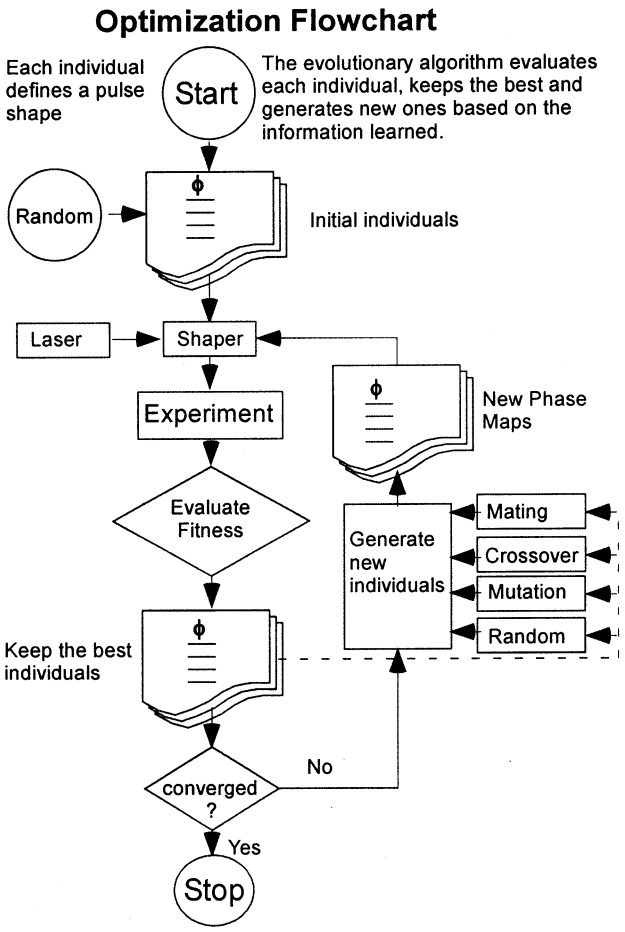

Figure 19. Flowchart for phase optimization with a GA.

The experimental implementation of coherent control with GAs requires a computer program that controls a pulse shaper and evaluates the experimental signal. Most computer programs used for coherent control are based on GAs with flowcharts similar to the one shown in Figure 19. Assuming the program controls the phase of 128 pixels in the SLM of a pulse shaper, an individual is defined by a list of 128 numbers (genes). The computer program evaluates the experimental signal resulting from excitation with 100 randomly generated phase functions and picks the 10 individuals whose signals more closely approach the target. The next generation of pulses to be evaluated is generated by combining attributes of the 10 best individuals. This is achieved through the exchange of one or more genes (spectral phases), by averaging, and by mutating them. Special mutation operators are written in the code to change the value or one or more genes. A number of new randomly chosen genes are introduced, to ensure global optimization. Once a pool of 100 new individuals is prepared, they are evaluated and the 10 best are selected again. After a number of iterations, the program converges toward the best solution. This type of program, similar to the one used by Wilson[384] and Gerber's[386] groups, is relatively easy to implement. More-advanced programs adapt their search plan as the program evolves toward the best solution. Bucksbaum and co-workers have implemented an adaptive program in which the operators that control the generation of new individuals change as the

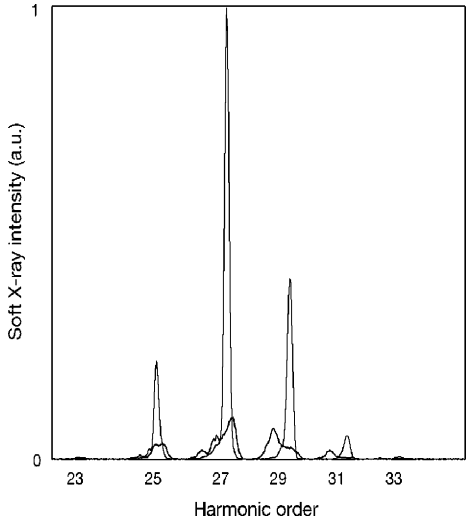

Figure 20. Optimization of the 27th harmonic, using a GA. The spectra shown correspond to the signal before (thick line) and after (thin line) optimization. (Reprinted with permission from *Nature* (http://www.nature.com), ref 395. Copyright 2000 Nature Publishing Group.)

program converges toward the final solution.[26] For example, at the start of the search, individuals are composed of randomly generated genes, and their success is as good as any other guess; however, as the program evolves, the individuals improve to the point that they are much more efficient (more fit) than those composed of randomly generated genes. The computer program adapts the search algorithm, reducing the number of randomly generated individuals and increasing the contribution of other operators. Adaptive GAs have been shown to be very efficient at finding solutions to multiple parameter problems; however, one should be aware that this method is prone to converging on local minima and not on the global optimum solution.

The GA control method has two very appealing qualities. On the experimental side, when implemented properly, it is designed to explore a very broad parameter space without constant participation of the experimentalist. From the scientific point of view, the GA solution may contain a scheme that has not been considered before, and, in effect, lead to new methods for coherent control. GA, pulse-shaping technology, and strong ultrashort pulses make a very powerful combination of tools for exploring coherent control of physicochemical processes. The challenges related to these types of experiments are quickly changing from questioning the ability to exert control on a system to being able to understand how the control was achieved. Efforts along these lines are already in progress.

Recently, shaped femtosecond laser pulses were used to optimize the high-harmonic (X-ray) emission. In particular, the goal was to optimize the 27th harmonic while minimizing other frequencies.[395] The GA-controlled pulse shaper was able to converge on the desired goal (see Figure 20). High-harmonic generation takes place when electrons are accelerated by the electric field and allowed to scatter their excess energy upon recollision with the nuclei. From this classical point of view, the timing during which the electrons are accelerated determines the harmonic that is generated. Phase modulation is then used to match the sub-femtosecond timing of ionization and recollision to select a specific harmonic.

The second example in this category concerns the photodissociation of $CpMn(CO)_3$.[411] It was found that enhancement of the yield of parent ion $CpMn(CO)_3^+$ was enhanced for an optimized field consisting of two 40-fs subpulses separated by 87 fs. Theoretical simulation of the experiment combining ab initio calculations of the relevant potential energy surfaces demonstrated that the excited state reached by the first pulse evolves during the first 87 fs to a configuration where maximum multiphoton ionization occurs. The combination of experiments and theory was used to unravel the optimized bond-selective photodissociation of polyatomic molecules. Unfortunately, it is unclear how the 40-fs subpulses were formed by the pulse shaper starting with 87-fs TL pulses with a 10 nm bandwidth. The channel that was optimized in this study (the parent ion) should be enhanced by TL pulses, when field ionization is maximized and can be suppressed by any pulse shaping that lowers peak intensity. Perhaps a more challenging pathway should have been chosen for control. The autocorrelation of the optimum pulses provided very limited information about the spectral amplitude and phase of the laser pulse. In the future, unraveling optimal control should include complete laser pulse characterization and control among pathways that are not optimized by TL pulses.

In general, experimental limitations of the optimum control scheme range from the purity of the initial state due to temperature, homogeneous and inhomogeneous dephasing, molecular orientations, and inter and IVR. In addition, there are other limitations imposed by the laser system. Among these are laser intensity fluctuations due to noise, focusing gradients at the sample, phase characterization, available bandwidth, wavelength of the laser pulse, and intensity of the laser pulse with respect to the relevant physics. Among the challenges to be addressed, in future experiments, we mention the need to determine if the GA has converged on the global optimum solution or not. For a pulse shaper with N pixels, one can generate $(P^*A)^N$ different shaped pulses, where P and A are the number of different phases and amplitudes a pixel can take. If we assume 100 pixels, each taking 10 different amplitude values and 100 different phase values, the number of different pulses is on the order of 10^{300}. This number is extremely large; therefore, while, in principle, the field exists to achieve the desired laser−matter outcome, finding the global optimum solution is a great challenge, if not impossible. Realistically, in a few days, an experiment can only sample 10^9 differently shaped pulses, limited primarily by the update time of the shaper. The ability of finding the global optimum with a GA is problem specific. The simplest problems, such as optimization of SHG, can be solved quickly because the global optimum is surrounded by promising nearby solutions. The other extreme to the simple case would be the "needle-in-a-haystack," for which no method is superior to random search

without repetition. Reaching a global maximum will in many cases require a reduction in the search space down to a manageable range $\sim 10^{19}$.

Experimentalists using GAs have attempted to reduce the search space by restricting the number of active pixels, the type of phase functions that are allowed, modulating phase and not amplitude, and introducing phase functions with a reduced numbers of parameters.[389,392,414] For one-pulse experiments, the periodic nature of electromagnetic waves results in a great deal of redundancy in pulse shaping because nonlinear optical processes do not depend on the absolute phase or a linear variation of the spectral phase. This equivalence can be expressed by $\phi(\omega) \Leftrightarrow \phi(\omega) + a + b\omega$, where a and b are constants. This redundancy can be filtered out by programming a GA that works on the second derivative of the phase. The actual phase that is used in the SLM is obtained by integration setting $a = b = 0$. Comstock et al. has introduced a strategy for drastically reducing the search space in an optimization experiment, where amplitude is kept constant and spectral phase takes only two values, 0 and π.[106] With this approach, binary phase shaping (BPS), when used on 128 active pixels reduces the search space to 2^{128}. If the problem has 2-fold symmetry, for example, achieving two-photon excitation at a specific narrow frequency using a broad bandwidth femtosecond pulse, the final search space is of size 10^{19}, a number that is at least 281 orders of magnitude smaller than would be considered for arbitrary phase and amplitude pulse shaping as discussed above. The resulting space is small enough that a significant percent of possible outcomes could be computed and a large portion evaluated experimentally. A simple GA can quickly converge toward significantly improved solutions.

BPS may have significant technological advantages. Retardation equivalent to π is easy and fast to obtain and calibrate. Permanently etched masks can be made in advance and used for specific applications, such as selective two-photon microscopy.[62] Scanning the mask can yield two-photon excitation spectra. Problems in laser control, especially those dealing with two-photon transitions, are simplified by BPS allowing direct analysis to propose rational solutions, or using a GA to search for an optimum solution. BPS has yet to be tested on problems that are more complex.

New alternatives for pulse shaping equipment are emerging now that researchers are finding the experimental advantages of controlling phase and amplitude of femtosecond pulses. Pulse shapers can now be constructed with a large number of pixels (where 1024 is the present record). Different pulse shapers, based on acousto-optic modulators, provide very large retardation (exceeding 40 π) and are now commercially available. A number of groups are working on micro-electromechanical systems (MEMS)-based shapers. The particular experimental requirements will determine the optimal parameters in the pulse shaper that are better suited for a specific task.

4.4. Optimized Coherent Control by Design

Advancements in pulse shaping and laser technology are allowing experimentalists to synthesize, with precision, pulses with specific characteristics. This has led to a series of experiments that are considered, here, as control by design. The premise of these experiments is that the spectroscopy and the nonlinear interaction between the laser and the sample are known. In these cases, we can design the electric field to achieve the desired control optimally. This is in contrast to experiments in which the GA is used to optimize a process without knowledge of the field or the spectroscopy. In this section, we discuss experiments that are based on carefully controlled phase and relatively weak fields (no saturation).

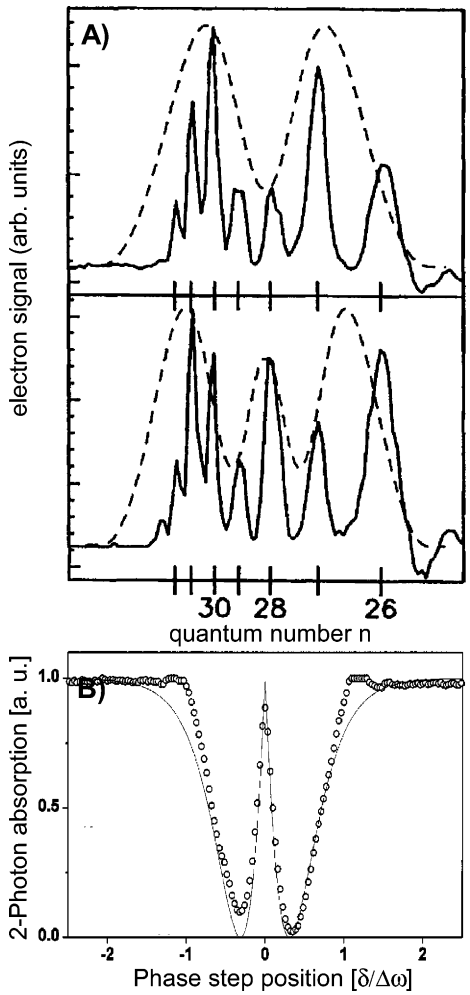

Figure 21. Control of two-photon processes with amplitude and phase modulation. (A) Two-photon excitation of Ru atoms with amplitude and phase shaped pulses. (Reprinted with permission from ref 309. Copyright 1992 American Physical Society.) (B) Excitation probability of a Cs atom two-photon transition, as a function of position, for a step-function phase that is scanned across the spectrum of the pulse. (Reprinted with permission from ref 418. Copyright 1999 American Physical Society.).

Some of the first experiments of coherent control by design were aimed at controlling two-photon transitions in isolated atoms. Broers and co-workers[56] realized, in 1992, that the spectral phase of a laser pulse could be considered to be analogous to the phase introduced by a Fresnel lens.[309] On the basis of the Fresnel analogy, Broers and Noordam demonstrated how amplitude modulation of linearly chirped pulses could be used to control the two-photon excitation of Rb atoms (see Figure 21A).[56,309]

They also showed that they could use amplitude and spectral phase to manipulate the SHG spectrum of their laser pulses.[416] Control of the two-photon transitions in Cs atoms was achieved by Silberberg in 1998,[417,418] who demonstrated similar control using phase-only modulation (see Figure 21B). Silberberg explained this control mechanism in terms of constructive interference that could be achieved at a specific frequency using a pulse shaper. Silberberg showed that the method did not work for large molecules in solution, because of their broad absorption spectrum.[418]

The explanation given by Broers, about focusing the available bandwidth at a specific frequency, necessitates starting with a heavily chirped pulse. The probability for two-photon excitation without an intermediate state is always maximized for TL pulses. The probability of two-photon excitation at a specific frequency is phase dependent; therefore, phase modulation can only lower the intensity of light at the specific frequency but cannot enhance it compared to TL pulses.[58,60,61] Broers work correctly described a theory that could be used to determine regions in the two-photon excitation spectrum where maximum (approaching TL) amplitude could be achieved. The Dantus group realized that the spectral phase modulated the probability for multiphoton excitation at many different frequencies.[60] In the case of isolated atoms with narrow absorption lines, it was easy to find conditions under which constructive or destructive interference could be identified. However, control of large molecules in condensed phase, with absorption bandwidths of hundreds of wavenumbers, required very short pulses with very broad bandwidth. In 2001, Walowicz et al. demonstrated coherent control of two- and three-photon transitions in large molecules in solution, using this principle.[60]

The multiphoton intrapulse interference (MII) experiments can be understood based on the explanation given in Section 2.5. about the dependence of nonlinear optical transitions on the spectral phase of the pulse. In general, TL pulses produce the maximum probability for multiphoton transitions in the absence of an intermediate state and saturation, because all frequencies are in phase. However, TL pulses induce indiscriminate excitation of all molecules. With MII, one is able to discriminate the order of excitation (two- vs three-photon excitation, for example) and the type of molecules that becomes excited in a mixture.[61,123] In principle, multiphoton excitation with broad bandwidth femtosecond pulses requires the combination of frequency components (photons) to induce multiphoton excitation or nonlinear optical signals. The combination of these photons depends on their phase, giving rise to constructive and destructive interference. It is possible to calculate the power spectrum of a shaped laser pulse centered at ω_0 using MII. The power spectrum has components near $2\omega_0$, $3\omega_0$, and higher. These harmonics are responsible for multiphoton excitation. The formula that can be used to calculate the complex amplitude of the nth order nonlinear power spectrum at a frequency $n(\Delta+\omega)$ is given by

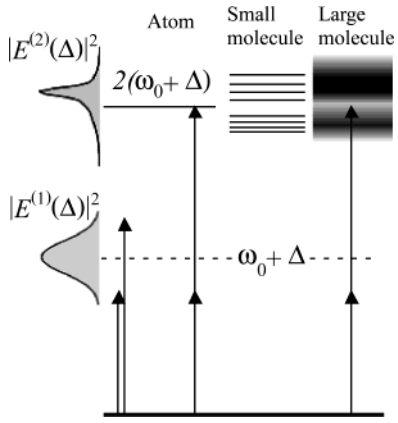

Figure 22. Schematic illustration of coherent control of two-photon excitation, using MII. Phase modulation changes the power spectrum responsible for two-photon excitation. Differences in the spectroscopy between atoms, small molecules, and large molecules require different phase-modulation parameters.

$$E^{(n)}(\Delta) \propto \int_{-\infty}^{\infty} E^n(t) \exp\{in(\Delta + \omega_0)t\} dt \qquad (8)$$

where Δ is a frequency detuning from the carrier frequency ω_0.

Equation 8 can be used to predict second- or third-harmonic generation spectra as well as n-photon excitation probabilities. Noordam and Hacker have used an analytical formula, applicable for two-photon processes to predict changes in the SHG spectra of the pulses with sinusoidal phase modulation.[58] Equation 8 was used to generate the power spectra shown in Figure 22. The goal of coherent control experiments based on MII is to control a multiphoton transition during the excitation process. This concept is shown in Figure 22. Notice that, for atoms, the condition is reduced to a single frequency. This case was treated by Silberberg.[341,419] As the molecule increases in complexity, the spectrum becomes crowded, due to the large number of degrees of freedom. When the molecule is placed in a solvent, the surroundings lead to broadening of the absorption lines, leading to continuous absorption bands. To control such systems, it is important to have very short pulses (because of their broad bandwidth) and specially designed phase functions that lead to broadband power spectra near the harmonic frequency of interest. The interference that results from MII is especially useful in preventing multiphoton excitation at specific frequencies, as discussed below.

The signal in MII experiments depends on the absorption spectrum of the molecule near the harmonics of the incident field. For weak fields we obtain

$$S^{(n)} \propto \int_{-\infty}^{\infty} g^{(n)}(\Delta)|E^{(n)}(\Delta)|^2 d\Delta \qquad (9)$$

where $g^{(n)}(\Delta)$ is n-photon absorption spectrum, and $|E^{(n)}(\Delta)|^2$ is calculated from eq 8.

MII experiments have been proven to be very robust, and amenable to simulation. The Dantus group has demonstrated control over two- and three-photon excitation of large molecules, including organic dyes and proteins in solution.[61] For these experiments, phase modulation functions were cho-

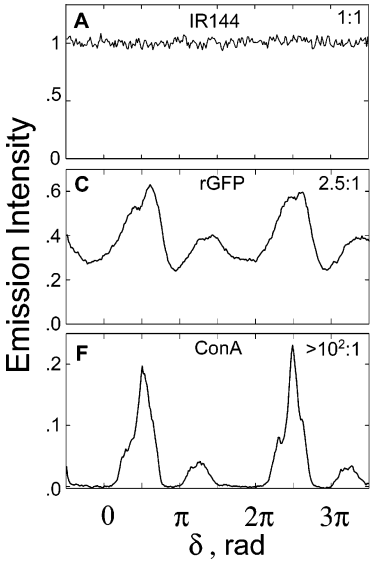

Figure 23. One-, two-, and three-photon excitation of macromolecules in solution (an IR-fluorescent dye, recombinant green fluorescent protein, and concanavalin A, respectively) with phase-shaped femtosecond pulses. The signal intensity versus phase function, defined by d (see text), is unchanged for one-photon excitation, but changes by a factor of 2.5 and >100 for two- and three-photon excitation, respectively. (Reprinted with permission from ref 60. Copyright 2002 American Chemical Society.).

sen, using the formula $f(\Delta) = \alpha \cos(\gamma\Delta - \delta)$, where Δ is the detuning frequency from the fundamental ω_0, and is used to determine the probability for multiphoton excitation at $n(\omega_0 + \Delta)$. The maximum phase modulation is controlled by α and is usually set between 1 to 2 π. The periodicity of the phase function is controlled by γ. In general, γ should be similar to the inverse of the absorption bandwidth that is being controlled, so long as the value is greater or equal to the pulse duration. For isolated atoms and small molecules, γ can be much greater than the pulse duration. The position of the phase function, with respect to the carrier frequency of the pulse, is determined by δ, a parameter that is usually scanned between 0 and 4 π. The experimental results, shown in Figure 23, demonstrate control of two- and three-photon transitions in macromolecules using MII. Notice that, for first-order absorption and induced fluorescence (see Figure 23A), phase modulation has no effect. For two- and three-photon induced fluorescence, though, phase modulation has an important effect (Figure 23B,C).

MII is very sensitive to changes in the nonlinear absorption spectrum of the sample. This sensitivity can be used to achieve selective excitation of molecules, depending on their immediate chemical environment. On the basis of this principle, the Dantus group has demonstrated selective two-photon excitation of molecules in different pH environments.[123,124] In their experiment, they used 8-hydroxypyrene-1,3,6-trisulfonic acid (HPTS), a large organic molecule with unit fluorescence quantum yield. Because the pK_a of HPTS is 7.5, it is protonated in acidic environments and deprotonated in alkaline environments. The state of protonation affects the absorption spectrum of HPTS in the region corresponding to two-photon excitation near 820 nm. These changes can

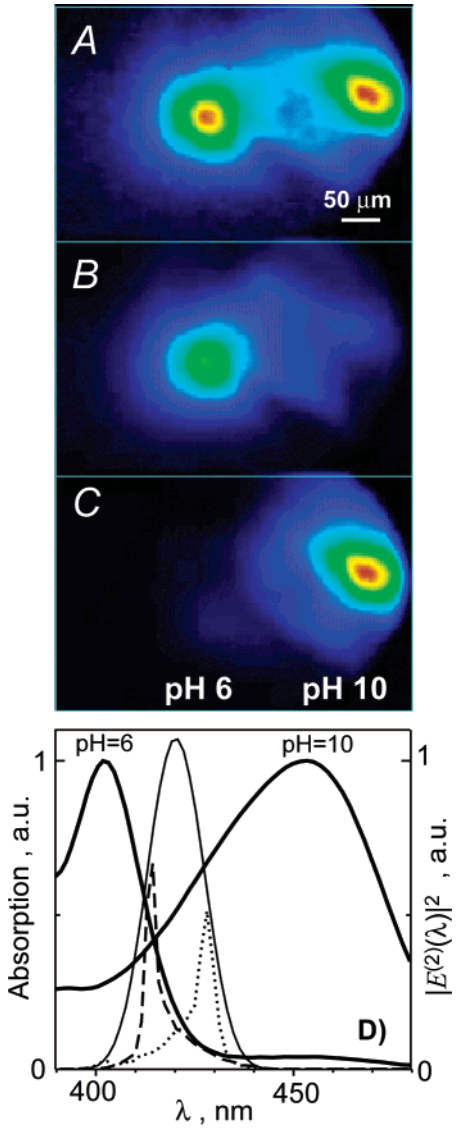

Figure 24. pH-selective two-photon microscopy. The images show two-photon induced fluorescence from a sample labeled with a pH-sensitive dye. Frame A shows fluorescence of the acidic (left side) and basic (right side) regions of the sample, as obtained with TL pulses. Frames B and C show images of the sample obtained with pulses optimized for selective excitation in an acidic and in a basic environment, respectively. The diagram below shows the absorption spectrum of the dye in acidic and basic solution (thick lines), and the square of the electric field for the shaped laser pulses used to optimize selective excitation (dashed and dotted lines). (Reprinted with permission from ref 123. Copyright 2003 American Chemical Society.)

be used to cause selective pH-sensitive excitation, using MII. The experiments, shown in Figure 24, show a polymer that has been doped with HPTS. In the polymer, there are two distinct regions, one cured at pH 6 and one cured at pH 8. When 23-fs TL pulses centered at 842 nm are used, both regions show two-photon induced fluorescence. Using MII, one can determine the required spectral phase modulation that is required to selectively excite the acidic or the alkaline regions.[123,124] In the bottom of Figure 24, the absorption spectra of the probe molecule, under different pH conditions, are shown (thick line). Because of the pronounced changes, MII can be used to selectively excite multiphoton transitions at wave-

Table 6. Shaped Pump

method	system	refs
ns, shaped pump, LIF	I_2, X → B, gas	119
fs, shaped pump, Raman scattering	α-perylene crystal	98
ps, shaped pump, e^-	Rb, → n 25−30, beam	309
ps, strong pump, ion probe	Na, 3s−7p, 3s−4p, beam	420
ps, strong pump, ion probe	Na, 3s−7p, 3s−4p, 3s−7p, beam	421
ps, shaped pump, e^-	Cs; 7s → 20−32p, beam	422
fs, shaped pump, ion probe	Li_2; X → A → E → X, gas	362
fs, shaped pump, LIF	Cs, 6S → 8S, gas	417
fs, shaped pump, ion probe	Li_2; X → A → E → X, gas	335
fs, shaped pump, e^- probe	Cs; 7s → 20−32p, gas	330
fs, shaped pump, LIF	Rh610, solution	423
fs, shaped pump, LIF probe	SNAFL-2,	353
fs, shaped pump, LIF	Cs, 6S → 8S, gas	418
fs, shaped pump, ion probe	Li_2; X → A → E → X, gas	364
fs, shaped pump, e^- probe	Cs; 7s → 20−32p, gas	331
fs, shaped pump, ion probe	Li_2; X → A → E → X^+, gas	336
fs, shaped pump, LIF	Rb, 5S → 5P → 4D, gas	341
fs, shaped pump, ion probe	Li_2; X → A → E → X, gas	424
fs, shaped pump, ion probe	Li_2; X → A → E → X, gas	337
fs, shaped pump, ion probe	Li_2; X → A → E → X^+, gas	338
fs, shaped pump, Raman probe	CCl_4, vibrations, liquid	425
fs, shaped pump, LIF probe	Rb, 5s → 5p-nd,ns, gas	426
fs, shaped pump, LIF	Rb, 5S → 5P → 4D, gas	342
fs, shaped pump, ion probe	Li_2; X → A → E → X^+, gas	339
fs, shaped pump, ion probe	Li_2; X → A → E → X^+, gas	344
fs, shaped pump, LIF	dyes, crystals, macromolecules	60
fs, shaped pump, LIF	dyes, crystals, macromolecules	61
fs, shaped pump, LIF	dyes, crystals, macromolecules	62
fs, chirped MIR pump, dissociation	$Cr(CO)_6$, gas	427

lengths shorter or greater than 420 nm. During the experiment, the spectrum and intensity of the beam remain constant; however, the energy where multiphoton transitions occur changes according to changes in the spectral phase. This principle is used to shape the pulse and illuminate a 250-μm region in the sample with the laser. A microscope is used to collect the images in Figure 24, demonstrating selective multiphoton excitation using MII.

The first application of phase-tailored pulses for sensing pH involved intense linearly chirped laser pulses that saturated the one-photon resonant transition of a pH-sensitive dye.[353] Wilson's group found that the ratio between the LIF signals obtained for positively and negatively chirped pulses was found to vary from 1.9 to 1.2 for different pH values. Unfortunately, this ratio did not vary monotonically, being the same for pH 7 and pH 9.

In Table 6, we give references to experiments in which pulse shaping has been used to control excitation.[60−62,98,119,309,330,331,335−339,341,342,344,353,362,364,417,418,420−427] Most experiments are characterized by the introduction of a specific phase function by the experimentalists. The choice of phase was based on physical principles. In general, the degree of control shown in most of these experiments is extremely good. The method has been applied to isolated atoms as well as large molecules, including proteins and crystals. The remaining limitations to control methods based on the design of specific phase shaped pulses are both technical and conceptual. On the technical side, experimentalists would like to have shorter pulses with greater energy per pulse. Presently, pulses as short as 15 fs have been shaped to control the excitation of macromolecules.[62] Kobayashi's research group has a shaped femtosecond source capable of generating 4-fs pulses.[68,169] They have used a pulse shaper to reduce spectral phase deformations, but, to our knowledge, not to carry out a coherent control experiment. Regarding conceptualization of the experiments, there is always the possibility that a nonlinear excitation electromagnetic field exists that has not been explored. For these reasons, GA controlled experiments (discussed in the previous section) that are programmed to explore a wide range of pulse shapes can prove extremely valuable.

5. Coherent Control and Four-Wave Mixing

One of the most important contributions from the field of coherent control has been a greater understanding of laser−molecule interactions. This has led to the development of enhanced spectroscopic methods. Among the most salient of such enhancements, we discuss here is the PE effect and mode suppression. In Table 7, we give reference to a number of experiments that have taken advantage of optical coherence and molecular coherence to control nonlinear spectroscopic signals recognized under the rubric of FWM.[20,74,75,114,340,360,419,428−480]

5.1. Suppression of Inhomogeneous Broadening

Inhomogeneous broadening is the spectroscopic manifestation of the fact that every molecule or atom in the sample may have a slightly different environment, which leads to differences in their absorption and emission spectroscopy. These differences make it difficult to obtain spectroscopic information that is not convoluted by all the locally perturbed species. From the point of view of coherent control, it important to design electric fields able to control an inhomogeneous sample. Otherwise, coherent control would only be applicable to isolated molecules.

In 1964, the PE method was demonstrated,[481] and it was realized that it played an analogous role to that of the Hahn spin−echo.[482] The PE phenomenon is best explained as the interaction of three electromagnetic waves on a sample. The three waves need not be three separate laser pulses, as a laser pulse can accomplish the role of one, two, or three interactions. Here, we explain the two-pulse PE for illustration. Consider the polarization that a laser induces on the sample at time $t = 0$. The time evolution of that polarization between the first and second pulses is described by $\exp(i\omega t_{12})$, where ω represents every quantum-mechanical state within resonance of the excitation pulse (See Figure 25). Interaction with a second laser pulse at time $t = t_{12}$ stimulates the transition of the excited molecules back to the ground state, thereby arresting the evolution of their polarization. The third laser pulse (or the second for a two laser experiment) induces a new polarization evolving with $\exp(-i\omega t_{23})$, as shown in Figure 25. The output signal is proportional to the third-order polarization

Table 7. Coherent Control with FWM

method	system	refs
ns, phase-locked, multipulse	I_2 gas	428
fs, chirped pump, CSRS	GaAs/AlAs QW	429
fs, chirped pump, CSRS, CARS	resorufin, solution	430
fs, chirped pump, DFWM	resorufin, solution	431
fs, DFWM	K, buffer gas	432
fs, phase locked DFWM	DTTCI, solution	433
fs, phase locked, HSPE	DTTCI, solution	434
fs, mode suppression, HSPE	DTTCI, solution	435
fs, DFWM	NaI, gas	436
fs, phase locked, HSPE	DTTCI, solution	437
fs, CARS	I_2, gas, vibrations	438
fs, DFWM, CARS, CSRS	I_2, gas, vibrations	439
fs, CARS	I_2, gas, vibrations	440
fs, DFWM,	DTTCI, solution	441
fs, CARS	I_2, gas, vibrations	442
fs, phase locked, HSPE	DTTCI, solution	443
fs, CARS	benzene/toluene gas	444
fs, DFWM,	I_2, gas, vibrations	445
fs, DFWM,	I_2, gas, vibrations	360
fs, DFWM, CARS, CSRS	I_2, gas, vibrations	452
fs, PE	CO in hemoglobin	453
fs, DFWM,	I_2, gas, vibrations	340
fs, DFWM, CARS	I_2, gas, vibrations	454
fs, DFWM,	I_2, gas, vibrations	446
fs, DFWM,	I_2, gas, vibrations	447
fs, CARS	K_2, jet, vibrations	455
fs, CARS	PDA, crystal, vibrations	456
fs, DFWM, CARS, CSRS	I_2, gas, vibrations	457
fs, CARS	benzene/toluene gas	457
fs, CARS	PDA, crystal, vibrations	457
fs, CARS	I_2, gas, rovibrations	459
fs, CARS	PDA, crystal, vibrations	460
fs, DFWM	K_2, molecular beam, vibrations	461
fs, DFWM	I_2, gas, vibrations	448
fs, DFWM	I_2, gas, vibrations	74
fs, DFWM	K_2, molecular beam, vibrations	462
fs, DFWM	I_2, gas, rovibrations	463
fs, CARS	I_2, gas, vibrations	464
fs, CARS	I_2, gas, vibrations	561
fs, CARS	porphyrin, solution	465
fs, CARS	porphyrin, solution	466
fs, DFWM	I_2, gas, vibrations	20
fs, DFWM, shaped pump	K_2, gas, vibrations	467
fs, CARS	I_2, solid Ar, rovibrations	468
fs, CARS	I_2, gas, vibrations	469
fs, CARS	porphyrin, solution	470
fs, DFWM	I_2, gas, vibrations	450
fs, DFWM	I_2, gas, vibrations	451
fs, CARS	PDA, crystal, vibrations	458
fs, DFWM	I_2, gas, vibrations	449
fs, CARS	I_2, gas, vibrations	471
fs, CARS, shaped	CH_3OH, CH_2Br_2, $(CH_2Cl)_2$, liquid	419
fs, DFWM	I_2, gas, vibrations	75
fs, CARS	I_2, gas, vibrations	472
fs, CARS	PDA, crystal, vibrations	472
fs, DFWM	I_2, gas, vibrations	473
fs, CARS, shaped	C_6H_6, $C_6H_5CH_3$, pyridine, liquid,	474
fs, CARS, shaped	CH_3OH, CH_3I, CCl_4, CS_2, $C_6H_3(CH_3)_3$ liquid	475
fs, CARS, shaped	$Ba(NO_3)_2$ crystal, pyridine liquid	476
fs, CARS	porphyrin, solution	477
fs, CARS	-carotene, solution	478
fs, CARS	β-carotene, solution	479
fs, CARS, shaped	diamond, $Ba(NO_3)_2$, $C_6H_5CH_3$, Lexan,	480
fs, CARS, shaped	CH_3I, $C_2H_4Cl_2$, *p*-xylene, liquids	114

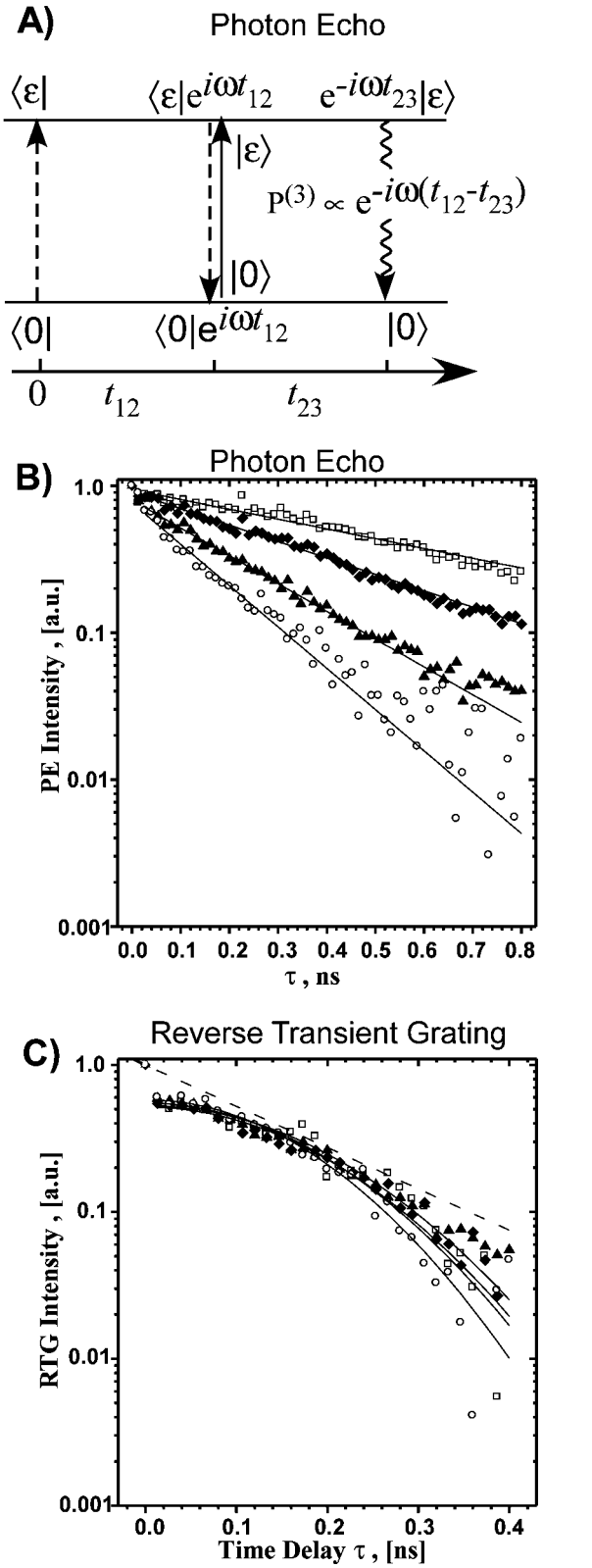

Figure 25. (A) Ladder diagram for PE excitation. (B and C) PE and reverse transient grating measurements on gaseous iodine molecules. The decay observed arises from homogeneous (PE) and inhomogeneous (TG) electronic dephasing. (Reprinted with permission from ref 449. Copyright 2001 Elsevier Science B. V.)

squared, which is proportional to $\exp\{-i\omega(t_{12} - t_{23})\}$. Notice that, when $t_{12} = t_{23}$ the signal reaches a maximum, the PE. In the presence of inhomogeneous broadening, the time evolution of every molecule

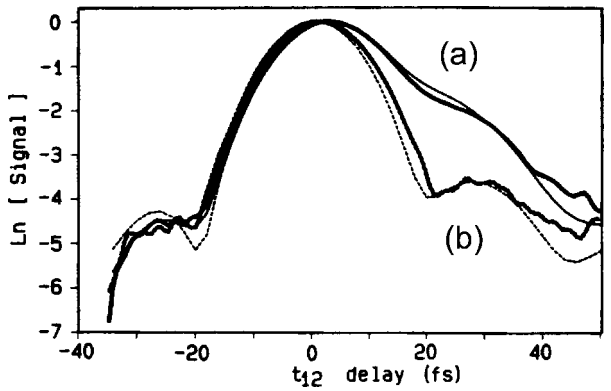

Figure 26. Electronic dephasing time measurements on LD690 in solution, using PE (a) with and (b) without vibrational mode suppression. (Reprinted with permission from ref 484. Copyright 1993 Elsevier Science B. V.)

proceeds at a different frequency; however, the echo time depends only on the timing between the two pulses and not on the frequency. The homogeneous electronic dephasing, measured using a PE sequence, decays exponentially (Figure 25B), while the inhomogeneous electronic dephasing, measured with the same laser pulses, but using a reverse transient grating sequence, decays nonexponentially (Figure 25C). The PE pulse sequence should be expressly studied for coherent control, because inhomogeneous broadening is essentially canceled.[74,75,360,445−449,483] The PE sequence could play a critical role in laser control in condensed-phase media.

5.2. Mode Suppression; Macroscopic and Microscopic Interference

PE experiments have typically been used to determine the homogeneous dephasing of molecules and materials. In some instances, vibrational dynamics of the molecules can interfere with these types of measurements, particularly when the vibrational period is similar to the dephasing time. Shank and co-workers realized that, if the time delay between the first two pulses in a PE measurement corresponds to the vibrational period that interferes with the measurement, that vibration is suppressed from the transient.[484] In Figure 26, we show experimental results in which mode suppression was used to reveal the true electronic dephasing of LD690, an organic laser dye, in solution. The mode suppression method was not developed expressly as a coherent control method, but we include it here for two reasons. First, it depends on the coherent interaction of two or more pulses. Second, the method depends on the vibrational coherence of the sample. Therefore, mode suppression depends on the interaction between the optically induced electronic coherence, and vibrational coherence. Mode suppression and other pulse sequences have been studied in the gas phase and interpreted using wave packet simulations as well as the density matrix approach.[74,75,451] These types of experiments can teach us valuable lessons that can be used to interpret present experiments and plan future experiments, especially in condensed phases. From the example in Figure 26, we learn that electronic coherence survives for times less than 50 fs, for large molecules in solution. Consequently, coherent control experiments in condensed phase should involve very short pulses (τ <20 fs) or not depend on electronic coherence.

5.3. Ground-State Dynamics

In Section 4.1, we discussed the pump−probe method. Here, we remark that, in most cases, the pump−probe method leads to the observation of excited-state dynamics. Observation of ground-state dynamics can be achieved by different approaches that can be understood under the rubric of FWM. Experiments using three separated pulses give the best illustration of this approach. The first pulse creates a wave packet in an excited state; the second pulse induces a transition back to the ground state; and the third pulse, after some time delay, probes the ground-state dynamics by inducing a transition to the excited state.[451] The coherent FWM signal emission is then collected as a function of time delay between the first two pulses and the probe pulse. These experiments take advantage of optical coherence with the electric field. In addition, it is possible to use the timing between the first two pulses, taking advantage of intramolecular coherence, to determine if ground- or excited-state dynamics are to be observed. This experiment is shown in Figure 27, where excited-state or ground-state dynamics are observed exclusively when the time delay between the first two pulses is 460 or 614 fs. When the wave packet prepared by the first pulse moves to a Franck−Condon region with good overlap to the ground state, the second pulse can stimulate a transition back to the ground state. When the wave packet in the upper state is in a region that has minimal overlap with the ground state, the second pulse cannot stimulate back to the ground state. In this case, excited-state dynamics are observed.[20,74,75] The results shown in Figure 27 required both electronic and vibrational phase coherence.

Many groups have taken advantage of FWM methods to study ground-state dynamics. By tuning the wavelength of the laser pulses, groups have been able to prepare wave packets in the ground state with as much as 10 000 cm^{-1} of excess energy above the ground state.[394,427,471] In these experiments, the dynamics of such highly excited wave packets are monitored by the third laser pulse.

Impulsive excitation by an off-resonance pulse leads to the creation of coherent superpositions of rotational and vibrational states. The time evolution of these superpositions can be followed by a probe beam, and the measurement is known as a transient grating (see Section 2.3.2). This method is very useful to follow ground-state dynamics. As the rotational wave packets evolve in time, the index of refraction of the vapor that has been irradiated by the first pulse changes as well. These transient changes have been demonstrated to be useful for inducing changes in the spectral phase of ultrashort pulses and have been used for pulse compression.[361,485]

The time evolution of molecular wave packets is followed by tracking the changes in the third-order susceptibility of the sample, affecting the third-order

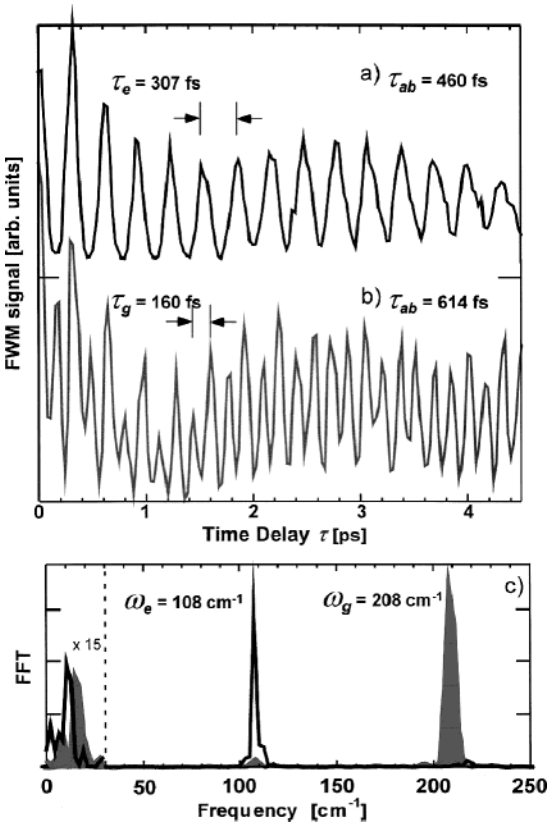

Figure 27. Experimental demonstration of population control, using three-pulse FWM. (a) Transient showing excited-state vibrational dynamics with a period of 307 fs. (b) Transient showing ground-state vibrational dynamics with a period of 160 fs. (c) Power FFT corresponding to each transient. For the FFT of the first transient (black line), the most prominent peak is centered at 108 cm^{-1} corresponding to the vibrational dynamics of iodine in the excited state. For the FFT of the second transient (gray line), the most prominent peak is centered at 208 cm^{-1} corresponding to the vibrational dynamics of iodine in the ground state. The peak centered at 16 cm^{-1} corresponds to the rotational motion. (Reprinted with permission from ref 445. Copyright 1999 American Institute of Physics.)

polarization. The intensity of the emitted wave in FWM is proportional to the square of the third-order polarization of the sample.[36] Given that FWM is a macroscopic phenomenon, the signal is affected by intramolecular coherence as well as by coherence between different molecules. If a mixture of two vapors is prepared, for example, benzene and toluene, the transient grating signal will contain the regular features corresponding to each of the constituents (microscopic coherence) and cross-features (macroscopic coherence).[457] This phenomenon was shown for a mixture of oxygen and nitrogen in which the signal was found to be proportional to $|\chi^{(3)}(O_2) + \chi^{(3)}(N_2)|^2$.[20] Macroscopic coherences have also been shown to play an important role in controlling the type of dynamics (ground or excited state) that are observed in a FWM experiment.[451]

6. Challenges in Coherent Control

Thus far, we have covered a number of systems in which coherent control strategies have been very successful. Here, we address some of the most important challenges in the field. Predominantly, we discuss the area of coherent control of chemical reactions. We make a distinction between unimolecular photodissociation, a process that is at least controllable in principle, and bimolecular chemical reactions, a problem which, in many cases, may not be controllable. We later discuss inhomogeneous and homogeneous broadening and its impact on coherent control strategies. Finally, we discuss IVR and the limited time window available for coherent control of chemical reactions.

6.1. Chemical Reactions

Clearly, one of the most challenging problems in coherent control is achieving coherent control of chemical reactions. There are several examples where a laser, or a combination of lasers, has been used to control the products that are observed, but these exciting results are still far from the goal of having a protocol that can be followed to control a number of different chemical reactions. It is too early to determine if laser-controlled chemical synthesis will ever replace conventional synthetic methods, even for a single molecular system. This prospect raises the fact that coherent laser photons are expensive. Fortunately, advances in laser technology have brought the cost of a mole of femtosecond-shaped photons, a unit called an Einstein, to the level that is comparable to the cost of a mole of the average pure chemical reagent.[486] This implies that at least in some special cases, laser-controlled synthesis could be considered as a realistic alternative.

The landmark experiment that demonstrated that shaped femtosecond laser control could be used to enhance one reactive pathway over another was carried out by Gerber's group.[386] The experiment concerned the photodissociation of dicarbonylchloro-(η^5-cyclopentadienyl)iron CpFe(CO)$_2$Cl, using intense 80-fs shaped pulses.[386] An illustration from that report is shown in Figure 28. The most important result from that experiment was that small changes in the phase of the incident pulse could alter different product ion ratios, as detected in the mass spectrometer (absolute yield was not measured). It was possible to enhance or suppress the different ratios, regardless of the strength of their chemical bonds. These pioneering results from Gerber's group have inspired a number of experiments on other chemical systems.[26,365,387−390,392−394,412−415]

The article by Assion et al., when first published, left some questions regarding the effect of peak intensity of the femtosecond pulses on the observed changes in fragmentation. Because phase modulation affects pulse duration, it serves to regulate peak intensity. The Gerber group has devised clever experiments in which they track the intensity of SHG concurrently with an optimization experiment to determine if the highest or lowest peak intensity pulse shape is also optimum.[415] This study has shown that optimization of specific fragment ions are not correlated to SHG intensity. In that study, the fragment ion required an intermediate intensity; therefore, the experiment only proved that TL pulses were not optimum. Currently, it is too early to de-

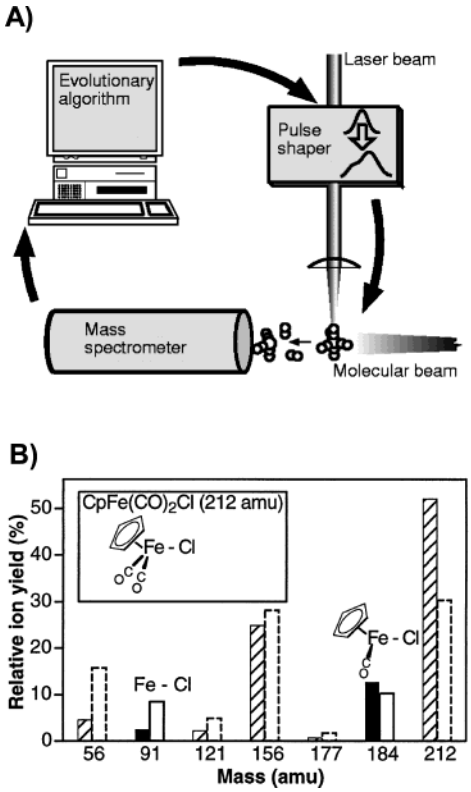

Figure 28. (A, B) Control over a chemical reaction with shaped femtosecond pulses, using a GA. (Reprinted with permission from *Science* (http://www.aaas.org), ref 386. Copyright 1998 The American Association for the Advancement of Science.).

termine if the original results from Assion et al. depended on laser-driven intramolecular coherence, on the manipulation of the potential energy surfaces by the intense field, or on intensity regulation. This determination will require complete spectral phase characterization of the pulses interacting with the sample and a demonstration that changing some phases, while keeping peak intensity constant, strongly affects the outcome. Unfortunately, only an autocorrelation of the pulse was provided, making it virtually impossible to reconstruct the phase−amplitude characteristics of the pulse in the time and frequency domains. Ultimately, the experiment was subject to one of the limitations of ion detection discussed in Section 2.3.3, namely, which processes occurred in the neutral species and which occurred after ionization.

The effect of photo fragmentation in strong fields had been studied with nanosecond and picosecond pulses. Earlier studies had noted that polyatomic molecules, upon irradiation with intense lasers showed direct ionization or "ladder switching," a process in which intermediate excited states were populated, leading to the observation of fragment ions in the mass spectrum.[487,488] More modern studies make the distinction between adiabatic single active electron (SAE) ionization, an approximation that works well for atoms and small molecules,[489−491] and nonadiabatic multielectron excitation and ionization (NME), a new model proposed by Stolow and co-workers.[89] The NME model includes the increasing participation of multiple electrons in a molecule during strong field excitation. Experimentally, small molecules under high intensity excitation become singly or multiply ionized. Larger molecules, however, may exhibit extensive fragmentation, due to the participation of multiple electrons. In general, longer wavelengths are more likely to include SAE ionization, while shorter wavelengths are more likely to induce NME ionization.

An example of multiple fragmentation and control is the study by Levis et al. on acetophenone,[407] where the sample, at a static pressure of 10^{-6} Torr, was irradiated by shaped pulses, and the ions were collected by TOF. TL pulses were found to cause extensive fragmentation, the most intense fragment ions found at M/Z values of 18(H_2O^+?), 28(CO^+), 43(CH_3CO^+?), 58($C_3H_6O^+$?), 68($C_4H_4O^+$), 77($C_6H_5^+$), 92($C_7H_8^+$), and 105($C_6H_5CO^+$). The species with a question mark were observed with significant intensity but not assigned by the authors. As mentioned earlier, large organic molecules are known to exhibit multiple fragmentation under intense laser fields.[89] Using a phase-amplitude pulse shaper (128 pixels, in 8 groups of 16 pixels each), where each group of pixels could take 360 different voltage values (corresponding to different values of phase retardance and/or amplitude, undeterminable without SLM calibration), the authors defined the search space. A learning algorithm was then used to optimize the ratio of peaks with mass (92)/(77). The results showed that after 20 generations (approximately 14 min) the ratio had improved from 1 observed for TL pulses to 1.6. Of particular interest is the fact that the peak at $M/Z = 92$ results from a rearrangement where the bridging CO is lost. They performed a second experiment with deuterated acetophenone $C_6H_5COCD_3$, and after a new optimization, the $C_6H_5CD_3$ mass was observed (data not shown). The authors concluded that the peak with $M/Z = 92$ must be toluene ions, although structural information is not available in mass spectrometry.

The experiment by Levis et al.[407] shows that for large molecules, where intense radiation causes multiple fragmentation, changes in the phase-amplitude profile of the laser, can be used to alter the relative amplitude between different peaks. A deeper interpretation of the experiment is impossible because no information (not even spectrum, pulse duration, or spectral phase) was given about the optimized laser pulses. No information is known about the fate of neutral species because they are not detected in this experiment. Unfortunately, the mass spectrum obtained after optimization was not shown, so one cannot tell how the amplitude for all the other fragments changed after pulse optimization. Molecular rearrangements, and specific fragmentation patterns, are common in electron impact mass spectrometry. It would be instructive to know which processes occurred while the field was interacting with the molecule, and which processes occurred afterward.

Current challenges in coherent control of chemical reactions can be divided into a number of categories. First, we mention unimolecular reactions involving isomerization. These kinds of chemical reactions have

been shown to be controllable, at least in theory.[15] Second, we mention chemical reactions where one is able to detect all neutral fragments from the reaction without bias, and one is able to show changes in the production of neutral species. In this regard, no such experiments have been reported to date.

There are two laser-based approaches capable of controlling photochemistry that are not based on coherence. One is bond-selective excitation,[492−508] an approach that works only for molecules with unusually slow IVR. The second approach entails excitation of different excited states, for example, in the photodissociation of CH_2IBr, different excitation wavelengths produce different products.[509] These approaches do not involve coherent control; however, they are mentioned because it is possible to cause bond-selective excitation by multiphoton-excitation processes, where the total energy is equivalent to spectroscopic transitions, known to lead to selective photochemistry. In Table 8, we summarize experimental research where laser control of chemical reactions has been demonstrated.[82,265,306,386,402−411,492−515] In this table, we begin with experiments aimed at bond-selective excitation, and we conclude with some of the more recent experiments with shaped laser pulses optimized using GAs.

6.2. Bimolecular Reactions

For unimolecular reactions, especially those involving bond cleavage or isomerization, it is conceivable that an electric field does exist to achieve the desired chemical change. However, for bimolecular reactions, those involving bond formation between two separate atoms or molecules, controllability of the outcome by an electromagnetic field can be questioned. There have been a few experimental successes in this extremely challenging problem. The first successful intervention of a laser to alter the outcome of a bimolecular reaction can be traced to an experiment by Brooks and Curl.[516] In their study, a nanosecond laser, not resonant with the asymptotic transitions of reactants or products, was used to open a chemiluminescent product channel. The experiment tracked the bimolecular reaction $K + HgBr_2 \rightarrow KBr + HgBr$. When a laser beam at 590 nm, far from resonance with any of the reactants or products, was introduced, a new product was detected. The new product had the distinct emission of HgBr*, an excited state that could only have been reached if the collision complex, while chemical bonds were being formed and broken, had been excited. This was perhaps one of the first attempts to change the course of a bimolecular reaction by excitation of the transient collision complex.

It is well-known that vibrational excitation leads in most cases to enhanced bimolecular reaction rates. In fact, vibrational excitation of specific eigenstates was the basis for bond-selective bimolecular reaction control,[180] a method not reviewed here, because it does not involve coherence. The observation of vibrational coherence in photodissociation products[517−520] leads one to consider the transition-state geometry being such that vibrational coherence ensues upon dissociation. If we consider the photodissociation process in reverse, as a bimolecular encounter, then the cross section would be found to depend on vibrational coherence. The cross section would be greatest when the interatomic distances of the reagents are closest to those corresponding to the

Table 8. Control over Reaction Channels

method	system	refs
ns, IR + UV	$OCS \rightarrow {}^{33}S/{}^{34}S$, gas	492
ns, IR + UV	$O_3 \rightarrow O(^1D)/O(^1\Delta_g)$, gas	493
ns, 193, 210, 248	$CH_2IBr \rightarrow I/Br/Ibr$, beam	509
ns, IR + UV	HNCO, $NH(a^1\Delta)/NH(X^3\Sigma^-)$, gas	494
ns, VUV	HOD → H + OD/D + OH, gas	495
ns, IR(OH) + UV	HOD → H + OD/D + OH, gas	496
ns, Raman(OH) + VUV	HOD → H + OD/D + OH, gas	497
ns, IR(OH)	H+HOD → H_2 + OD/HD + OH, gas	498
ns, IR(OH)	H + HOD → H_2 + OD/HD + OH, gas	499
ns, Raman (OH/OD) + VUV	HOD → H + OD/D + OH, gas	500
ns, IR(OH/OD)	H + HOD → H_2 + OD/HD + OH, gas	501
fs excitation−ionization	$Na_2 \rightarrow Na_2^+/Na^+$, beam	265
ns, IR(OH)	Cl + HOD → OH + DCl/OD + HCl, gas	510
ns, 222,248	$CH_3SH \rightarrow CH_3 + SH/CH_3S + H$, beam	511
ns, IR(OH/OD) + UV	H + HOD → H_2 + OD/HD+OH, gas	502
ns, IR(OH/OD) + UV	H + HOD → H_2 + OD/HD + OH, gas	512
ns, IR(OH/OD) + UV	H + HOD → H_2 + OD/HD + OH, gas	503
fs, pump-dump-probe	$NaI \rightarrow Na + I/Na^+ + I^-$, gas	513
fs excitation−ionization	$Na_2 \rightarrow Na_2^+/Na^+$, beam	562
ns, IR(CH) + 248/193	$C_2H_2 \rightarrow C_2H(A^2\Pi)/C_2H(X^2\Sigma^+)$, beam	504
ns, IR(OH/OD) + UV	Cl + HOD → OH + DCl/OD + HCl, gas	505
ns, IR + UV	HNCO, NCO/NH, gas	506
ns, IR + UV	HNCO, NCO/NH, gas	507
fs, chirped pump−probe	$Na_2 \rightarrow Na_2^+/Na^+$, beam	306
ns	$Na_2 \rightarrow Na(3s) + Na(3p)/Na(3s) + Na(3d)$	514
fs, shaped pump, GA	$CpFe(CO)_5 \rightarrow Fe(CO)_5^+/Fe^+$, beam	386
fs, shaped pump, GA	$CpFe(CO)_2Cl \rightarrow FeCOCl^+/FeCl^+$, beam	386
fs tailored pump, GA	$CpFe(CO)_5 \rightarrow CpFe(CO)_5^+/Fe^+$, beam	402
fs polarized pump,	$I_2 \rightarrow I + I^*/I + I$, ss jet	515
fs, chirped pump−probe	$Na_2 \rightarrow Na_2^+/Na^+$, beam	82
fs, pump−probe, GA	$CsCl \rightarrow Cs + Cl/Cs^+ + Cl^-$, beam	403
fs, pump−probe, GA	$CsCl \rightarrow Cs + Cl/Cs^+ + Cl^-$, beam	404
fs, shaped pump, GA	$CpMn(CO)_3 \rightarrow CpMn(CO)_3^+/CpMn(CO)^+$, beam	405
fs, shaped pump, GA	$CpFe(CO)_2Cl \rightarrow CpFeCOCl^+/FeCl^+$	406
fs, shaped pump, GA	$CH_3COCF_3 \rightarrow CH_3^+/CF_3^+$, beam	407
fs, shaped pump, GA	$C_6H_5COCH_3 \rightarrow C_6H_5CO^+/C_6H_5^+$, beam	407
fs, shaped pump, GA	$C_6H_5COCH_3 \rightarrow C_6H_5CH_3^+$, beam	407
ns, IR + UV	HNCO, H + NCO/^{3}NH + CO, beam	508
fs, shaped pump, GA	$CH_3COCH_3 \rightarrow CH_3CO^+$, beam	408
fs, shaped pump, GA	$CH_3COCF_3 \rightarrow CF_3^+$, beam	408
fs, shaped pump, GA	$C_6H_5COCH_3 \rightarrow C_6H_5CO^+/C_6H_5^+$, beam	408
fs, shaped pump, GA	$C_6H_5COCH_3 \rightarrow C_6H_5CH_3^+$, beam	408
fs, shaped pump, GA	$CH_2BrCl \rightarrow CH_2Cl^+/CH_2Br^+$, beam	409
fs, shaped pump, GA	$CpFe(CO)_2Cl \rightarrow CpFeCOCl^+/FeCl^+$, beam	410
fs, shaped pump, GA	$CpFe(CO)_2Br \rightarrow CpFeCOBr^+/FeBr^+$, beam	410
fs, shaped pump, GA	$CpMn(CO)_3 \rightarrow CpMn(CO)_3^+/CpMn(CO)_2^+$, beam	411

transition-state geometry for the reaction.

Potter et al. performed the first experiments aimed at measuring the dependence of the probability of a bimolecular reaction on the interatomic distance of a coherently vibrating reagent, using femtosecond laser pulses:[521]

$$I_2(X) + h\nu\ (515\ nm) \rightarrow I_2(B) \qquad (10a)$$

$$I_2(B)\text{—}Xe + h\nu\ (260\ nm) \rightarrow Xe\text{-}I_2{}^{*\neq} \rightarrow XeI^* + I \qquad (10b)$$

where the first femtosecond pulse prepares a coherent superposition of vibrational states in the B electronic state of iodine. The second laser pulse captures $I_2(B)$—Xe collision pairs and produces the transition state $Xe\text{-}I_2{}^{*\neq}$, which decomposes to produce the electronically excited ion-pair state XeI*. The fluorescence intensity of XeI* was found to be modulated as the delay between the two femtosecond pulses was varied. In principle, the cross section for the bimolecular reaction is modulated by the wave packet motion in the electronic B state of iodine. Therefore, the reaction yield reflects the vibrationally coherent nuclear motions of the reactants.[521] There is an alternative explanation offered in the original article, which should also be considered.[263,521,522] It is possible that XeI* is not formed in one step, as shown in eq 10b, but is formed after the I_2 ion-pair state formed by the probe pulse collides, on a nanosecond time-scale,[523,524] with Xe atoms. Apkarian and Manz independently have indicated that probing the intermediate species $Xe\text{-}I_2{}^{*\neq}$ directly would resolve the question regarding the importance of the direct (10) and the alternate pathways.[263,522] This experiment has not been performed, so the role of vibrational coherence in this reaction cannot be ruled out.

Studies from the Dantus group have established that free-to-bound photoassociation is possible with femtosecond laser pulses, bringing the technique to the time scale of vibrational motion (10^{-14}—10^{-12} s).[525−527] Experiments performed on the reaction $Hg + Hg \rightarrow Hg_2{}^*$ (shown in Figure 29) demonstrated selective control over the total energy of the reaction, the time of bond formation, the alignment of the product, and the range of impact parameters. These experiments showed that time-resolved measurements of transition-state dynamics during reactive bimolecular collisions were possible and that the laser wavelength could be used to control the impact parameter of the bimolecular encounter through the Franck—Condon dependence of the photoassociation process.

One of the remaining questions is whether coherent control of bimolecular reactions is possible. This challenge could be addressed in condensed phase, with prearranged precursors on a surface, or as van der Waals clusters.[528−531] However, the question posed here implies unrestricted reagents. Could shaped laser pulses improve the yield of a bimolecular encounter? In the case of two atoms, as they come together during a chemical collision, the difference potential between the repulsive ground state and the outer branch of the potential energy curve of the upper bound state decreases. A negatively chirped pulse, in principle, would be able to match this decrease, thereby improving the probability of photoassociation. A positively chirped pulse would be able to photoassociate atoms just after a collision as they begin to separate. Only careful experimental work that takes into account the dependence of the bimolecular encounter on the vibrational coherence and the coherent laser field will be able to determine to what extent bimolecular collisions can be coherently controlled.

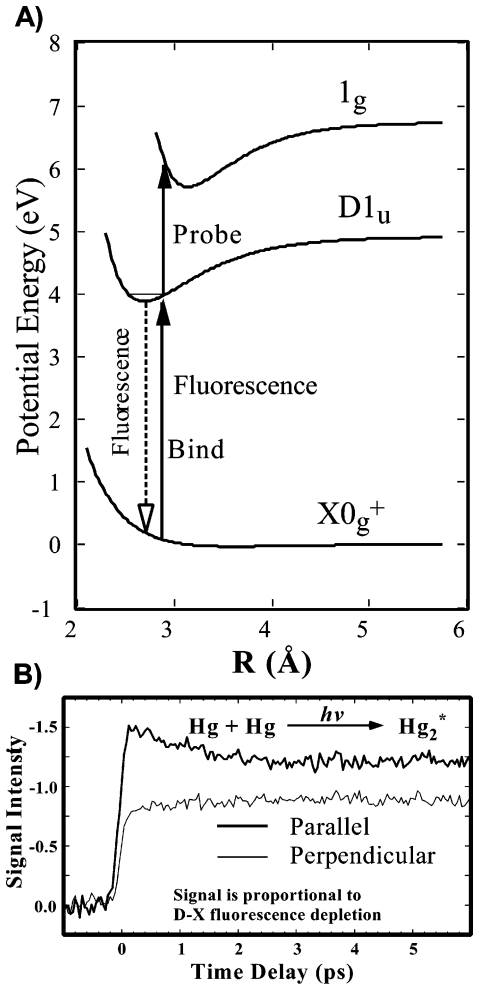

Figure 29. (A) FPAS experiment on Hg. The initial (binding) pulse forms Hg_2 in the D state; the depletion of the D → X fluorescence is monitored, as probe causes excitation to the 1g state. The region of most probable excitation from the ground state is shown in the inset. (B) FPAS transients showing depletion of the D → X fluorescence, as shown in A. Data are for the binding and probe lasers polarized parallel or perpendicular to one another. Note the rotational dephasing of the initial anisotropy. (Reprinted with permission from ref 525. Copyright 1995 Elsevier Science B. V.).

6.3. Coherent Control in Liquids

The general concept of coherent control hinges on the existence of an electric field that can be used to achieve a specific outcome through a coherent laser—matter interaction while other outcomes are suppressed. In most cases, the system is assumed a single molecule or an ensemble of identical molecules. However, in most cases, the sample molecules have

different surroundings that perturb each molecule, causing differences in their spectroscopy. These differences are recognized as inhomogeneous broadening. In the gas phase, inhomogeneous broadening has two different sources: Doppler broadening and differences in the thermal distribution of the sample before it interacts with the laser. In most cases, inhomogeneous broadening is small, and it becomes negligible when the molecules are expanded in molecular beams.

Whereas inhomogeneous broadening can be neglected in gas-phase samples, inhomogeneous broadening can be extremely large in liquid-phase samples. Typical values for inhomogeneous broadening in large organic molecules dissolved in polar solvents range from 10 to 100 fs.[350,484,532] Given these very large perturbations, one can appreciate that the control field no longer can address distinct quantum states in the molecular ensemble as desired. The percentage of molecules that produce the desired outcome becomes diluted by the extent of the inhomogeneous broadening. The most interesting aspect about inhomogeneous broadening, though, is that there is a way to cancel its influence on the spectroscopy of the sample, as described below.

These inhomogeneities in the sample are considered explicitly in the density matrix formulation of nonlinear optical spectroscopy.[36] Inhomogeneities can also be included using the more common wave function approach; however, summing over a weighted number of different available contributions is required to take into account the differences between individual molecules. Upon excitation of the system, the time evolution for each molecule is slightly different. The PE pulse sequence defines a point in time when the temporal evolution of all molecules in the ensemble coincide (see Section 5.1). This provides a means to coherently manipulate an inhomogeneous ensemble of molecules coherently.

A second challenge for coherent control experiments is the presence of homogeneous broadening. Homogeneous broadening is a term that is used to describe the statistical loss of coherence that all molecules in the sample experience. Usually, homogeneous broadening arises from collision of the system with the surroundings. As can be expected, homogeneous broadening is greatest in liquids where the close proximity of the sample to the solvent gives rise to extremely large broadening (0.1−20 nm), arising from the fast coherence decay 20−200 fs, for room temperature samples. Because homogeneous broadening arises from statistical events, there is no pulse sequence capable of reversing its effects in a way similar to that which PE reverses inhomogeneous broadening. Two different approaches have been used to reduce the detrimental loss of coherence due to homogeneous broadening. The first requires the use of very fast pulses. With the commercial availability of lasers with pulse durations shorter than 20 fs, it is now possible to generate fields that can interact with the sample on a time scale that is faster than homogeneous broadening. The second approach is to develop methods that are not dependent on the persistence of coherence, which can be separated into two categories. The first corresponds to those methods that do not require electronic coherence. For example, vibrational coherence is much longer lived; even in condensed samples, vibrational coherence can persist for tens of picoseconds. The second category requires electronic coherence only while the pulse interacts with the sample. As an example of this category, we mention MII, where the interference occurs only while the laser interacts with the sample during the nonlinear excitation process.

Weinacht and Bucksbaum demonstrated Raman scattering from selected vibrational modes in methanol, benzene, deuterated benzene, and carbon tetrachloride, using a GA and phase-amplitude modulation.[26] Recent experiments aimed at control in condensed phases, using shaped laser pulses under the control of a GA, are very encouraging.[388,414] Brixner et al. explored the use of adaptive femtosecond pulse shaping for selective excitation of two different organic dye mixtures.[388] The linear absorption spectrum in the 400−500 nm wavelength range for methanol solutions of each of the two compounds (DCM and $[Ru(dpb)_3]^{2+}$) chosen is very similar. Changes on single parameters such as pulse energy (50−250 μJ), linear chirp ($-2 \times 10^{4-}$ 2×10^4 fs^2), and wavelength (796−810 nm) were tested, and no significant change in the ratio of multiphoton induced fluorescence detected from each of the two sample containers was noticed. However, using the adaptive femtosecond pulse shaper, a ∼50% increase in the DCM/$[Ru(dpb)_3]^{2+}$ signal ratio was obtained. The conclusion of this carefully performed experiment was that the shaped field had found a nontrivial manipulation of excited-state photophysics to enhance the ratio and that phase coherences must exist that are not destroyed by interaction with the surrounding solvent on the time scale of the optimized pulse shape (100 fs to 1 ps).[388] The results are intriguing and inspire a number of questions. The first question, relevant to the problem, concerns possible differences in the two-photon absorption spectrum of the two dyes in the 398−404-nm wavelength range, where such excitation by the femtosecond pulses is expected. The linear spectrum of the two dyes changes drastically below 400 nm, and similar drastic changes could be expected for two-photon transitions. This question was partially answered by a wavelength-tuning experiment. A 5-nm window was scanned over the laser spectrum, in the 796−810 nm wavelength range, with only a small ∼10% influence on the signal, approximately of similar amplitude to the experimental noise. Changes caused by three-photon transitions (at 267 nm) can be ruled out as the reason for the improved ratio, because the intensity dependence and the chirp experiments would have revealed the difference. Finally, if the control mechanism involves coherence, one would like to determine what kind of coherence was involved. The optimized pulse shows three lobes in the Husimi plot, the wings extending from −1.0 to 1.5 ps and a center lobe of ∼150 fs in duration; the authors conclude that a coherent laser-

sample interaction takes place within the entire time scale. Homogeneous electronic coherence of organic laser dyes in solution decays in a sub-100-fs time scale;[350,484,532] the inhomogeneous dephasing is an order of magnitude faster. Vibrational coherence, however, could certainly survive for several picoseconds. One could also postulate a three-step process, similar to FWM, consisting of excitation to the ground state, stimulated emission, and re-excitation. Clearly, further experimentation will be needed to unravel the results from this study.

Herek et al. used a combination of an adaptive femtosecond pulse shaper to excite the light-harvesting antenna complex LH2 in the S_2 excited-state region (single-photon 525 nm) and two probe pulses monitoring the carotenoid system absorption (588 nm) and the B850 bchl Q_y bleach/stimulated emission (880 nm).[414] A pulse shaper controlling 128 pixels (32 groups of 4 pixels) was used, the phase and amplitude were varied from 0 to 2π and from 4 to 100% transmission. The laser intensity of the unshaped pulses was above saturation to permit multiphoton interactions. After optimization, a 35% increase in the internal conversion over energy transfer IC/ET ratio was obtained. Pulse characterization using SHG-FROG revealed seven major subpulses separated by 250 fs, each with a pulse duration similar to that of the TL pulses ~30 fs. When a sinusoidal phase function was used to optimize the process, again a seven subpulse solution was obtained. Shifting the sinusoidal phase function by π resulted in a lower IC/ET ratio, this result leading the authors to conclude that the control mechanism involved coherent control. If the control mechanism involved the linear preparation of an "optimized" wave packet that evolves preferentially toward IC, then a π shift should make a large difference. If nonlinear excitation, such as two-photon excitation, plays an important role, then a π shift can have a significant change in the peak intensity as well, independent of intramolecular dynamics (see Figure 4A,B). Further experimentation will be required to determine if the 250 fs periodicity is significant and is responsible for driving relevant intramolecular vibrational modes. It will be even more important to determine if a coherently driven mechanism exists, which can improve light-induced ET, the biologically desired product, while lowering IC losses.

6.4. Energy Randomization and Wave-Packet Revivals

When the sample to be controlled is a polyatomic molecule, it becomes very difficult to localize excitation to a specific chemical bond where one is interested in exerting control. The large numbers of degrees of freedom in a molecule provide a large number of vibrational overtones that participate in the randomization of the energy, initially deposited into a particular state. Within a couple of picoseconds, the localized excitation begins to explore the energy landscape of the molecule. This initial randomization does not implicate dissipation. Even in condensed phases, the energy is still within the molecule. In some cases, especially in the gas phase, vibrational quantum beats can be observed when the energy has only a discrete number of states to explore. As the number grows, it becomes more difficult to discern the coherent evolution of the energy among the different states. Zewail's group demonstrated this behavior in a number of polyatomic molecules. In their experiments on anthracene, a molecule with 24 atoms, they demonstrated that, upon excitation, the vibrational energy evolved in a coherent superposition of vibrational states for a number of nanoseconds.[533−536] These results demonstrated that energy did not spread to all degrees of freedom statistically.[537]

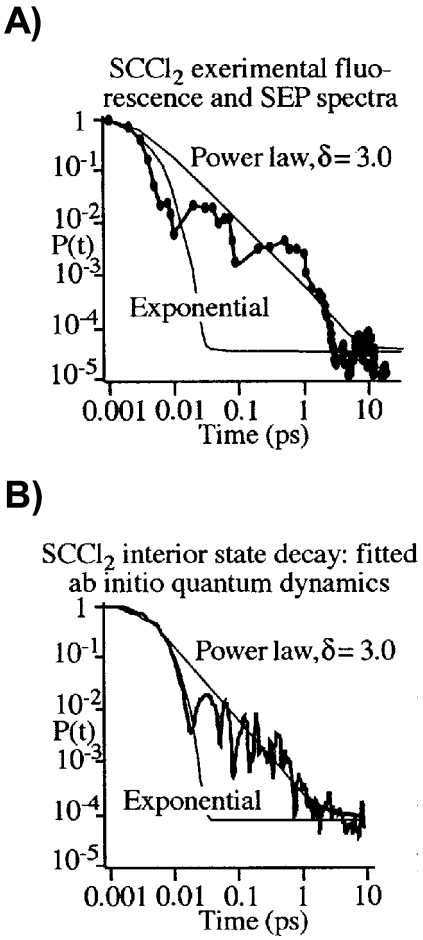

Figure 30. IVR decays on a log−log scale. (A) Experimental data for $SCCl_2$. (B) Accurate quantum simulation for an $SCCl_2$ interior state. (Reprinted with permission from ref 538. Copyright 2002 Springer Verlag.)

A number of researchers have explored the randomization of vibrational energy in polyatomic molecules. If energy dissipates statistically throughout the molecule, then the rate of dissipation should increase exponentially as a function of time, as more and more pathways become available. If the energy remains trapped in certain vibrational modes or combinations of modes, then the dissipation follows a power law that is much slower than the exponential decay. Gruebele has carried out experiments and high-level ab initio calculations regarding energy dissipation in $SCCl_2$.[538] The results of the work are shown in Figure 30; they include experiment and theory. The power law derived from the experiments

and calculations, with an exponent of 3.0, much slower than exponential behavior, as can be seen in the plots. The additional structure in the data shows multiple bottlenecks that are encountered during energy randomization.

The fact that early energy randomization is not statistical and is not dissipative opens the opportunity for coherent control of chemical reactivity in large molecules. It is conceivable that the energy that is trapped in a coherent superposition of states can be refocused at a particular point in time to achieve bond-selective chemistry. This refocusing effect could be obtained by wave packet manipulations, as discussed in Section 4.2. Experimental demonstration of wave packet refocusing, in large polyatomic molecules in gas or condensed phase, remains to be demonstrated.

7. Future Outlook and Applications

In this review, we have presented some of the most successful experimental demonstrations of coherent control. The field has led to the development of new equipment and techniques and to improved understanding of laser−molecule interactions. However, beyond the academic contributions, few applications have emerged. It is quite possible that recent advances in the field will lead to a number of applications. This is an indication that the field is reaching maturity, and below we review some of the applications that seem to be the closest to implementation.

7.1. Coherent Control Methods in Microscopy

There are presently two methods based on coherent control that are being used for microscopy. The first method is based on CARS.[419] The experiment uses a single, shaped femtosecond pulse that replaces the three fields required for the CARS process, as discussed in Section 2.3.2. The shaped pulse induces the initial Raman transitions and stimulates the anti-Stokes scattering. During the shaping process, the blue end of the spectrum of the pulse is clipped, to reduce background photons near the signal. As this shaped beam is focused on the sample, the CARS signal is collected, providing high-resolution images that depend on the molecular identity of the sample. In Figure 31A, we show an image obtained using this method. The sample imaged is a collection of capillaries filled with CH_2Br_2.[419] The contrast between the two figures shows the sensitivity of the method to different sample compositions.

The second imaging method based on coherent control has been termed selective multiphoton microscopy.[62,123] The method is based on the principle of multiphoton intrapulse interference discussed in Section 4.4. Here, MII is used to selectively excite certain chromophores in the sample. Whereas TL pulses excite all chromophores in the field of focus, a shaped pulse can excite only specific chromophores. In Figure 31B, we show how this method is used to selectively excite two different microscopic fluorescent beads. One of the beads is labeled with (4′-6-diamidino-2-phenylindole) DAPI and the other with

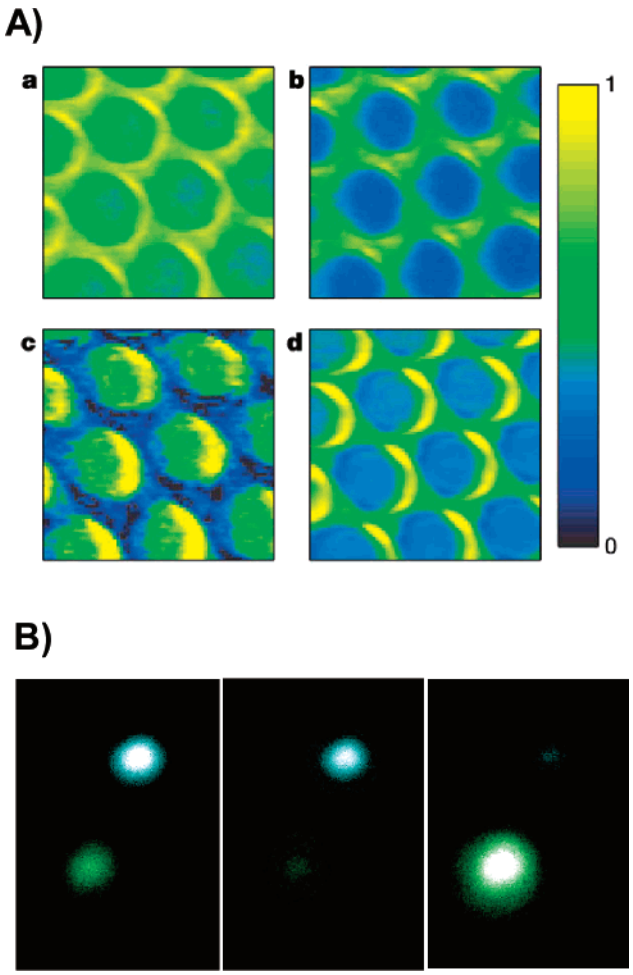

Figure 31. (A) CARS spectroscopy. Depth-resolved, single-pulse CARS images of a glass capillary plate with 10-mm holes filled with CH_2Br_2. (Reprinted with permission from Nature (http://www.nature.com), ref 419. Copyright 2002 Nature Publishing Group.) (B) Selective two-photon microscopy. The image on the left shows fluorescence from blue and green microspheres induced by TL pulses. The middle and right panels show selective fluorescence from the same micrsopheres using shaped pulses.

AlexaFluor 430, two fluorescent chromophores that are commonly used to stain biological samples. When TL pulses are used both regions show strong fluorescence, but, when shaped pulses are used, it is possible to selectively excite either of the two.[62,123] This method can be used for imaging microscopic as well as macroscopic biomedical samples. Selective multiphoton excitation afforded by coherent control results in additional contrast and better differentiation.

One of the main goals in coherent control is to achieve the greatest contrast between different pathways following optical excitation of a sample. In microscopy, as well as in imaging in general, the goal has always been to achieve the greatest contrast possible. We expect a number of new developments in the area of imaging that can be traced to advances in the field of coherent control. Incorporation of the binary phase shaping concept[106] enables the combination of rational design with very fast and efficient optimization, a strategy that we are presently following in our laboratory.

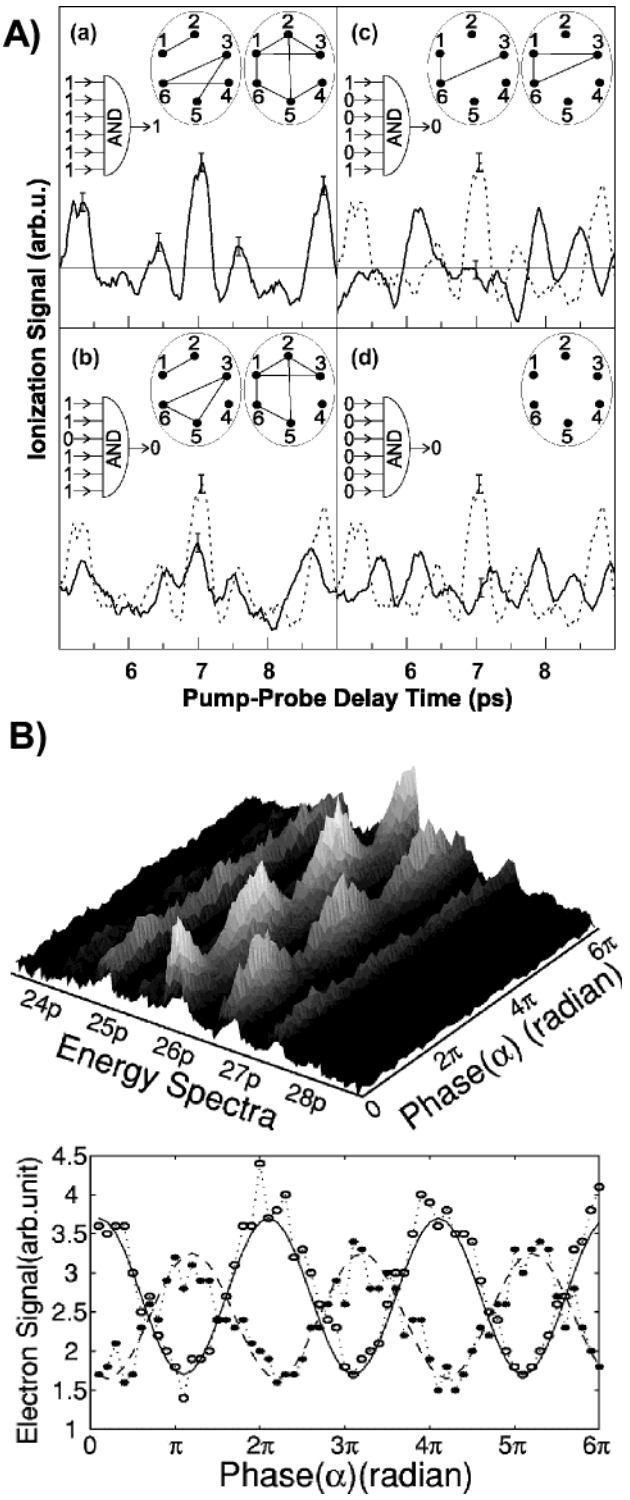

Figure 32. (A) Experimental results showing coherent computation of multiple-input AND gates using pure molecular superpositions. (Reprinted with permission from ref 543. Copyright 2002 Elsevier Science B. V.) (B) Quantum-state information retrieval from a Rydberg-atom data register. Reprinted with permission from ref 544. Copyright 2002 American Physical Society.)

7.2. Quantum Information

During the last 20 years, the field of quantum information has grown from an interesting proposition to an effort involving hundreds of scientists. The field has been described in a number of review articles and books; here, we only give a couple of them.[539,540] The main goal behind this new field has been to treat information as quantum objects that are subject to the laws of quantum mechanics. The rationale for such a seemingly complex proposition comes from the expected advantages. Classical information is limited to zeros and ones. When each byte of information is processed, special instructions are required to communicate the result to other parts of the algorithm. These requirements result in an exponential growth in the resources needed to solve particular problems, for example, Fourier transformation. The quantum-mechanical "qubit" is in a superposition of zero and one; when two or more qubits are entangled, a transformation of one qubit is instantaneously transmitted to the other qubits. The means of communication is provided by quantum-mechanical entanglement.[539,540] We have included this section in the review because the quantum gates, responsible for the coherent transformation of quantum information, will very likely be shaped laser pulses, as described in this review.

The implementation of a quantum information processor has received considerable attention. The most important requirement for such a device is the ability to manipulate each quantum bit of information coherently, without loss of phase. The best ideas on how to achieve unitary transformations make use of electromagnetic radiation, either in the radio frequency range, as in nuclear magnetic resonance (NMR), or in the visible range, using coherent laser pulses. While there has been considerable progress in the use of multiple-pulse NMR for quantum information processing, similar methods based on laser pulses have a number of advantages. Because of the size of the quantum transitions, optical methods are 8 orders of magnitude faster and are 10 orders of magnitude less prone to thermal noise.[541,542]

In Figure 32A we show experimental results from Amitay et al.,[543] where an experimental implementa-

Table 9. Quantum Phase Information Experiments

method	system	refs
third harmonic generation	surface	545
third harmonic generation	BaF_2	546
third harmonic generation	BaF_2	547
fs, SPE	dye, cryogenic solution in polymer	548
fs, SPE	dye, cryogenic solution in polymer	549
fs, SPE	dye, cryogenic solution in polymer	550
fs, shaped pulse	Cs; $7s \rightarrow 20-32p \rightarrow e^-$	86
fs, shaped pulse	Cs; $7s \rightarrow 20-32p \rightarrow e^-$	551
fs, shaped pulse	Cs; $7s \rightarrow 20-32p \rightarrow e^-$	552
fs, shaped pulse	Cs; $7s \rightarrow 20-32p \rightarrow e^-$	544
fs, shaped pulse	Cs; $7s \rightarrow 20-32p \rightarrow e^-$	553
fs, shaped pump, ion	Li_2, $X \rightarrow A \rightarrow E \rightarrow X^+$, rovibrations	543
fs, shaped pulse	I_2, $X \rightarrow B$, vibrations	542
fs, shaped pump, ion	Li_2, $X \rightarrow A \rightarrow E \rightarrow X^+$, rovibrations	554
fs, CARS	I_2, $X \rightarrow B$, rovibrations	555
fs, CARS	I_2, $X \rightarrow B$, rovibrations	556
fs, shaped pump	Li_2, $X \rightarrow A \rightarrow E \rightarrow X^+$, rovibrations	346
fs, CARS	I_2, $X \rightarrow B$ rovibrations, (proposal)	557

tion of a multiple-input AND gates, based on molecular superpositions, is demonstrated. In Figure 32B, we show quantum-state information retrieval from a Rydberg-atom data register.[544] Superpositions of quantum-mechanical states containing quantum information are manipulated by shaped laser pulses. The resulting output signal demonstrates successful coherent manipulation of the quantum-mechanical information. Both of these examples are still far from the dream of quantum computation, but they demonstrate how principles of coherent control are used to manipulate information stored in quantum mechanical states. In Table 9, we summarize experiments in which concepts of coherent control have been used for quantum information manipulation and processing.[86,542−557] This field is still in its infancy; advances in the field of coherent control may play an important role in its development and the future creation of a large-scale quantum computer.

8. Conclusions

Controlling matter with light has been a conceptual goal for many decades. Here, we have presented some of the most important experimental demonstrations in which laser pulses are used to control a number of physical and chemical processes, taking advantage of coherence in the laser pulses and/or the system. It is interesting to analyze all of these experiments and summarize some of the most important lessons. They combine the need for ultrashort pulses that can compete with relaxation processes and interference among multiple pathways. In the weak-field limit, they can be fully explained within the framework of frequency-resolved spectroscopy. Strong fields can modify the potentials to the extent that a frequency-resolved picture is no longer relevant. Here, we list a number of important conclusions.

(i) Interference remains the most powerful tool of coherent control. Different interference processes include linear and nonlinear optical interference in microscopic (intramolecular), and macroscopic (intermolecular) coherences.

(ii) The phase of femtosecond pulses can be used to sculpt a wave packet and control its evolution.

(iii) Strong fields can be used to exert forces that can reshape the potential energy surface as well as control the external degrees of freedom.

(iv) Nonlinear optical processes, such as multiphoton absorption, and FWM, inherently provide multiple pathways of excitation; therefore, they are ideally suited for coherent control.

(v) Shorter pulses have a greater bandwidth available, opening multiple pathways that can be controlled by interference. Single-optical-cycle pulses, in the visible range, and phase shaped will provide the greatest flexibility.

(vi) Learning algorithms are extremely powerful in the search of successful control strategies, provided redundant pulse shapes are eliminated and pulse characterization is accurate and reliable.

The probability for reaching a quantum-mechanical transition is equal to the amplitude-squared of the sum over all possible pathways between the initial and final states. From this point of view, and assuming weak field excitation, control strategies can be designed in the frequency domain. When a single state can be reached by two distinct optical pathways, then Brumer and Shapiro have explained how the relative phase between the two optical pathways modulates the probability of excitation. This concept has been expanded to control excitation between two different degenerate states, provided there is an intrinsic phase lag between them. A pulse shaper can be used to control the phase between several frequencies, which connect multiple quantum-mechanical states, by distinct optical pathways. For multiphoton excitation experiments, when broad-bandwidth femtosecond pulses are used, the resulting interference can be controlled with specific phase functions, designed using the principles of MII, and can be introduced using a programmable pulse shaper. Strong fields, however, modify the potential energy surfaces to the extent that there is no longer a spectroscopic map to follow. The intermediate regime, where the frequency-domain picture begins to fail, remains to be explored.

Strong-field control cannot be explained in the frequency domain. The electric field can exert a force directly on the electrons, forcing them into high-Rydberg states or causing them to field ionize. These strong fields can also exert forces on the molecule and its constituent atoms. Strong-field control has the greatest possibility for manipulating molecular structure and chemical transformations. The experiments discussed under this rubric[26,365,386−390,392−394,412−415] show tremendous promise. Experiments are expected to proceed toward control of more complex systems, and to provide a more thorough understanding of the control mechanism. The ultimate goal might be to directly demonstrate the coherent manipulation of molecules *during* the presence of the field.

It is reasonable to say that we have reached the point where the technology, in the form of ultrashort intense pulses and pulse shaping equipment, is available for synthesizing arbitrarily defined electromagnetic fields. Under the control of GAs, or by strategically designed fields, one can address a large number of systems and expect significant results, so long as the systems are controllable. Certainly, most nonlinear optical excitation processes are controllable; however, chemical reactions must be analyzed one at a time and in detail. In principle, unimolecular reactions are controllable, at least at the conceptual level of a single, fixed, isolated molecule, where all the atoms are present and their initial position is well defined. Theoretical studies have shown that unimolecular reactions can be controlled to yield the desired product with 100% probability, but experimental results usually show modest changes, of the order of 50−80%. Experimental work will determine the degree of success for each system that is attempted.

9. Abbreviations

AOPDF	acousto-optic programmable dispersive filter
BPS	binary phase shaping
CARS	coherent anti-Stokes Raman scattering
CHIRAP	chirped rapid adiabatic passage

COIN	coherence observation by interference noise
CRS	coherent Raman scattering
CSRS	coherent Stokes Raman scattering
DFWM	degenerate four-wave mixing
ET	energy transfer
FPAS	femtosecond photoassociation spectroscopy
FROG	frequency-resolved optical gating
FWHM	full-width at half maximum
FWM	four-wave mixing
GA	genetic algorithm
HSPE	heterodyne detected stimulated photon echo
$I^{(2)}$CRS (two noisy fields)	interferometric coherent Raman scattering
IC	internal conversion
IR	infrared
IVR	intramolecular vibrational energy redistribution
LIF	laser-induced fluorescence
MII	multiphoton intrapulse interference
MIIPS	multiphoton intrapulse interference phase scan
NME	nonadiabatic multielectron
NMR	nuclear magnetic resonance
NOPA	noncollinear optical parametric amplification
PE	photon echo
RAP	rapid adiabatic passage
SAE	single active electron
SHG	second-harmonic generation
SLM	spatial light modulator
SPE	stimulated photon echo
SPIDER	spectral phase interferometry for direct electric-field reconstruction
STIRAP	stimulated transition induced by Raman adiabatic passage
TG	transient grating
TL	transform limited (same as bandwidth limited)
TOF-MS	time-of-flight mass spectrometer
UV	ultraviolet
VE	virtual echo

10. Acknowledgments

Our research on coherent control has been supported primarily by the Chemical Sciences, Geosciences and Biosciences Division, Office of Basic Energy Sciences, Office of Science, U.S. Department of Energy. The National Science Foundation has provided funds for our work on four-wave mixing and related methods to observe and control molecular dynamics. Their funding is gratefully acknowledged. M.D. is a Camille Dreyfus Teacher−Scholar. The efforts and dedication of K. A. Walowicz, I. Pastirk, J. Dela Cruz, M. Comstock, B. I. Grimberg, and E. J. Brown, referenced in this review, have made our contributions possible. M.D. wishes to thank A. Stolow, A. H. Zewail, G. J. Blanchard, and J. K. McCusker for many stimulating discussions. We are grateful to our colleagues who provided us with preprints and reprints of their work. We hope that we were successful in including all relevant contributions and apologize to those whose work we did not have a chance to discuss. We thank J. Dela Cruz for helping us obtain all the copyright permissions, and R. Darrow and A. L. Smeigh for proofreading this manuscript.

11. References

(1) Rice, S. A. *Science* **1992**, *258*, 412.
(2) Kohler, B.; Krause, J. L.; Raksi, F.; Rosepetruck, C.; Whitnell, R. M.; Wilson, K. R.; Yakovlev, V. V.; Yan, Y. J.; Mukamel, S. *J. Phys. Chem.* **1993**, *97*, 12602.
(3) Warren, W. S. *Science* **1993**, *262*, 1008.
(4) Warren, W. S.; Rabitz, H.; Dahleh, M. *Science* **1993**, *259*, 1581.
(5) Brumer, P.; Shapiro, M. *Sci. Am.* **1995**, *272*, 56.
(6) Crim, F. F. *J. Phys. Chem.* **1996**, *100*, 12725.
(7) Gordon, R. J.; Rice, S. A. *Annu. Rev. Phys. Chem.* **1997**, *48*, 601.
(8) Baumert, T.; Helbing, J.; Gerber, G.; Woste, L.; Zewail, A. H.; Troe, J.; Manz, J.; Kobayashi, T.; Letokhov, V. S.; Even, U.; Chergui, M.; Neumark, D. M.; Rice, S. A. In *Chemical Reactions and Their Control on the Femtosecond Time Scale, Xxth Solvay Conference on Chemistry*; John Wiley & Sons: New York, 1997; Vol. 101.
(9) Noordam, L. D.; Jones, R. R. *J. Mod. Opt.* **1997**, *44*, 2515.
(10) Bergmann, K.; Theuer, H.; Shore, B. W. *Rev. Mod. Phys.* **1998**, *70*, 1003.
(11) Zare, R. N. *Science* **1998**, *279*, 1875.
(12) Shapiro, M.; Brumer, P. *Adv. Atom. Mol. Opt. Phys.* **2000**, *42*, 287.
(13) Rice, S. A. *Nature* **2000**, *403*, 496.
(14) Rice, S. A. *J. Stat. Phys.* **2000**, *101*, 187.
(15) Rice, S. A.; Zhao, M. *Optical Control of Molecular Dynamics*; Wiley: New York, 2000.
(16) Rabitz, H.; de Vivie-Riedle, R.; Motzkus, M.; Kompa, K. *Science* **2000**, *288*, 824.
(17) Rabitz, H.; Zhu, W. S. *Acc. Chem. Res.* **2000**, *33*, 572.
(18) Brixner, T.; Damrauer, N. H.; Gerber, G. *Adv. Atom. Mol. Opt. Phys.* **2001**, *46*, 1.
(19) Dantus, M. In *Femtochemistry: With the Nobel Lecture of A. Zewail*; De Schryver, F. C., De Feyter, S., Schweizter, G., Eds.; Wiley-VCH Verlag: Weinheim, 2001.
(20) Dantus, M. *Annu. Rev. Phys. Chem.* **2001**, *52*, 639.
(21) Rice, S. A. *Nature* **2001**, *409*, 422.
(22) Verlet, J. R. R.; Fielding, H. H. *Int. Rev. Phys. Chem.* **2001**, *20*, 283.
(23) Vitanov, N. V.; Fleischhauer, M.; Shore, B. W.; Bergmann, K. *Adv. Atom. Mol. Opt. Phys.* **2001**, *46*, 55.
(24) *Laser Control and Manipulation of Molecules*; Bandrauk, A. D.; Fujimura, Y.; Gordon, R. J., Eds.; American Chemical Society: Washington, 2002; Vol. 821.
(25) Henriksen, N. E. *Chem. Soc. Rev.* **2002**, *31*, 37.
(26) Weinacht, T. C.; Bucksbaum, P. H. *J. Opt. B.* **2002**, *4*, R35.
(27) Roberts, G. *Philos. Trans. R. Soc. London Ser. A.* **2002**, *360*, 987.
(28) Rice, S. A.; Shah, S. P. *Phys. Chem. Chem. Phys.* **2002**, *4*, 1683.
(29) Brixner, T.; Gerber, G. *ChemPhysChem* **2003**, *4*, 418.
(30) Goswami, D. *Phys. Rep.* **2003**, *374*, 385.
(31) Rabitz, H. *Science* **2003**, *299*, 525.
(32) Shapiro, M.; Brumer, P. *Principles of the Quantum Control of Molecular Processes*; Wiley-Interscience: Hoboken, NJ, 2003.
(33) Shen, Y. R. *The Principles of Nonlinear Optics*; 2nd ed.; Wiley: New York, 1984.
(34) Boyd, R. W. *Nonlinear Optics*; Academic Press: Boston, MA, 1992.
(35) Bloembergen, N. *Nonlinear Optics*; 4th ed.; World Scientific: River Edge, NJ, 1996.
(36) Mukamel, S. *Principles of Nonlinear Optical Spectroscopy*; Oxford University Press: New York, 1995.
(37) Park, S. M.; Lu, S. P.; Gordon, R. J. *J. Chem. Phys.* **1991**, *94*, 8622.
(38) Vysloukh, V. A.; Chirkin, A. S.; Akhmanov, S. A. *Optics of Femtosecond Laser Pulses*; Springer-Verlag, New York, 1992.
(39) Duling, I. N. *Compact Sources of Ultrashort Lasers*; Cambridge University Press: New York, 1995.
(40) Diels, J.-C.; Wolfgamg, R. *Ultrashort Laser Pulse Phenomena: Fundamentals, Techniques, and Applications on a Femtosecond Time Scale (Optics and Photonics)*; Academic Press: New York, 1996.
(41) Rulliere, C. *Femtosecond Laser Pulses: Principles and Experiments*; Springer-Verlag: New York, 1998.
(42) *Femtosecond Technology: From Basic Research to Application Prospects*; Kamiaya, T.; Saito, F.; Wada, O.; Yajima, H., Eds.; Springer-Verlag: New York, 1999; Vol. 2.
(43) Trebino, R. *Frequency-Resolved Optical Gating: The Measurement of Ultrashort Laser Pulses*; Kluwer Academic Publishers: Boston, 2002.
(44) Shelton, R. K.; Foreman, S. M.; Ma, L. S.; Hall, J. L.; Kapteyn, H. C.; Murnane, M. M.; Notcutt, M.; Ye, J. *Opt. Lett.* **2002**, *27*, 312.
(45) Shelton, R. K.; Ma, L. S.; Kapteyn, H. C.; Murnane, M. M.; Hall, J. L.; Ye, J. *J. Mod. Opt.* **2002**, *49*, 401.
(46) Fortier, T. M.; Jones, D. J.; Ye, J.; Cundiff, S. T.; Windeler, R. S. *Opt. Lett.* **2002**, *27*, 1436.
(47) Kobayashi, Y.; Torizuka, K. *Opt. Lett.* **2003**, *28*, 746.

(48) Kobayashi, Y.; Takada, H.; Kakehata, M.; Torizuka, K. *Appl. Phys. Lett.* **2003**, *83*, 839.
(49) Ye, J.; Cundiff, S. T.; Foreman, S.; Fortier, T. M.; Hall, J. L.; Holman, K. W.; Jones, D. J.; Jost, J. D.; Kapteyn, H. C.; Leeuwen, K.; Ma, L. S.; Murnane, M. M.; Peng, J. L.; Shelton, R. K. *Appl. Phys. B* **2002**, *74*, S27.
(50) Scherer, N. F.; Carlson, R. J.; Matro, A.; Du, M.; Ruggiero, A. J.; Romerorochin, V.; Cina, J. A.; Fleming, G. R.; Rice, S. A. *J. Chem. Phys.* **1991**, *95*, 1487.
(51) Telle, H. R.; Steinmeyer, G.; Dunlop, A. E.; Stenger, J.; Sutter, D. H.; Keller, U. *Appl. Phys. B - Lasers Opt.* **1999**, *69*, 327.
(52) Shelton, R. K.; Ma, L. S.; Kapteyn, H. C.; Murnane, M. M.; Hall, J. L.; Ye, J. *Science* **2001**, *293*, 1286.
(53) Yariv, A. *Quantum Electronics*, 3rd ed.; Wiley: New York, 1989.
(54) Glenn, W. H. *IEEE J. Quantum Electron.* **1969**, *5*, 284.
(55) Baltuska, A.; Pshenichnikov, M. S.; Wiersma, D. A. *IEEE J. Quantum Electron.* **1999**, *35*, 459.
(56) Broers, B.; Vandenheuvell, H. B. V.; Noordam, L. D. *Opt. Commun.* **1992**, *91*, 57.
(57) Zheng, Z.; Weiner, A. M. *Opt. Lett.* **2000**, *25*, 984.
(58) Hacker, M.; Netz, R.; Roth, M.; Stobrawa, G.; Feurer, T.; Sauerbrey, R. *Appl. Phys. B: Lasers Opt.* **2001**, *73*, 273.
(59) Zheng, Z.; Weiner, A. M. *Chem. Phys.* **2001**, *267*, 161.
(60) Walowicz, K. A.; Pastirk, I.; Lozovoy, V. V.; Dantus, M. *J. Phys. Chem. A* **2002**, *106*, 9369.
(61) Lozovoy, V. V.; Pastirk, I.; Walowicz, K. A.; Dantus, M. *J. Chem. Phys.* **2003**, *118*, 3187.
(62) Pastirk, I.; Dela Cruz, J. M.; Walowicz, K. A.; Lozovoy, V. V.; Dantus, M. *Opt. Express* **2003**, *11*, 1695.
(63) Wilhelm, T.; Piel, J.; Riedle, E. *Opt. Lett.* **1997**, *22*, 1494.
(64) Riedle, E.; Beutter, M.; Lochbrunner, S.; Piel, J.; Schenkl, S.; Sporlein, S.; Zinth, W. *Appl. Phys. B* **2000**, *71*, 457.
(65) Piel, J.; Beutter, M.; Riedle, E. *Opt. Lett.* **2000**, *25*, 180.
(66) Kobayashi, T.; Shirakawa, A.; Fuji, T. *IEEE J. Sel. Top. Quantum Electron.* **2001**, *7*, 525.
(67) Baltuska, A.; Kobayashi, T. *Appl. Phys. B* **2002**, *75*, 427.
(68) Kobayashi, T.; Baltuska, A. *Meas. Sci. Technol.* **2002**, *13*, 1671.
(69) Zeidler, D.; Hornung, T.; Proch, D.; Motzkus, M. *Appl. Phys. B: Lasers Opt.* **2000**, *70*, S125.
(70) Zeidler, D.; Witte, T.; Proch, D.; Motzkus, M. *Opt. Lett.* **2001**, *26*, 1921.
(71) Tan, H. S.; Warren, W. S.; Schreiber, E. *Opt. Lett.* **2001**, *26*, 1812.
(72) Shirley, J. A.; Hall, R. J.; Eckbreth, A. C. *Opt. Lett.* **1980**, *5*, 380.
(73) Prior, Y. *Appl. Opt.* **1980**, *19*, 1741.
(74) Lozovoy, V. V.; Pastirk, I.; Brown, E. J.; Grimberg, B. I.; Dantus, M. *Int. Rev. Phys. Chem.* **2000**, *19*, 531.
(75) Grimberg, B. I.; Lozovoy, V. V.; Dantus, M.; Mukamel, S. *J. Phys. Chem. A* **2002**, *106*, 697.
(76) Gallagher, S. M.; Albrecht, A. W.; Hybl, T. D.; Landin, B. L.; Rajaram, B.; Jonas, D. M. *J. Opt. Soc. Am. B - Opt. Phys.* **1998**, *15*, 2338.
(77) Faeder, S. M. G.; Jonas, D. M. *Phys. Rev. A* **2000**, *62*, art. no. 033820.
(78) Hybl, J. D.; Faeder, S. M. G.; Albrecht, A. W.; Tolbert, C. A.; Green, D. C.; Jonas, D. M. *J. Lumin.* **2000**, *87*−*9*, 126.
(79) Hybl, J. D.; Ferro, A. A.; Jonas, D. M. *J. Chem. Phys.* **2001**, *115*, 6606.
(80) Wollenhaupt, M.; Assion, A.; Bazhan, O.; Horn, C.; Liese, D.; Sarpe-Tudoran, C.; Winter, M.; Baumert, T. *Phys. Rev. A* **2003**, *68*, art. no. 015401.
(81) Wollenhaupt, M.; Assion, A.; Bazhan, O.; Liese, D.; Sarpe-Tudoran, C.; Baumert, T. *Appl. Phys. B* **2002**, *74*, S121.
(82) Frohnmeyer, T.; Baumert, T. *Appl. Phys. B* **2000**, *71*, 259.
(83) Pisharody, S. N.; Jones, R. R. *Phys. Rev. A* **2002**, *65*, art. no. 033418.
(84) van Leeuwen, R.; Vijayalakshmi, K.; Jones, R. R. *Phys. Rev. A* **2001**, *63*, art. no. 033403.
(85) van Leeuwen, R.; Bajema, M. L.; Jones, R. R. *Phys. Rev. Lett.* **1999**, *82*, 2852.
(86) Ahn, J.; Weinacht, T. C.; Bucksbaum, P. H. *Science* **2000**, *287*, 463.
(87) Assion, A.; Baumert, T.; Weichmann, U.; Gerber, G. *Phys. Rev. Lett.* **2001**, *86*, 5695.
(88) Neumark, D. M. *Annu. Rev. Phys. Chem.* **2001**, *52*, 255.
(89) Lezius, M.; Blanchet, V.; Ivanov, M. Y.; Stolow, A. *J. Chem. Phys.* **2002**, *117*, 1575.
(90) Stolow, A. *Int. Rev. Phys. Chem.* **2003**, *22*, 377.
(91) Stolow, A. *Annu. Rev. Phys. Chem.* **2003**, *54*, 89.
(92) Schultz, T.; Quenneville, J.; Levine, B.; Toniolo, A.; Martinez, T. J.; Lochbrunner, S.; Schmitt, M.; Shaffer, J. P.; Zgierski, M. Z.; Stolow, A. *J. Am. Chem. Soc.* **2003**, *125*, 8098.
(93) Hanold, K. A.; Sherwood, C. R.; Garner, M. C.; Continetti, R. E. *Rev. Sci. Instrum.* **1995**, *66*, 5507.
(94) Davies, J. A.; LeClaire, J. E.; Continetti, R. E.; Hayden, C. C. *J. Chem. Phys.* **1999**, *111*, 1.
(95) Hanold, K. A.; Luong, A. K.; Clements, T. G.; Continetti, R. E. *Rev. Sci. Instrum.* **1999**, *70*, 2268.
(96) Rohrbacher, A.; Continetti, R. E. *Rev. Sci. Instrum.* **2001**, *72*, 3386.
(97) Continetti, R. E. *Annu. Rev. Phys. Chem.* **2001**, *52*, 165.
(98) Weiner, A. M.; Leaird, D. E.; Wiederrecht, G. P.; Nelson, K. A. *Science* **1990**, *247*, 1317.
(99) Weiner, A. M.; Leaird, D. E.; Patel, J. S.; Wullert, J. R. *IEEE J. Quantum Electron.* **1992**, *28*, 908.
(100) Weiner, A. M. *Rev. Sci. Instrum.* **2000**, *71*, 1929.
(101) Vaughan, J. C.; Feurer, T.; Nelson, K. A. *J. Opt. Soc. Am. B* **2002**, *19*, 2489.
(102) Feurer, T.; Vaughan, J. C.; Koehl, R. M.; Nelson, K. A. *Opt. Lett.* **2002**, *27*, 652.
(103) Feurer, T.; Vaughan, J. C.; Nelson, K. A. *Science* **2003**, *299*, 374.
(104) Heritage, J. P.; Weiner, A. M.; Thurston, R. N. **1985**, *10*, 609.
(105) Wang, H.; Zheng, Z.; Leaird, D. E.; Weiner, A. M.; Dorschner, T. A.; Fijol, J. J.; Friedman, L. J.; Nguyen, H. Q.; Palmaccio, L. A. **2001**, *7*, 718.
(106) Comstock, M.; Lozovoy, V. V.; Pastirk, I.; Dantus, M. *Opt. Express* **2004**, in press.
(107) Wefers, M. M.; Nelson, K. A. *Opt. Lett.* **1993**, *18*, 2032.
(108) Wefers, M. M.; Nelson, K. A. *Opt. Lett.* **1995**, *20*, 1047.
(109) Kawashima, H.; Wefers, M. M.; Nelson, K. A. *Annu. Rev. Phys. Chem.* **1995**, *46*, 627.
(110) Brixner, T.; Gerber, G. *Opt. Lett.* **2001**, *26*, 557.
(111) Brixner, T.; Krampert, G.; Niklaus, P.; Gerber, G. *Appl. Phys. B* **2002**, *74*, S133.
(112) Brixner, T.; Damrauer, N. H.; Krampert, G.; Niklaus, P.; Gerber, G. *J. Opt. Soc. Am. B* **2003**, *20*, 878.
(113) Nelson, R. D.; Leaird, D. E.; Weiner, A. M. *Opt. Express* **2003**, *11*, 1763.
(114) Oron, D.; Dudovich, N.; Silberberg, Y. *Phys. Rev. Lett.* **2003**, *90*, art. no. 213902.
(115) Xu, L.; Nakagawa, N.; Morita, R.; Shigekawa, H.; Yamashita, M. *IEEE J. Quantum Electron.* **2000**, *36*, 893.
(116) Zeek, E.; Bartels, R.; Murnane, M. M.; Kapteyn, H. C.; Backus, S.; Vdovin, G. *Opt. Lett.* **2000**, *25*, 587.
(117) Hacker, M.; Stobrawa, G.; Sauerbrey, R.; Buckup, T.; Motzkus, M.; Wildenhain, M.; Gehner, A. *Appl. Phys. B* **2003**, *76*, 711.
(118) Haner, M.; Warren, W. S. *Appl. Opt.* **1987**, *26*, 3687.
(119) Lin, C. P.; Bates, J.; Mayer, J. T.; Warren, W. S. *J. Chem. Phys.* **1987**, *86*, 3750.
(120) Verluise, F.; Laude, V.; Cheng, Z.; Spielmann, C.; Tournois, P. *Opt. Lett.* **2000**, *25*, 575.
(121) Monmayrant, A.; Joffre, M.; Oksenhendler, T.; Herzog, R.; Kaplan, D.; Tournois, P. *Opt. Lett.* **2003**, *28*, 278.
(122) Itoh, H.; Urakami, T.; Yoshida, N.; Igasaki, Y.; Hosoda, M. *Rev. Laser Eng.* **2000**, *28*, 511.
(123) Dela Cruz, J. M.; Pastirk, I.; Walowicz, K. A.; Lozovoy, V. V.; Dantus, M. *J. Phys. Chem.* **2003**, *108*, 53
(124) Lozovoy, V. V.; Pastirk, I.; Dantus, M. *Opt. Lett.* **2004**, *29*, 775.
(125) Kane, D. J.; Trebino, R. *IEEE J. Quantum Electron.* **1993**, *29*, 571.
(126) Kane, D. J.; Trebino, R. *Opt. Lett.* **1993**, *18*, 823.
(127) Trebino, R.; Kane, D. J. *J. Opt. Soc. Am. A* **1993**, *10*, 1101.
(128) Kane, D. J.; Taylor, A. J.; Trebino, R.; Delong, K. W. *Opt. Lett.* **1994**, *19*, 1061.
(129) Delong, K. W.; Trebinoi, R.; Kane, D. J. *J. Opt. Soc. Am.* **1994**, *11*, 1595.
(130) Delong, K. W.; Ladera, C. L.; Trebino, R.; Kohler, B.; Wilson, K. R. *Opt. Lett.* **1995**, *20*, 486.
(131) Kohler, B.; Yakovlev, V. V.; Wilson, K. R.; Squier, J.; Delong, K. W.; Trebino, R. *Opt. Lett.* **1995**, *20*, 483.
(132) Clement, T. S.; Taylor, A. J.; Kane, D. J. *Opt. Lett.* **1995**, *20*, 70.
(133) Taft, G.; Rundquist, A.; Murnane, M. M.; Kapteyn, H. C.; Delong, K. W.; Trebino, R.; Christov, I. P. *Opt. Lett.* **1995**, *20*, 743.
(134) Tsang, T.; Krumbugel, M. A.; DeLong, K. W.; Fittinghoff, D. N.; Trebino, R. *Opt. Lett.* **1996**, *21*, 1381.
(135) LutherDavies, B.; Samoc, M.; Swiatkiewicza, J.; Samoc, A.; Woodruff, M.; Trebino, R.; Delong, K. W. *Opt. Commun.* **1996**, *131*, 301.
(136) DeLong, K. W.; Fittinghoff, D. N.; Trebino, R. *IEEE J. Quantum Electron.* **1996**, *32*, 1253.
(137) Kwok, A.; Jusinski, L.; Krumbugel, M. A.; Sweetser, J. N.; Fittinghoff, D. N.; Trebino, R. *IEEE J. Sel. Top. Quantum Electron.* **1998**, *4*, 271.
(138) O'Shea, P.; Kimmel, M.; Gu, X.; Trebino, R. *Opt. Express* **2000**, *7*, 342.
(139) O'Shea, P.; Kimmel, M.; Gu, X.; Trebino, R. *Opt. Lett.* **2001**, *26*, 932.
(140) O'Shea, D.; Kimmel, M.; O'Shea, P.; Trebino, R. *Opt. Lett.* **2001**, *26*, 1442.
(141) O'Shea, P.; Kimmel, M.; Trebino, R. *J. Opt. B* **2002**, *4*, 44.
(142) Trebino, R.; DeLong, K. W.; Fittinghoff, D. N.; Sweetser, J. N.; Krumbugel, M. A.; Richman, B. A.; Kane, D. J. *Rev. Sci. Instrum.* **1997**, *68*, 3277.
(143) Chilla, J. L. A.; Martinez, O. E. *Opt. Lett.* **1991**, *16*, 39.
(144) Chu, K. C.; Heritage, J. P.; Grant, R. S.; Liu, K. X.; Dienes, A.; White, W. E.; Sullivan, A. *Opt. Lett.* **1995**, *20*, 904.

(145) Chu, K. C.; Heritage, J. P.; Grant, R. S.; White, W. E. *Opt. Lett.* **1996**, *21*, 1842.
(146) Iaconis, C.; Walmsley, I. A. *Opt. Lett.* **1998**, *23*, 792.
(147) Iaconis, C.; Walmsley, I. A. *IEEE J. Quantum Electron.* **1999**, *35*, 501.
(148) Gallmann, L.; Sutter, D. H.; Matuschek, N.; Steinmeyer, G.; Keller, U.; Iaconis, C.; Walmsley, I. A. *Opt. Lett.* **1999**, *24*, 1314.
(149) Dorrer, C.; de Beauvoir, B.; Le Blanc, C.; Ranc, S.; Rousseau, J. P.; Rousseau, P.; Chambaret, J. P. *Opt. Lett.* **1999**, *24*, 1644.
(150) Dorrer, C.; Walmsley, I. A. *J. Opt. Soc. Am. B* **2002**, *19*, 1019.
(151) Dorrer, C.; Walmsley, I. A. *J. Opt. Soc. Am. B* **2002**, *19*, 1030.
(152) Gallmann, L.; Steinmeyer, G.; Sutter, D. H.; Rupp, T.; Iaconis, C.; Walmsley, I. A.; Keller, U. *Opt. Lett.* **2001**, *26*, 96.
(153) Dorrer, C.; Kosik, E. M.; Walmsley, I. A. *Opt. Lett.* **2002**, *27*, 548.
(154) Dorrer, C.; Kosik, E. M.; Walmsley, I. A. *App. Phys. B* **2002**, *74*, S209.
(155) Gallmann, L.; Sutter, D. H.; Matuschek, N.; Steinmeyer, G.; Keller, U. *Appl. Phys. B* **2000**, *70*, S67.
(156) Nicholson, J. W.; Rudolph, W. *J. Opt. Soc. B* **2002**, *19*, 330.
(157) Meshulach, D.; Yelin, D.; Silberberg, Y. *Opt. Commun.* **1997**, *138*, 345.
(158) Yelin, D.; Meshulach, D.; Silberberg, Y. *Opt. Lett.* **1997**, *22*, 1793.
(159) Meshulach, D.; Yelin, D.; Silberberg, Y. *J. Opt. Soc. Am. B* **1998**, *15*, 1615.
(160) Efimov, A.; Reitze, D. H. *Opt. Lett.* **1998**, *23*, 1612.
(161) Efimov, A.; Moores, M. D.; Beach, N. M.; Krause, J. L.; Reitze, D. H. *Opt. Lett.* **1998**, *23*, 1915.
(162) Efimov, A.; Moores, M. D.; Mei, B.; Krause, J. L.; Siders, C. W.; Reitze, D. H. *Appl. Phys. B* **2000**, *70*, S133.
(163) Baumert, T.; Brixner, T.; Seyfried, V.; Strehle, M.; Gerber, G. *Appl. Phys. B* **1997**, *65*, 779.
(164) Brixner, T.; Strehle, M.; Gerber, G. *Appl. Phys. B* **1999**, *68*, 281.
(165) Brixner, T.; Oehrlein, A.; Strehle, M.; Gerber, G. *Appl. Phys. B* **2000**, *70*, S119.
(166) Zeek, E.; Maginnis, K.; Backus, S.; Russek, U.; Murnane, M.; Mourou, G.; Kapteyn, H.; Vdovin, G. *Opt. Lett.* **1999**, *24*, 493.
(167) Armstrong, M. R.; Plachta, P.; Ponomarev, E. A.; Miller, R. J. D. *Opt. Lett.* **2001**, *26*, 1152.
(168) Armstrong, M.; Plachta, P.; Ponomarev, E. A.; Ogilvie, J. P.; Nagy, A. M.; Miller, R. J. D. *Appl. Phys. B* **2002**, *74*, S127.
(169) Baltuska, A.; Fuji, T.; Kobayashi, T. *Opt. Lett.* **2002**, *27*, 306.
(170) Siegner, U.; Haiml, M.; Kunde, J.; Keller, U. *Opt. Lett.* **2002**, *27*, 315.
(171) Takada, H.; Kakehata, M.; Torizuka, K. *Appl. Phys. B* **2002**, *74*, S253.
(172) Ohno, K.; Tanabe, T.; Kannari, F. *J. Opt. Soc. Am. B* **2002**, *19*, 2781.
(173) Legare, F. L.; Fraser, J. M.; Villeneuve, D. M.; Corkum, P. B. *Appl. Phys. B* **2002**, *74*, S279.
(174) Baum, P.; Lochbrunner, S.; Gallmann, L.; Steinmeyer, G.; Keller, U.; Riedle, E. *Appl. Phys. B* **2002**, *74*, S219.
(175) Verluise, F.; Laude, V.; Huignard, J. P.; Tournois, P.; Migus, A. *J. Opt. Soc. Am. B* **2000**, *17*, 138.
(176) Yeremenko, S.; Baltuska, A.; Pshenichnikov, M. S.; Wiersma, D. A. *Appl. Phys. B* **2000**, *70*, S109.
(177) Hong, K. H.; Kim, J. H.; Kang, Y. H.; Nam, C. H. *Appl. Phys. B* **2002**, *74*, S231.
(178) Letokhov, V. S. *Phys. Today* **1980**, *33*, 34.
(179) Crim, F. F. *Annu. Rev. Phys. Chem.* **1993**, *44*, 397.
(180) Crim, F. F. *Acc. Chem. Res.* **1999**, *32*, 877.
(181) Shapiro, M.; Brumer, P. *J. Chem. Phys.* **1986**, *84*, 4103.
(182) Kurizki, G.; Shapiro, M.; Brumer, P. *Phys. Rev. B* **1989**, *39*, 3435.
(183) Ohmura, H.; Nakanaga, T. *J. Chem. Phys.* **2004**, in press.
(184) Fiss, J. A.; Zhu, L. C.; Gordon, R. J.; Seideman, T. *Phys. Rev. Lett.* **1999**, *82*, 65.
(185) Gordon, R. J.; Zhu, L. C.; Seideman, T. *Comment Mod. Phys.* **2002**, *2*, D262.
(186) Khachatrian, A.; Billotto, R.; Zhu, L. C.; Gordon, R. J.; Seideman, T. *J. Chem. Phys.* **2002**, *116*, 9326.
(187) Chen, C.; Yin, Y. Y.; Elliott, D. S. *Phys. Rev. Lett.* **1990**, *64*, 507.
(188) Muller, H. G.; Bucksbaum, P. H.; Schumacher, D. W.; Zavriyev, A. *J. Phys. B* **1990**, *23*, 2761.
(189) Chen, C.; Elliott, D. S. *Phys. Rev. Lett.* **1990**, *65*, 1737.
(190) Lu, S. P.; Park, S. M.; Xie, Y. G.; Gordon, R. J. *J. Chem. Phys.* **1992**, *96*, 6613.
(191) Yin, Y. Y.; Chen, C.; Elliott, D. S.; Smith, A. V. *Phys. Rev. Lett.* **1992**, *69*, 2353.
(192) Gordon, R. J.; Lu, S. P.; Park, S. M.; Trentelman, K.; Xie, Y. J.; Zhu, L. C.; Kumar, A.; Meath, W. J. *J. Chem. Phys.* **1993**, *98*, 9481.
(193) Schumacher, D. W.; Weihe, F.; Muller, H. G.; Bucksbaum, P. H. *Phys. Rev. Lett.* **1994**, *73*, 1344.
(194) Yin, Y. Y.; Elliott, D. S.; Shehadeh, R.; Grant, E. R. *Chem. Phys. Lett.* **1995**, *241*, 591.
(195) Xing, G. Q.; Wang, X. B.; Huang, X.; Bersohn, R.; Katz, B. *J. Chem. Phys.* **1996**, *104*, 826.
(196) Wang, X. B.; Bersohn, R.; Takahashi, K.; Kawasaki, M.; Kim, H. L. *J. Chem. Phys.* **1996**, *105*, 2992.
(197) Chen, C.; Elliott, D. S. *Phys. Rev. A* **1996**, *53*, 272.
(198) Karapanagioti, N. E.; Xenakis, D.; Charalambidis, D.; Fotakis, C. *J. Phys. B* **1996**, *29*, 3599.
(199) Schumacher, D. W.; Bucksbaum, P. H. *Phys. Rev. A* **1996**, *54*, 4271.
(200) Pratt, S. T. *J. Chem. Phys.* **1996**, *104*, 5776.
(201) Wang, F.; Chen, C.; Elliott, D. S. *Phys. Rev. Lett.* **1996**, *77*, 2416.
(202) Wang, F.; Elliott, D. S. *Phys. Rev. A* **1997**, *56*, 3065.
(203) Xenakis, D.; Karapanagioti, N. E.; Faucher, O.; Hertz, E.; Charalambidis, D. *J. Phys. B* **1999**, *32*, 341.
(204) Wang, Z. M.; Elliott, D. S. *Phys. Rev. Lett.* **2001**, *87*, art. no. 173001.
(205) Zhu, L. C.; Kleiman, V.; Li, X. N.; Lu, S. P.; Trentelman, K.; Gordon, R. J. *Science* **1995**, *270*, 77.
(206) Sheehy, B.; Walker, B.; Dimauro, L. F. *Phys. Rev. Lett.* **1995**, *74*, 4799.
(207) Kleiman, V. D.; Zhu, L. C.; Allen, J.; Gordon, R. J. *J. Chem. Phys.* **1995**, *103*, 10800.
(208) Kleiman, V. D.; Zhu, L. C.; Li, X. N.; Gordon, R. J. *J. Chem. Phys.* **1995**, *102*, 5863.
(209) Zhu, L.; Suto, K.; Fiss, J. A.; Wada, R.; Seideman, T.; Gordon, R. J. *Phys. Rev. Lett.* **1997**, *79*, 4108.
(210) Fiss, J. A.; Zhu, L. C.; Suto, K.; He, G. Z.; Gordon, R. J. *Chem. Phys.* **1998**, *233*, 335.
(211) Loy, M. M. T. *Phys. Rev. Lett.* **1974**, *32*, 814.
(212) Loy, M. M. T. *Phys. Rev. Lett.* **1978**, *41*, 473.
(213) Gaubatz, U.; Rudecki, P.; Becker, M.; Schiemann, S.; Kulz, M.; Bergmann, K. *Chem. Phys. Lett.* **1988**, *149*, 463.
(214) Gaubatz, U.; Rudecki, P.; Schiemann, S.; Bergmann, K. *J. Chem. Phys.* **1990**, *92*, 5363.
(215) Dam, N.; Oudejans, L.; Reuss, J. *Chem. Phys.* **1990**, *140*, 217.
(216) Melinger, J. S.; Hariharan, A.; Gandhi, S. R.; Warren, W. S. *J. Chem. Phys.* **1991**, *95*, 2210.
(217) Melinger, J. S.; Gandhi, S. R.; Hariharan, A.; Tull, J. X.; Warren, W. S. *Phys. Rev. Lett.* **1992**, *68*, 2000.
(218) Dittmann, P.; Pesl, F. P.; Martin, J.; Coulston, G. W.; He, G. Z.; Bergmann, K. *J. Chem. Phys.* **1992**, *97*, 9472.
(219) Broers, B.; Vandenheuvell, H. B. V.; Noordam, L. D. *Phys. Rev. Lett.* **1992**, *69*, 2062.
(220) Schiemann, S.; Kuhn, A.; Steuerwald, S.; Bergmann, K. *Phys. Rev. Lett.* **1993**, *71*, 3637.
(221) Melinger, J. S.; Gandhi, S. R.; Hariharan, A.; Goswami, D.; Warren, W. S. *J. Chem. Phys.* **1994**, *101*, 6439.
(222) Sussmann, R.; Neuhauser, R.; Neusser, H. J. *J. Chem. Phys.* **1994**, *100*, 4784.
(223) Sussmann, R.; Neuhauser, R.; Neusser, H. J. *J. Chem. Phys.* **1995**, *103*, 3315.
(224) Kulz, M.; Kortyna, A.; Keil, M.; Schellhaass, B.; Bergmann, K. *Z. Phys. D* **1995**, *33*, 109.
(225) Halfmann, T.; Bergmann, K. *J. Chem. Phys.* **1996**, *104*, 7068.
(226) Martin, J.; Shore, B. W.; Bergmann, K. *Phys. Rev. A* **1996**, *54*, 1556.
(227) Vrijen, R. B.; Duncan, D. I.; Noordam, L. D. *Phys. Rev. A* **1997**, *56*, 2205.
(228) Maas, D. J.; Duncan, D. I.; Vrijen, R. B.; van der Zande, W. J.; Noordam, L. D. *Chem. Phys. Lett.* **1998**, *290*, 75.
(229) Kuhn, A.; Steuerwald, S.; Bergmann, K. *Eur. Phys. J. D* **1998**, *1*, 57.
(230) Theuer, H.; Bergmann, K. *Eur. Phys. J. D* **1998**, *2*, 279.
(231) Keil, M.; Kolling, T.; Bergmann, K.; Meyer, W. *Eur. Phys. J. D* **1999**, *7*, 55.
(232) Clark, B. K.; Standard, J. M.; Boostrom, T. S. *Opt. Commun.* **1999**, *164*, 145.
(233) Maas, D. J.; Rella, C. W.; Antoine, P.; Toma, E. S.; Noordam, L. D. *Phys. Rev. A* **1999**, *59*, 1374.
(234) Zewail, A. H. *Phys. Today* **1980**, *33*, 27.
(235) Yan, Y. X.; Gamble, E. B.; Nelson, K. A. *J. Chem. Phys.* **1985**, *83*, 5391.
(236) Ruhman, S.; Joly, A. G.; Kohler, B.; Williams, L. R.; Nelson, K. A. **1987**, *22*, 1717.
(237) Ruhman, S.; Kohler, B.; Joly, A. G.; Nelson, K. A. *Chem. Phys. Lett.* **1987**, *141*, 16.
(238) Ruhman, S.; Joly, A. G.; Nelson, K. A. *J. Chem. Phys.* **1987**, *86*, 6563.
(239) Ruhman, S.; Williams, L. R.; Joly, A. G.; Kohler, B.; Nelson, K. A. *J. Phys. Chem.* **1987**, *91*, 2237.
(240) Yan, Y. X.; Nelson, K. A. *J. Chem. Phys.* **1987**, *87*, 6240.
(241) Yan, Y. X.; Nelson, K. A. *J. Chem. Phys.* **1987**, *87*, 6257.
(242) Ruhman, S.; Joly, A. G.; Nelson, K. A. *IEEE J. Quantum Electron.* **1988**, *24*, 460.
(243) Ruhman, S.; Kohler, B.; Joly, A. G.; Nelson, K. A. *IEEE J. Quantum Electron.* **1988**, *24*, 470.
(244) Yan, Y. X.; Cheng, L. T.; Nelson, K. A. *J. Chem. Phys.* **1988**, *88*, 6477.
(245) Baskin, J. S.; Felker, P. M.; Zewail, A. H. **1986**, *84*, 4708.
(246) Baskin, J. S.; Felker, P. M.; Zewail, A. H. *J. Chem. Phys.* **1987**, *86*, 2483.
(247) Felker, P. M.; Hartland, G. V. **1987**, *134*, 503.
(248) Felker, P. M.; Zewail, A. H. *J. Chem. Phys.* **1987**, *86*, 2460.

(249) Hartland, G. V.; Felker, P. M. **1987**, *91*, 5527.
(250) Hartland, G. V.; Henson, B. F.; Felker, P. M. **1989**, *91*, 1478.
(251) Dantus, M.; Rosker, M. J.; Zewail, A. H. *J. Chem. Phys.* **1987**, *87*, 2395.
(252) Rosker, M. J.; Dantus, M.; Zewail, A. H. *Science* **1988**, *241*, 1200.
(253) Zewail, A. H. *Femtochemistry: Ultrafast Dynamics of the Chemical Bond*; World Scientific: 1994; Vol. 1.
(254) Zewail, A. H. *Femtochemistry: Ultrafast Dynamics of the Chemical Bond, Vol. 2*; World Scientific: 1994.
(255) Zewail, A. H. *Femtochemistry: Ultrafast Dynamics of the Chemical Bond, Vol.3*; World Scientific: River Edge, NJ, 1994.
(256) *Femtochemistry: With the Nobel Lecture of A. Zewail*; De Schryver, F. C., De Feyter, S., Schweiter, G., Eds.; Wiley-VCH: New York, 2001.
(257) *Femtochemistry and Femtobiology*; Douhal, A., Santamaria, J., Eds.; World Scientific: River Edge, NJ, 2002.
(258) Sundstrèom, V. *Femtochemistry and femtobiology: ultrafast reaction dynamics at atomic-scale resolution: Nobel Symposium 101*; Imperial College Press: Distributed by World Scientific Pub. Co.: London River Edge, NJ, 1997.
(259) Manz, J.; Wèoste, L. *Femtosecond Chemistry*; VCH: Weinheim; New York, 1995.
(260) Tannor, D. J.; Rice, S. A.; Weber, P. M. *J. Chem. Phys.* **1985**, *83*, 6158.
(261) Tannor, D. J.; Rice, S. A. *J. Chem. Phys.* **1985**, *83*, 5013.
(262) Tannor, D. J.; Kosloff, R.; Rice, S. A. *J. Chem. Phys.* **1986**, *85*, 5805.
(263) Manz, J. In *Femtochemistry and Femtobiology: Ultrafast Reaction Dynamics at Atomic-Scale Resolution*; Sundstrum, V., Ed.; Imperial College Press: London, 1996.
(264) Bowman, R. M.; Dantus, M.; Zewail, A. H. *Chem. Phys. Lett.* **1990**, *174*, 546.
(265) Baumert, T.; Grosser, M.; Thalweiser, R.; Gerber, G. *Phys. Rev. Lett.* **1991**, *67*, 3753.
(266) Salour, M. M.; Cohentannoudji, C. *Phys. Rev. Lett.* **1977**, *38*, 757.
(267) Teets, R.; Eckstein, J.; Hansch, T. W. *Phys. Rev. Lett.* **1977**, *38*, 760.
(268) Sleva, E. T.; Glasbeek, M.; Zewail, A. H. *J. Phys. Chem.* **1986**, *90*, 1232.
(269) Scherer, N. F.; Ruggiero, A. J.; Du, M.; Fleming, G. R. *J. Chem. Phys.* **1990**, *93*, 856.
(270) Scherer, N. F.; Matro, A.; Ziegler, L. D.; Du, M.; Carlson, R. J.; Cina, J. A.; Fleming, G. R. *J. Chem. Phys.* **1992**, *96*, 4180.
(271) Jones, R. R.; Raman, C. S.; Schumacher, D. W.; Bucksbaum, P. H. *Phys. Rev. Lett.* **1993**, *71*, 2575.
(272) Scherer, N. F.; Jonas, D. M.; Fleming, G. R. *J. Chem. Phys.* **1993**, *99*, 153.
(273) Blanchet, V.; Bouchene, M. A.; Cabrol, O.; Girard, B. *Chem. Phys. Lett.* **1995**, *233*, 491.
(274) Noel, M. W.; Stroud, C. R. *Phys. Rev. Lett.* **1995**, *75*, 1252.
(275) Noel, M. W.; Stroud, C. R. *Phys. Rev. Lett.* **1996**, *77*, 1913.
(276) Blanchet, V.; Nicole, C.; Bouchene, M. A.; Girard, B. *Phys. Rev. Lett.* **1997**, *78*, 2716.
(277) Bellini, M.; Bartoli, A.; Hansch, T. W. *Opt. Lett.* **1997**, *22*, 540.
(278) Noel, M. W.; Stroud, J. C. R. *Opt. Express* **1997**, *1*, 176.
(279) Blanchet, V.; Bouchene, M. A.; Girard, B. *J. Chem. Phys.* **1998**, *108*, 4862.
(280) Bouchene, M. A.; Blanchet, V.; Nicole, C.; Melikechi, N.; Girard, B.; Ruppe, H.; Rutz, S.; Schreiber, E.; Woste, L. *Eur. Phys. J. D* **1998**, *2*, 131.
(281) Kunde, J.; Siegner, U.; Arlt, S.; Steinmeyer, G.; Morier-Genoud, F.; Keller, U. *J. Opt. Soc. Am. B* **1999**, *16*, 2285.
(282) Bouchene, M. A.; Nicole, C.; Girard, B. *J. Phys. B* **1999**, *32*, 5167.
(283) Nicole, C.; Bouchene, M. A.; Zamith, S.; Melikechi, N.; Girard, B. *Phys. Rev. A* **1999**, *60*, R1755.
(284) Bouchene, M. A.; Nicole, C.; Girard, B. *Opt. Commun.* **2000**, *181*, 327.
(285) Wetzels, A.; Gurtler, A.; Muller, H. G.; Noordam, L. D. *Eur. Phys. J. D* **2001**, *14*, 157.
(286) Wollenhaupt, M.; Assion, A.; Liese, D.; Sarpe-Tudoran, C.; Baumert, T.; Zamith, S.; Bouchene, M. A.; Girard, B.; Flettner, A.; Weichmann, U.; Gerber, G. *Phys. Rev. Lett.* **2002**, *89*, art. no. 173001.
(287) Netz, R.; Nazarkin, A.; Sauerbrey, R. *Phys. Rev. Lett.* **2003**, *90*, art. no. 063001.
(288) Kinrot, O.; Averbukh, I. S.; Prior, Y. *Phys. Rev. Lett.* **1995**, *75*, 3822.
(289) Leichtle, C.; Schleich, W. P.; Averbukh, I. S.; Shapiro, M. *J. Chem. Phys.* **1998**, *108*, 6057.
(290) Warmuth, C.; Tortschanoff, A.; Milota, F.; Shapiro, M.; Prior, Y.; Averbukh, I. S.; Schleich, W.; Jakubetz, W.; Kauffmann, H. F. *J. Chem. Phys.* **2000**, *112*, 5060.
(291) Warmuth, C.; Tortschanoff, A.; Milota, F.; Leibscher, M.; Shapiro, M.; Prior, Y.; Averbukh, I. S.; Schleich, W.; Jakubetz, W.; Kauffmann, H. F. *J. Chem. Phys.* **2001**, *114*, 9901.
(292) Morita, N.; Yajima, T. *Phys. Rev A* **1984**, *30*, 2525.
(293) Beach, R.; Hartmann, S. R. *Phys. Rev. Lett.* **1984**, *53*, 663.
(294) Asaka, S.; Nakatsuka, H.; Fujiwara, M.; Matsuoka, M. *Phys. Rev. A* **1984**, *29*, 2286.
(295) Nicole, C.; Bouchene, M. A.; Blanchet, V.; Melikechi, N.; Girard, B. *Ann. Phys.-Paris* **1998**, *23*, 119.
(296) Dugan, M. A.; Melinger, J. S.; Albrecht, A. C. *Chem. Phys. Lett.* **1988**, *147*, 411.
(297) Dugan, M. A.; Albrecht, A. C. *Phys. Rev. A* **1991**, *43*, 3877.
(298) Dugan, M. A.; Albrecht, A. C. *Phys. Rev. A* **1991**, *43*, 3922.
(299) Schaertel, S. A.; Albrecht, A. C.; Lau, A.; Kummrow, A. *Appl. Phys. B* **1994**, *59*, 377.
(300) Schaertel, S. A.; Lee, D.; Albrecht, A. C. *J. Raman Spectrosc.* **1995**, *26*, 889.
(301) Gershgoren, E.; Bartels, R. A.; Fourkas, J. T.; Tobey, R.; Murnane, M. M.; Kapteyn, H. C. *Opt. Lett.* **2003**, *28*, 361.
(302) Ulness, D. J.; Stimson, M. J.; Kirkwood, J. C.; Albrecht, A. C. *J. Phys. Chem. A* **1997**, *101*, 4587.
(303) Kohler, B.; Krause, J. L.; Raksi, F.; Wilson, K. R.; Yakovlev, V. V.; Whitnell, R. M.; Yan, Y. J. *Acc. Chem. Res.* **1995**, *28*, 133.
(304) Kohler, B.; Yakovlev, V. V.; Che, J. W.; Krause, J. L.; Messina, M.; Wilson, K. R.; Schwentner, N.; Whitnell, R. M.; Yan, Y. J. *Phys. Rev. Lett.* **1995**, *74*, 3360.
(305) Bardeen, C. J.; Che, J. W.; Wilson, K. R.; Yakovlev, V. V.; Apkarian, V. A.; Martens, C. C.; Zadoyan, R.; Kohler, B.; Messina, M. *J. Chem. Phys.* **1997**, *106*, 8486.
(306) Assion, A.; Baumert, T.; Helbing, J.; Seyfried, V.; Gerber, G. *Chem. Phys. Lett.* **1996**, *259*, 488.
(307) Fork, R. L.; Martinez, O. E.; Gordon, J. P. *Opt. Lett.* **1984**, *9*, 150.
(308) Cruz, C. H. B.; Becker, P. C.; Fork, R. L.; Shank, C. V. *Opt. Lett.* **1988**, *13*, 123.
(309) Broers, B.; Noordam, L. D.; Vandenheuvell, H. B. V. *Phys. Rev. A* **1992**, *46*, 2749.
(310) Foing, J. P.; Joffre, M.; Oudar, J. L.; Hulin, D. **1993**, *10*, 1143.
(311) Christian, J. F.; Broers, B.; Hoogenraad, J. H.; Vanderzande, W. J.; Noordam, L. D. *Opt. Commun.* **1993**, *103*, 79.
(312) Balling, P.; Maas, D. J.; Noordam, L. D. *Phys. Rev. A* **1994**, *50*, 4276.
(313) Lozovoi, V. V.; Sarkisov, O. M.; Umanskii, S. Y. *Khim. Fiz.* **1995**, *14*, 83.
(314) Bardeen, C. J.; Che, J. W.; Wilson, K. R.; Yakovlev, V. V.; Cong, P. J.; Kohler, B.; Krause, J. L.; Messina, M. *J. Phys. Chem. A* **1997**, *101*, 3815.
(315) Maas, D. J.; Duncan, D. I.; vanderMeer, A. F. G.; vanderZande, W. J.; Noordam, L. D. *Chem. Phys. Lett.* **1997**, *270*, 45.
(316) Bardeen, C. J.; Yakovlev, V. V.; Squier, J. A.; Wilson, K. R. *J. Am. Chem. Soc.* **1998**, *120*, 13023.
(317) Kleiman, V. D.; Arrivo, S. M.; Melinger, J. S.; Heilweil, E. J. *Chem. Phys.* **1998**, *233*, 207.
(318) Lozovoi, V. V.; Titov, A. A.; Gostev, F. E.; Tovbin, D. G.; Antipin, S. A.; Umanskii, S. Y.; Sarkisov, O. M. *Chem. Phys. Rep.* **1998**, *17*, 1267.
(319) Lozovoy, V. V.; Antipin, S. A.; Gostev, F. E.; Titov, A. A.; Tovbin, D. G.; Sarkisov, O. M.; Vetchinkin, A. S.; Umanskii, S. Y. *Chem. Phys. Lett.* **1998**, *284*, 221.
(320) Pastirk, I.; Brown, E. J.; Zhang, Q. G.; Dantus, M. *J. Chem. Phys.* **1998**, *108*, 4375.
(321) Vetchinkin, A. S.; Lozovoi, V. V.; Sarkisov, O. M.; Umanskii, S. Y. *Chem. Phys. Rep.* **1998**, *17*, 1031.
(322) Yakovlev, V. V.; Bardeen, C. J.; Che, J. W.; Cao, J. S.; Wilson, K. R. *J. Chem. Phys.* **1998**, *108*, 2309.
(323) Zadoyan, R.; Schwentner, N.; Apkarian, V. A. *Chem. Phys.* **1998**, *233*, 353.
(324) Maas, D. J.; Vrakking, M. J. J.; Noordam, L. D. *Phys. Rev. A* **1999**, *60*, 1351.
(325) Sarkisov, O. M.; Tovbin, D. G.; Lozovoy, V. V.; Gostev, F. E.; Titov, A. A.; Antipin, S. A.; Umanskiy, S. Y. *Chem. Phys. Lett.* **1999**, *303*, 458.
(326) Lozovoi, V. V.; Gostev, F. E.; Titov, A. A.; Tovbin, D. G.; Antipin, S. A.; Umanskii, S. Y.; Sarkisov, O. M. *Chem. Phys. Rep.* **2000**, *18*, 1197.
(327) Sarkisov, O. M.; Petrukhin, A. N.; Gostev, F. E.; Titov, A. A. *Quantum Electron.* **2001**, *31*, 483.
(328) Zamith, S.; Degert, J.; Stock, S.; de Beauvoir, B.; Blanchet, V.; Bouchene, M. A.; Girard, B. *Phys. Rev. Lett.* **2001**, *87*, art. no. 033001.
(329) Netz, R.; Feurer, T.; Roberts, G.; Sauerbrey, R. *Phys. Rev. A* **2002**, *65*, art. no. 043406.
(330) Weinacht, T. C.; Ahn, J.; Bucksbaum, P. H. *Phys. Rev. Lett.* **1998**, *80*, 5508.
(331) Weinacht, T. C.; Ahn, J.; Bucksbaum, P. H. *Nature* **1999**, *397*, 233.
(332) Verlet, J. R. R.; Stavros, V. G.; Minns, R. S.; Fielding, H. H. *Phys. Rev. Lett.* **2002**, 89.
(333) Verlet, J. R. R.; Stavros, V. G.; Minns, R. S.; Fielding, H. H. *J. Phys. B-At. Mol. Opt. Phys.* **2003**, *36*, 3683.
(334) Minns, R. S.; Patel, R.; Verlet, J. R. R.; Fielding, H. H. *Phys. Rev. Lett.* **2003**, *91*, art. no. 243601.
(335) Uberna, R.; Khalil, M.; Williams, R. M.; Papanikolas, J. M.; Leone, S. R. *J. Chem. Phys.* **1998**, *108*, 9259.
(336) Amitay, Z.; Ballard, J. B.; Stauffer, H. U.; Leone, S. R. *Chem. Phys.* **2001**, *267*, 141.

(337) Uberna, R.; Amitay, Z.; Qian, C. X. W.; Leone, S. R. *J. Chem. Phys.* **2001**, *114*, 10311.
(338) Ballard, J. B.; Stauffer, H. U.; Mirowski, E.; Leone, S. R. *Phys. Rev. A* **2002**, *66*, art. no. 043402.
(339) Mirowski, E.; Stauffer, H. U.; Ballard, J. B.; Zhang, B.; Hetherington, C. L.; Leone, S. R. *J. Chem. Phys.* **2002**, *117*, 11228.
(340) Lozovoy, V. V.; Sarkisov, O. M.; Vetchinkin, A. S.; Umanskii, S. Y. *Chem. Phys.* **1999**, *243*, 97.
(341) Dudovich, N.; Dayan, B.; Faeder, S. M. G.; Silberberg, Y. *Phys. Rev. Lett.* **2001**, *86*, 47.
(342) Dudovich, N.; Oron, D.; Silberberg, Y. *Phys. Rev. Lett.* **2002**, *88*, art. no. 123004.
(343) Degert, J.; Wohlleben, W.; Chatel, B.; Motzkus, M.; Girard, B. *Phys. Rev. Lett.* **2002**, *89*, art. no. 203003.
(344) Stauffer, H. U.; Ballard, J. B.; Amitay, Z.; Leone, S. R. *J. Chem. Phys.* **2002**, *116*, 946.
(345) Chatel, A.; Degert, J.; Stock, S.; Girard, B. *Phys. Rev. A* **2003**, *68*, art. no. 041402.
(346) Ballard, J. B.; Arrowsmith, A. N.; Huewel, L.; X., D.; Leone, S. R. *Phys. Rev. A.* **2003**, *68*, art. no. 043409.
(347) Bardeen, C. J.; Wang, Q.; Shank, C. V. *Phys. Rev. Lett.* **1995**, *75*, 3410.
(348) Cerullo, G.; Bardeen, C. J.; Wang, Q.; Shank, C. V. *Chem. Phys. Lett.* **1996**, *262*, 362.
(349) Bardeen, C. J.; Wang, Q.; Shank, C. V. *J. Phys. Chem. A* **1998**, *102*, 2759.
(350) Bardeen, C. J.; Rosenthal, S. J.; Shank, C. V. *J. Phys. Chem. A* **1999**, *103*, 10506.
(351) Cao, J. S.; Wilson, K. R. *J. Chem. Phys.* **1997**, *107*, 1441.
(352) Bardeen, C. J.; Cao, J. S.; Brown, F. L. H.; Wilson, K. R. *Chem. Phys. Lett.* **1999**, *302*, 405.
(353) Buist, A. H.; Muller, M.; Ghauharali, R. I.; Brakenhoff, G. J.; Squier, J. A.; Bardeen, C. J.; Yakovlev, V. V.; Wilson, K. R. *Opt. Lett.* **1999**, *24*, 244.
(354) Cao, J. S.; Bardeen, C. J.; Wilson, K. R. *J. Chem. Phys.* **2000**, *113*, 1898.
(355) Cao, J. S.; Bardeen, C. J.; Wilson, K. R. *Phys. Rev. Lett.* **1998**, *80*, 1406.
(356) Heritage, J. P.; Gustafson, T. K.; Lin, C. H. *Phys. Rev. Lett.* **1975**, *34*, 1299.
(357) Bowman, R. M.; Dantus, M.; Zewail, A. H. *Chem. Phys. Lett.* **1989**, *161*, 297.
(358) Dantus, M.; Bowman, R. M.; Zewail, A. H. *Nature* **1990**, *343*, 737.
(359) Gruebele, M.; Roberts, G.; Dantus, M.; Bowman, R. M.; Zewail, A. H. *Chem. Phys. Lett.* **1990**, *166*, 459.
(360) Brown, E. J.; Zhang, Q. G.; Dantus, M. *J. Chem. Phys.* **1999**, *110*, 5772.
(361) Comstock, M.; Lozovoy, V. V.; Dantus, M. *Chem. Phys. Lett.* **2003**, *372*, 739.
(362) Papanikolas, J. M.; Williams, R. M.; Leone, S. R. *J. Chem. Phys.* **1997**, *107*, 4172.
(363) Williams, R. M.; Papanikolas, J. M.; Rathje, J.; Leone, S. R. *J. Chem. Phys.* **1997**, *106*, 8310.
(364) Uberna, R.; Amitay, Z.; Loomis, R. A.; Leone, S. R. *Faraday Discuss.* **1999**, *113*, 385.
(365) Ballard, J. B.; Stauffer, H. U.; Amitay, Z.; Leone, S. R. *J. Chem. Phys.* **2002**, *116*, 1350.
(366) Friedrich, B.; Herschbach, D. *J. Phys. Chem.* **1995**, *99*, 15686.
(367) Friedrich, B.; Herschbach, D. *Phys. Rev. Lett.* **1995**, *74*, 4623.
(368) Kim, W.; Felker, P. M. *J. Chem. Phys.* **1996**, *104*, 1147.
(369) Kim, W. S.; Felker, P. M. *J. Chem. Phys.* **1997**, *107*, 2193.
(370) Larsen, J. J.; Sakai, H.; Safvan, C. P.; Wendt-Larsen, I.; Stapelfeldt, H. *J. Chem. Phys.* **1999**, *111*, 7774.
(371) Sakai, H.; Safvan, C. P.; Larsen, J. J.; Hilligsoe, K. M.; Hald, K.; Stapelfeldt, H. *J. Chem. Phys.* **1999**, *110*, 10235.
(372) Larsen, J. J.; Hald, K.; Bjerre, N.; Stapelfeldt, H.; Seideman, T. *Phys. Rev. Lett.* **2000**, *85*, 2470.
(373) Seideman, T. *J. Chem. Phys.* **1995**, *103*, 7887.
(374) Posthumus, J. H.; Plumridge, J.; Thomas, M. K.; Codling, K.; Frasinski, L. J.; Langley, A. J.; Taday, P. F. *J. Phys. B* **1998**, *31*, L553.
(375) Ellert, C.; Corkum, P. B. *Phys. Rev. A* **1999**, *59*, R3170.
(376) Comstock, M.; Senekerimyan, V. A.; Dantus, M. *J. Phys. Chem. A* **2003**, *107*, 8271.
(377) Yamanouchi, K. *Science* **2002**, *295*, 1659.
(378) Villeneuve, D. M.; Aseyev, S. A.; Dietrich, P.; Spanner, M.; Ivanov, M. Y.; Corkum, P. B. *Phys. Rev. Lett.* **2000**, *85*, 542.
(379) Ashkin, A.; Dziedzic, J. M.; Bjorkholm, J. E.; Chu, S. *Opt. Lett.* **1986**, *11*, 288.
(380) Ashkin, A.; Dziedzic, J. M.; Yamane, T. *Nature* **1987**, *330*, 769.
(381) Ashkin, A.; Dziedzic, J. M. *Science* **1987**, *235*, 1517.
(382) Ashkin, A.; Dziedzic, J. M. *Proc. Natl. Acad. Sci. U.S.A.* **1989**, *86*, 7914.
(383) DeCamp, M. F.; Reis, D. A.; Bucksbaum, P. H.; Merlin, R. *Phys. Rev. B* **2001**, *64*, art. no. 092301.
(384) Bardeen, C. J.; Yakovlev, V. V.; Wilson, K. R.; Carpenter, S. D.; Weber, P. M.; Warren, W. S. *Chem. Phys. Lett.* **1997**, *280*, 151.
(385) Judson, R. S.; Rabitz, H. *Phys. Rev. Lett.* **1992**, *68*, 1500.
(386) Assion, A.; Baumert, T.; Bergt, M.; Brixner, T.; Kiefer, B.; Seyfried, V.; Strehle, M.; Gerber, G. *Science* **1998**, *282*, 919.
(387) Hornung, T.; Meier, R.; Zeidler, D.; Kompa, K. L.; Proch, D.; Motzkus, M. *Appl. Phys. B* **2000**, *71*, 277.
(388) Brixner, T.; Damrauer, N. H.; Niklaus, P.; Gerber, G. *Nature* **2001**, *414*, 57.
(389) Zeidler, D.; Frey, S.; Kompa, K. L.; Motzkus, M. *Phys. Rev. A* **2001**, *64*, art. no. 023420.
(390) Ando, T.; Urakami, T.; Itoh, H.; Tsuchiya, Y. *Appl. Phys. Lett.* **2002**, *80*, 4265.
(391) Weinacht, T. C.; White, J. L.; Bucksbaum, P. H. *J. Phys. Chem. A* **1999**, *103*, 10166.
(392) Weinacht, T. C.; Bartels, R.; Backus, S.; Bucksbaum, P. H.; Pearson, B.; Geremia, J. M.; Rabitz, H.; Kapteyn, H. C.; Murnane, M. M. *Chem. Phys. Lett.* **2001**, *344*, 333.
(393) Pearson, B. J.; White, J. L.; Weinacht, T. C.; Bucksbaum, P. H. *Phys. Rev. A* **2001**, *6306*, art. no. 063412.
(394) Zeidler, D.; Frey, S.; Wohlleben, W.; Motzkus, M.; Busch, F.; Chen, T.; Kiefer, W.; Materny, A. *J. Chem. Phys.* **2002**, *116*, 5231.
(395) Bartels, R.; Backus, S.; Zeek, E.; Misoguti, L.; Vdovin, G.; Christov, I. P.; Murnane, M. M.; Kapteyn, H. C. *Nature* **2000**, *406*, 164.
(396) Bartels, R.; Backus, S.; Christov, I.; Kapteyn, H.; Murnane, M. *Chem. Phys.* **2001**, *267*, 277.
(397) Christov, I. P.; Bartels, R.; Kapteyn, H. C.; Murnane, M. M. *Phys. Rev. Lett.* **2001**, *86*, 5458.
(398) Bartels, R. A.; Backus, S.; Murnane, M. M.; Kapteyn, H. C. *Chem. Phys. Lett.* **2003**, *374*, 326.
(399) Fraser, J. M.; Shkrebtii, A. I.; Sipe, J. E.; van Driel, H. M. *Phys. Rev. Lett.* **1999**, *83*, 4192.
(400) Omenetto, F. G.; Taylor, A. J.; Moores, M. D.; Reitze, D. H. *Opt. Lett.* **2001**, *26*, 938.
(401) Omenetto, F. G.; Reitze, D. H.; Luce, B. P.; Moores, M. D.; Taylor, A. J. *IEEE J. Sel. Top. Quantum Electron.* **2002**, *8*, 690.
(402) Bergt, M.; Brixner, T.; Kiefer, B.; Strehle, M.; Gerber, G. *J. Phys. Chem. A* **1999**, *103*, 10381.
(403) Glass, A.; Rozgonyi, T.; Feurer, T.; Sauerbrey, R.; Szabo, G. *Appl. Phys. B* **2000**, *71*, 267.
(404) Feurer, T.; Glass, A.; Rozgonyi, T.; Sauerbrey, R.; Szabo, G. *Chem. Phys.* **2001**, *267*, 223.
(405) Daniel, C.; Full, J.; Gonzalez, L.; Kaposta, C.; Krenz, M.; Lupulescu, C.; Manz, J.; Minemoto, S.; Oppel, M.; Rosendo-Francisco, P.; Vajda, S.; Woste, L. *Chem. Phys.* **2001**, *267*, 247.
(406) Brixner, T.; Kiefer, B.; Gerber, G. *Chem. Phys.* **2001**, *267*, 241.
(407) Levis, R. J.; Menkir, G. M.; Rabitz, H. *Science* **2001**, *292*, 709.
(408) Levis, R. J.; Rabitz, H. A. *J. Phys. Chem. A* **2002**, *106*, 6427.
(409) Damrauer, N. H.; Dietl, C.; Krampert, G.; Lee, S. H.; Jung, K. H.; Gerber, G. *Eur. Phys. J. D* **2002**, *20*, 71.
(410) Bergt, M.; Brixner, T.; Dietl, C.; Kiefer, B.; Gerber, G. *J. Organomet. Chem.* **2002**, *661*, 199.
(411) Daniel, C.; Full, J.; Gonzalez, L.; Lupulescu, C.; Manz, J.; Merli, A.; Vajda, S.; Woste, L. *Science* **2003**, *299*, 536.
(412) Kunde, J.; Baumann, B.; Arlt, S.; Morier-Genoud, F.; Siegner, U.; Keller, U. *App. Phys. Lett.* **2000**, *77*, 924.
(413) Hornung, T.; Meier, R.; de Vivie-Riedle, R.; Motzkus, M. *Chem. Phys.* **2001**, *267*, 261.
(414) Herek, J. L.; Wohlleben, W.; Cogdell, R. J.; Zeidler, D.; Motzkus, M. *Nature* **2002**, *417*, 533.
(415) Brixner, T.; Damrauer, N. H.; Kiefer, B.; Gerber, G. *J. Chem. Phys.* **2003**, *118*, 3692.
(416) Bakker, H. J.; Joosen, W.; Noordam, L. D. *Phys. Rev. A* **1992**, *45*, 5126.
(417) Meshulach, D.; Silberberg, Y. *Nature* **1998**, *396*, 239.
(418) Meshulach, D.; Silberberg, Y. *Phys. Rev. A* **1999**, *60*, 1287.
(419) Dudovich, N.; Oron, D.; Silberberg, Y. *Nature* **2002**, *418*, 512.
(420) Jones, R. R. *Phys. Rev. Lett.* **1995**, *74*, 1091.
(421) Jones, R. R. *Phys. Rev. Lett.* **1995**, *75*, 1491.
(422) Schumacher, D. W.; Hoogenraad, J. H.; Pinkos, D.; Bucksbaum, P. H. *Phys. Rev. A* **1995**, *52*, 4719.
(423) Bardeen, C. J.; Yakovlev, V. V.; Squier, J. A.; Wilson, K. R.; Carpenter, S. D.; Weber, P. M. *J. Biomed. Opt.* **1999**, *4*, 362.
(424) Pesce, L.; Amitay, Z.; Uberna, R.; Leone, S. R.; Ratner, M.; Kosloff, R. *J. Chem. Phys.* **2001**, *114*, 1259.
(425) Bartels, R. A.; Weinacht, T. C.; Leone, S. R.; Kapteyn, H. C.; Murnane, M. M. *Phys. Rev. Lett.* **2002**, *88*, art. no. 033001.
(426) Degert, J.; Meier, C.; de Beauvoir, B.; Brakking, M. J. J.; Girard, B. *J. Phys. IV* **2002**, *12*, 253.
(427) Witte, T.; Hornung, T.; Windhorn, L.; Proch, D.; de Vivie-Riedle, R.; Motzkus, M.; Kompa, K. L. *J. Chem. Phys.* **2003**, *118*, 2021.
(428) Warren, W. S.; Zewail, A. H. *J. Chem. Phys.* **1983**, *78*, 2279.
(429) Koch, M.; Feldmann, J.; Vonplessen, G.; Gobel, E. O.; Thomas, P.; Kohler, K. *Phys. Rev. Lett.* **1992**, *69*, 3631.
(430) Nibbering, E. T. J.; Wiersma, D. A.; Duppen, K. *Phys. Rev. Lett.* **1992**, *68*, 514.
(431) Duppen, K.; Dehaan, F.; Nibbering, E. T. J.; Wiersma, D. A. *Phys. Rev. A* **1993**, *47*, 5120.
(432) Kinrot, O.; Prior, Y. *Phys. Rev. A* **1994**, *50*, R1999.
(433) de Boeij, W. P.; Pshenichnikov, M. S.; Wiersma, D. A. *Chem. Phys. Lett.* **1995**, *247*, 264.

(434) de Boeij, W. P.; Pshenichnikov, M. S.; Wiersma, D. A. *Chem. Phys. Lett.* **1995**, *238*, 1.
(435) de Boeij, W. P.; Pshenichnikov, M. S.; Wiersma, D. A. *J. Chem. Phys.* **1996**, *105*, 2953.
(436) Motzkus, M.; Pedersen, S.; Zewail, A. H. *J. Phys. Chem.* **1996**, *100*, 5620.
(437) Pshenichnikov, M. S.; de Boeij, W. P.; Wiersma, D. A. *Phys. Rev. Lett.* **1996**, *76*, 4701.
(438) Schmitt, M.; Knopp, G.; Materny, A.; Kiefer, W. *Chem. Phys. Lett.* **1997**, *280*, 339.
(439) Schmitt, M.; Knopp, G.; Materny, A.; Kiefer, W. *Chem. Phys. Lett.* **1997**, *270*, 9.
(440) Meyer, S.; Schmitt, M.; Materny, A.; Kiefer, W.; Engel, V. *Chem. Phys. Lett.* **1997**, *281*, 332.
(441) Emde, M. F.; de Boeij, W. P.; Pshenichnikov, M. S.; Wiersma, D. A. *Opt. Lett.* **1997**, *22*, 1338.
(442) Schmitt, M.; Knopp, G.; Materny, A.; Kiefer, W. *J. Phys. Chem. A* **1998**, *102*, 4059.
(443) de Boeij, W. P.; Pshenichnikov, M. S.; Wiersma, D. A. *Chem. Phys.* **1998**, *233*, 287.
(444) Rubner, O.; Schmitt, M.; Knopp, G.; Materny, A.; Kiefer, W.; Engel, V. *J. Phys. Chem. A* **1998**, *102*, 9734.
(445) Brown, E. J.; Pastirk, I.; Grimberg, B. I.; Lozovoy, V. V.; Dantus, M. *J. Chem. Phys.* **1999**, *111*, 3779.
(446) Pastirk, I.; Lozovoy, V. V.; Grimberg, B. I.; Brown, E. J.; Dantus, M. *J. Phys. Chem. A* **1999**, *103*, 10226.
(447) Pastirk, I.; Brown, E. J.; Grimberg, B. I.; Lozovoy, V. V.; Dantus, M. *Faraday Discuss.* **1999**, *113*, 401.
(448) Lozovoy, V. V.; Grimberg, B. I.; Brown, E. J.; Pastirk, I.; Dantus, M. *J. Raman Spectrosc.* **2000**, *31*, 41.
(449) Pastirk, I.; Lozovoy, V. V.; Dantus, M. *Chem. Phys. Lett.* **2001**, *333*, 76.
(450) Lozovoy, V. V.; Pastirk, I.; Comstock, M. G.; Dantus, M. *Chem. Phys.* **2001**, *266*, 205.
(451) Lozovoy, V. V.; Grimberg, B. I.; Pastirk, I.; Dantus, M. *Chem. Phys.* **2001**, *267*, 99.
(452) Chen, T.; Engel, V.; Heid, M.; Kiefer, W.; Knopp, G.; Materny, A.; Meyer, S.; Pausch, R.; Schmitt, M.; Schwoerer, H.; Siebert, T. *J. Mol. Struct.* **1999**, *481*, 33.
(453) Hamm, P.; Lim, M.; Asplund, M.; Hochstrasser, R. M. *Chem. Phys. Lett.* **1999**, *301*, 167.
(454) Meyer, S.; Schmitt, M.; Materny, A.; Kiefer, W.; Engel, V. *Chem. Phys. Lett.* **1999**, *301*, 248.
(455) Pausch, R.; Heid, M.; Chen, T.; Kiefer, W.; Schwoerer, H. *J. Chem. Phys.* **1999**, *110*, 9560.
(456) Vierheilig, A.; Chen, T.; Waltner, P.; Kiefer, W.; Materny, A.; Zewail, A. H. *Chem. Phys. Lett.* **1999**, *312*, 349.
(457) Materny, A.; Chen, T.; Schmitt, M.; Siebert, T.; Vierheilig, A.; Engel, V.; Kiefer, W. *Appl. Phys. B* **2000**, *71*, 299.
(458) Materny, A.; Chen, T.; Vierheilig, A.; Kiefer, W. *J. Raman Spectrosc.* **2001**, *32*, 425.
(459) Zadoyan, R.; Apkarian, V. A. *Chem. Phys. Lett.* **2000**, *326*, 1.
(460) Chen, T.; Vierheilig, A.; Waltner, P.; Heid, M.; Kiefer, W.; Materny, A. *Chem. Phys. Lett.* **2000**, *326*, 375.
(461) Heid, M.; Chen, T.; Pausch, R.; Schwoerer, H.; Kiefer, W. *J. Chin. Chem. Soc.* **2000**, *47*, 637.
(462) Pausch, R.; Heid, M.; Chen, T.; Schwoerer, H.; Kiefer, W. *J. Raman Spectrosc.* **2000**, *31*, 7.
(463) Siebert, T.; Schmitt, M.; Vierheilig, A.; Flachenecker, G.; Engel, V.; Materny, A.; Kiefer, W. *J. Raman Spectrosc.* **2000**, *31*, 25.
(464) Knopp, G.; Pinkas, I.; Prior, Y. *J. Raman Spectrosc.* **2000**, *31*, 51.
(465) Heid, M.; Chen, T.; Schmitt, U.; Kiefer, W. *Chem. Phys. Lett.* **2001**, *334*, 119.
(466) Chen, T.; Vierheilig, A.; Kiefer, W.; Materny, A. *Phys. Chem. Chem. Phys.* **2001**, *3*, 5408.
(467) Hornung, T.; Meier, R.; Motzkus, M. *Chem. Phys. Lett.* **2000**, *326*, 445.
(468) Karavitis, M.; Zadoyan, R.; Apkarian, V. A. *J. Chem. Phys.* **2001**, *114*, 4131.
(469) Faeder, J.; Pinkas, I.; Knopp, G.; Prior, Y.; Tannor, D. J. *J. Chem. Phys.* **2001**, *115*, 8440.
(470) Heid, M.; Schlucker, S.; Schmitt, U.; Chen, T.; Schweitzer-Stenner, R.; Engel, V.; Kiefer, W. *J. Raman Spectrosc.* **2001**, *32*, 771.
(471) Pinkas, I.; Knopp, G.; Prior, Y. *J. Chem. Phys.* **2001**, *115*, 236.
(472) Kiefer, W.; Materny, A.; Schmitt, M. *Naturwissenschaften* **2002**, *89*, 250.
(473) Lozovoy, V. V.; Comstock, M.; Dantus, M. In *Laser Control and Manipulation of Molecules*; Bandrauk, A. D., Fujimura, Y., Gordon, R. J., Eds.; American Chemical Society: Washington, DC, 2002; Vol. 821.
(474) Oron, D.; Dudovich, N.; Yelin, D.; Silberberg, Y. *Phys. Rev. A* **2002**, *65*, art. no. 043408.
(475) Oron, D.; Dudovich, N.; Silberberg, Y. *Phys. Rev. Lett.* **2002**, *89*, art. no. 273001.
(476) Oron, D.; Dudovich, N.; Yelin, D.; Silberberg, Y. *Phys. Rev. Lett.* **2002**, *88*, art. no. 063004.
(477) Schmitt, M.; Heid, M.; Schlucker, S.; Kiefer, W. *Biopolymers* **2002**, *67*, 226.
(478) Siebert, T.; Schmitt, M.; Engel, V.; Materny, A.; Kiefer, W. *J. Am. Chem. Soc.* **2002**, *124*, 6242.
(479) Siebert, T.; Maksimenka, R.; Materny, A.; Engel, V.; Kiefer, W.; Schmitt, M. *J. Raman Spectrosc.* **2002**, *33*, 844.
(480) Dudovich, N.; Oron, D.; Silberberg, Y. *J. Chem. Phys.* **2003**, *118*, 9208.
(481) Kurnit, N. A.; Abella, I. D.; Hartmann, S. R. *Phys. Rev. Lett.* **1964**, *13*, 567.
(482) Hahn, E. L. *Phys. Rev.* **1950**, *80*, 580.
(483) Comstock, M.; Lozovoy, V. V.; Dantus, M. *J. Chem. Phys.* **2003**, *119*, 6546.
(484) Bardeen, C. J.; Shank, C. V. *Chem. Phys. Lett.* **1993**, *203*, 535.
(485) Bartels, R. A.; Weinacht, T. C.; Wagner, N.; Baertschy, M.; Greene, C. H.; Murnane, M. M.; Kapteyn, H. C. *Phys. Rev. Lett.* **2002**, *88*, art. no. 013903.
(486) Dantus, M. *Chem. Eng. News* **2001**, *79*, 191.
(487) Schlag, E. W.; Grotemeyer, J.; Levine, R. D. *Chem. Phys. Lett.* **1992**, *190*, 521.
(488) Szaflarski, D. M.; Elsayed, M. A. *J. Phys. Chem.* **1988**, *92*, 2234.
(489) Walker, B.; Sheehy, B.; Dimauro, L. F.; Agostini, P.; Schafer, K. J.; Kulander, K. C. *Phys. Rev. Lett.* **1994**, *73*, 1227.
(490) Augst, S.; Strickland, D.; Meyerhofer, D. D.; Chin, S. L.; Eberly, J. H. *Phys. Rev. Lett.* **1989**, *63*, 2212.
(491) Talebpour, A.; Larochelle, S.; Chin, S. L. *J. Phys. B - At. Mol., Opt. Phys.* **1998**, *31*, 2769.
(492) Zittel, P. F.; Little, D. D. *J. Chem. Phys.* **1980**, *72*, 5900.
(493) Zittel, P. F.; Masturzo, D. E. *J. Chem. Phys.* **1986**, *85*, 4362.
(494) Berghout, H. L.; Brown, S. S.; Delgado, R.; Crim, F. F. *J. Chem. Phys.* **1998**, *109*, 2257.
(495) Shafer, N.; Satyapal, S.; Bersohn, R. *J. Chem. Phys.* **1989**, *90*, 6807.
(496) Vanderwal, R. L.; Scott, J. L.; Crim, F. F. *J. Chem. Phys.* **1990**, *92*, 803.
(497) Bar, I.; Cohen, Y.; David, D.; Rosenwaks, S.; Valentini, J. J. *J. Chem. Phys.* **1990**, *93*, 2146.
(498) Sinha, A.; Hsiao, M. C.; Crim, F. F. *J. Chem. Phys.* **1990**, *92*, 6333.
(499) Sinha, A.; Hsiao, M. C.; Crim, F. F. *J. Chem. Phys.* **1991**, *94*, 4928.
(500) Bar, I.; Cohen, Y.; David, D.; Arusiparpar, T.; Rosenwaks, S.; Valentini, J. J. *J. Chem. Phys.* **1991**, *95*, 3341.
(501) Bronikowski, M. J.; Simpson, W. R.; Girard, B.; Zare, R. N. *J. Chem. Phys.* **1991**, *95*, 8647.
(502) Metz, R. B.; Thoemke, J. D.; Pfeiffer, J. M.; Crim, F. F. *J. Chem. Phys.* **1993**, *99*, 1744.
(503) Bronikowski, M. J.; Simpson, W. R.; Zare, R. N. *J. Phys. Chem.* **1993**, *97*, 2204.
(504) Zhang, J.; Riehn, C. W.; Dulligan, M.; Wittig, C. *J. Chem. Phys.* **1995**, *103*, 6815.
(505) Thoemke, J. D.; Pfeiffer, J. M.; Metz, R. B.; Crim, F. F. *J. Phys. Chem.* **1995**, *99*, 13748.
(506) Brown, S. S.; Berghout, H. L.; Crim, F. F. *J. Chem. Phys.* **1995**, *102*, 8440.
(507) Brown, S. S.; Metz, R. B.; Berghout, H. L.; Crim, F. F. *J. Chem. Phys.* **1996**, *105*, 6293.
(508) Berghout, H. L.; Hsieh, S.; Crim, F. F. *J. Chem. Phys.* **2001**, *114*, 10835.
(509) Butler, L. J.; Hintsa, E. J.; Shane, S. F.; Lee, Y. T. *J. Chem. Phys.* **1987**, *86*, 2051.
(510) Sinha, A.; Thoemke, J. D.; Crim, F. F. *J. Chem. Phys.* **1992**, *96*, 372.
(511) Jensen, E.; Keller, J. S.; Waschewsky, G. C. G.; Stevens, J. E.; Graham, R. L.; Freed, K. F.; Butler, L. J. *J. Chem. Phys.* **1993**, *98*, 2882.
(512) Bronikowski, M. J.; Simpson, W. R.; Zare, R. N. *J. Phys. Chem.* **1993**, *97*, 2194.
(513) Herek, J. L.; Materny, A.; Zewail, A. H. *Chem. Phys. Lett.* **1994**, *228*, 15.
(514) Shnitman, A.; Sofer, I.; Golub, I.; Yogev, A.; Shapiro, M.; Chen, Z.; Brumer, P. *Phys. Rev. Lett.* **1996**, *76*, 2886.
(515) Larsen, J. J.; Wendt-Larsen, I.; Stapelfeldt, H. *Phys. Rev. Lett.* **1999**, *83*, 1123.
(516) Hering, P.; Brooks, P. R.; Curl, R. F.; Judson, R. S.; Lowe, R. S. *Phys. Rev. Lett.* **1980**, *44*, 687.
(517) Bowman, R. M.; Dantus, M.; Zewail, A. H. *Chem. Phys. Lett.* **1989**, *156*, 131.
(518) Dantus, M.; Bowman, R. M.; Gruebele, M.; Zewail, A. H. *J. Chem. Phys.* **1989**, *91*, 7437.
(519) Marvet, U.; Dantus, M. *Chem. Phys. Lett.* **1996**, *256*, 57.
(520) Marvet, U.; Zhang, Q. G.; Brown, E. J.; Dantus, M. *J. Chem. Phys.* **1998**, *109*, 4415.
(521) Potter, E. D.; Herek, J. L.; Pedersen, S.; Liu, Q.; Zewail, A. H. *Nature* **1992**, *355*, 66.
(522) Apkarian, V. A. *J. Chem. Phys.* **1997**, *106*, 5298.
(523) Ogrady, B. V.; Donovan, R. J. *Chem. Phys. Lett.* **1985**, *122*, 503.
(524) Donovan, R. J.; Holmes, A. J.; Langridgesmith, P. R. R.; Ridley, T. **1988**, *84*, 541.

(525) Marvet, U.; Dantus, M. *Chem. Phys. Lett.* **1995**, *245*, 393.
(526) Gross, P.; Dantus, M. *J. Chem. Phys.* **1997**, *106*, 8013.
(527) Backhaus, P.; Schmidt, B. *Chem. Phys.* **1997**, *217*, 131.
(528) Scherer, N. F.; Khundkar, L. R.; Bernstein, R. B.; Zewail, A. H. *J. Chem. Phys.* **1987**, *87*, 1451.
(529) Wittig, C.; Sharpe, S.; Beaudet, R. A. *Acc. Chem. Res.* **1988**, *21*, 341.
(530) Scherer, N. F.; Sipes, C.; Bernstein, R. B.; Zewail, A. H. *J. Chem. Phys.* **1990**, *92*, 5239.
(531) Ionov, S. I.; Brucker, G. A.; Jaques, C.; Valachovic, L.; Wittig, C. *J. Chem. Phys.* **1993**, *99*, 6553.
(532) Bardeen, C. J.; Shank, C. V. *Chem. Phys. Lett.* **1994**, *226*, 310.
(533) Lambert, W. R.; Felker, P. M.; Syage, J. A.; Zewail, A. H. *J. Chem. Phys.* **1984**, *81*, 2195.
(534) Lambert, W. R.; Felker, P. M.; Zewail, A. H. *J. Chem. Phys.* **1984**, *81*, 2209.
(535) Lambert, W. R.; Felker, P. M.; Zewail, A. H. *J. Chem. Phys.* **1984**, *81*, 2217.
(536) Syage, J. A.; Felker, P. M.; Zewail, A. H. *J. Chem. Phys.* **1984**, *81*, 2233.
(537) Diau, E. W. G.; Herek, J. L.; Kim, Z. H.; Zewail, A. H. *Science* **1998**, *279*, 847.
(538) Gruebele, M. *Theor. Chem. Acc.* **2003**, *109*, 53.
(539) Williams, C. P.; Clearwate, S. H. *Explorations in Quantum Computing*; TELOS: Anta Clara, CA, 1998.
(540) Nielsen, M. A.; Chuang, I. L. *Quantum Computation and Quantum Information*; Cambridge University Press: Cambridge, 2000.
(541) Warren, W. S. *Science* **1997**, *277*, 1688.
(542) Lozovoy, V. V.; Dantus, M. *Chem. Phys. Lett.* **2002**, *351*, 213.
(543) Amitay, Z.; Kosloff, R.; Leone, S. R. *Chem. Phys. Lett.* **2002**, *359*, 8.
(544) Ahn, J.; Rangan, C.; Hutchinson, D. N.; Bucksbaum, P. H. *Phys. Rev. A* **2002**, *66*, art. no. 022312.
(545) Reif, J.; Schmid, R. P.; Schneider, T. *Appl. Phys. B* **2002**, *74*, 745.
(546) Schmid, R. P.; Schneider, T.; Reif, J. *Opt. Commun.* **2002**, *207*, 155.
(547) Schmid, R. P.; Schneider, T.; Reif, J. *Appl. Phys. B* **2002**, *74*, S205.
(548) Ollikainen, O.; Nilsson, C.; Gallus, J.; Erni, D.; Rebane, A. *Opt. Commun.* **1998**, *147*, 429.
(549) Rebane, A.; Drobizhev, M.; Sigel, C.; Ross, W.; Gallus, J. *J. Lumin.* **1999**, *83−4*, 325.
(550) Ross, W.; Drobizhev, M.; Sigel, C.; Rebane, A. *Laser Phys.* **1999**, *9*, 1102.
(551) Ahn, J.; Hutchinson, D. N.; Rangan, C.; Bucksbaum, P. H. *Phys. Rev. Lett.* **2001**, *86*, 1179.
(552) Rangan, C.; Bucksbaum, P. H. *Phys. Rev. A* **2001**, *64*, art. no. 033417.
(553) Rangan, C.; Ahn, J.; Hutchinson, D. N.; Bucksbaum, P. H. *J. Mod. Opt.* **2002**, *49*, 2339.
(554) Vala, J.; Amitay, Z.; Zhang, B.; Leone, S. R.; Kosloff, R. *Phys. Rev. A* **2002**, *66*, art. no. 062316.
(555) Zadoyan, R.; Kohen, D.; Lidar, D. A.; Apkarian, V. A. *Chem. Phys.* **2001**, *266*, 323.
(556) Bihary, Z.; Glenn, D. R.; Lidar, D. A.; Apkarian, V. A. *Chem. Phys. Lett.* **2002**, *360*, 459.
(557) Naumov, A. N.; Materny, A.; Kiefer, W.; Motzkus, M.; Zheltikov, A. M. *Laser Phys.* **2001**, *11*, 1319.
(558) Ohmura, H.; Nakanaga, T.; Arakawa, H.; Tachiya, M. *Chem. Phys. Lett.* **2002**, *363*, 559.
(559) Zhang, Q.; Keil, M.; Shapiro, M. *J. Opt. Soc. Am. B* **2003**, *20*, 2255.
(560) Ohmori, K.; Sato, Y.; Nikitin, E. E.; Rice, S. A. *Phys. Rev. Lett.* **2003**, *91*, art no 243003.
(561) Prior, Y.; Pinkas, I.; Knopp, G. *Nonlinear Opt.* **2000**, *24*, 233.
(562) Baumert, T.; Gerber, G. *Isr. J. Chem.* **1994**, *34*, 103.

CR020668R